

# RCA REVIEW

*A Quarterly Journal of Radio Progress*

Published in July, October, January and April of Each Year by

RCA INSTITUTES TECHNICAL PRESS  
A Department of RCA Institutes, Inc.  
75 Varick Street, New York, N. Y.

---

VOLUME V

April, 1941

NUMBER 4

---

## CONTENTS

	PAGE
Short-Wave Radio Transmission and Geomagnetism.....	395
H. E. HALLBORG	
Video Output Systems.....	409
D. E. FOSTER AND J. A. RANKIN	
Deflection and Impedance of Electron Beams at High Frequencies in the Presence of a Magnetic Field.....	439
L. MALTER	
Engineering Factors Involved in Re-Locating WEAFF.....	455
RAYMOND F. GUY	
Frequency Modulation .....	468
S. W. SEELEY	
Cascade Amplifiers With Maximal Flatness, Part II.....	481
V. D. LANDON	
A New Series of Insulators for Ultra-High-Frequency Tubes.....	498
L. R. SHARDLOW	
Fluctuations in Space-Charge-Limited Currents at Moderately High Frequencies, Part V—Fluctuations in Vacuum Tube Amplifiers and Input Systems.....	505
W. A. HARRIS	
Announcement—RCA Laboratories .....	525
Our Contributors .....	529
Technical Articles by RCA Engineers.....	532
Index to RCA REVIEW, Vol. V.....	533

---

## SUBSCRIPTION:

United States, Canada and Postal Union: One Year \$2.00. Two Years \$3.00. Three Years \$4.00  
Other Foreign Countries: One Year \$2.55. Two Years \$3.70. Three Years \$5.05  
Single Copies: 75¢ each

Copyright, 1941, by RCA Institutes, Inc.

Entered as second-class matter July 17, 1936, at the Post Office at New York, New York,  
under the Act of March 3, 1879.

Printed in U.S.A.

## BOARD OF EDITORS

*Chairman*

CHARLES J. PANNILL  
*President, RCA Institutes, Inc.*

RALPH R. BEAL  
*Research Director,  
Radio Corporation of America*

DR. H. H. BEVERAGE  
*Vice President in Charge  
of Research and Development,  
R.C.A. Communications, Inc.*

ROBERT S. BURNAP  
*Engineer-in-Charge,  
Commercial Engineering Section,  
RCA Manufacturing Company,  
Radiotron Division*

IRVING F. BYRNES  
*Chief Engineer,  
Radiomarine Corporation of America*

DR. ALFRED N. GOLDSMITH  
*Consulting Engineer,  
Radio Corporation of America*

HARRY G. GROVER  
*General Patent Attorney,  
Radio Corporation of America*

O. B. HANSON  
*Vice President in Charge of Engineering  
National Broadcasting Company*

HORTON H. HEATH  
*Director of Advertising  
and Publicity  
Radio Corporation of America*

CHARLES W. HORN  
*Assistant Vice President and  
Director of Research and Development,  
National Broadcasting Company*

WILLSON HURT  
*Assistant General Counsel  
Radio Corporation of America*

DR. CHARLES B. JOLLIFFE  
*Engineer-in-Charge,  
RCA Frequency Bureau*

C. W. LATIMER  
*Vice President and Chief  
Operations Engineer  
R.C.A. Communications, Inc.*

FRANK E. MULLEN  
*Vice President and General Manager  
National Broadcasting Company*

E. W. RITTER  
*Vice President in Charge of  
Manufacturing and Production  
Engineering  
RCA Manufacturing Company*

CHARLES H. TAYLOR  
*R.C.A. Communications, Inc.*

ARTHUR F. VAN DYCK  
*Manager  
Radio Corporation of America  
License Laboratory*

C. S. ANDERSON  
*Secretary, Board of Editors*

---

Previously unpublished papers appearing in this book may be reprinted, abstracted or abridged, provided credit is given to RCA REVIEW and to the author, or authors, of the papers in question. Reference to the issue date or number is desirable.

Permission to quote other papers should be obtained from the publications to which credited.

# SHORT-WAVE RADIO TRANSMISSION AND GEOMAGNETISM\*

BY

H. F. HALLBORG

Engineering Department, R.C.A. Communications, Inc., New York, N. Y.

*Summary*—The most outstanding correlations connecting short-wave radio transmission with geomagnetism, observed by the author, are illustrated. Measurement methods are briefly described. Simultaneous recordings of London signal "GLH", and earth-current traces at Riverhead, for the disturbed month of April, 1936, are shown to be related in approximate accordance with the law of inverse earth-current variability. The transmission power required over a circuit is therefore proportional to the mean rate of geomagnetic change over that circuit. The power required over the North Atlantic, for various degrees of magnetic disturbance, and the relationship of power to geomagnetic latitude is illustrated. The latitude-power data are deduced from H-intensity-range values for all North American Magnetic Observatories supplied by the U. S. Coast & Geodetic Survey.

Short-wave circuit interruptions are studied, both with respect to geomagnetic latitude, and duration, up to four days immediately following the magnetic storm. A geomagnetic storm "knee" is seen to exist at 50°N geomagnetic latitude, thereby demarking a storm zone of non-communication for short waves.

World-wide short-wave circuit transmission conditions to New York from North Europe, South America, and San Francisco, and from the Orient to San Francisco are compared, for two solar rotations, with earth-current variability at Riverhead, N. Y. One of these solar rotations, March 7 to April 12, 1940, is unquestionably the most exciting in the history of long-distance short-wave communication.

Cheltenham magnetic activity and North Atlantic RCAC disturbance ratings are compared for a period of 12 solar rotations, beginning November 3, 1939 and ending September 21, 1940. The period selected is approximately at the peak of the current eleven-year geomagnetic cycle.

It is concluded that the data presented is further evidence that the ionosphere, short-wave radio transmission, and geomagnetism are closely related to the changing rotational complexions of the sun. The locations of magnetic and ionosphere observatories above 60° N geomagnetic latitude would provide further means to supplement our knowledge of all these broad fields of research.

IT HAS long been known that short-wave circuits passing over or near the North magnetic pole are subject to much disturbance, and severe fading. On the other hand, circuits at lower latitudes are very much less disturbed.

Extended study of magnetic and earth-current activity by R.C.A. Communications, together with the systematic recording of circuit conditions on a specified disturbance scale, has permitted an evaluation of magnetic activity, and circuit disturbance, with reference to the great-circle path of the circuit. This study has advanced to the

---

\* This paper was presented at the "Symposium on Geomagnetism" held at the American Philosophical Society, February 14-15, 1941.

extent that it is now possible to estimate the amount of power that will be required over the North Atlantic for various degrees of geomagnetic activity. It has also been possible to determine the relative freedom from interruption, during magnetic storms, of any circuit in terms of its great-circle bearing with respect to the North magnetic pole.

The magnetic data have been deduced from the RCAC earth-current recordings at Riverhead, and from Cheltenham, Md., magnetograms, which are received regularly. The U. S. Coast and Geodetic Survey has further cooperated in RCAC magnetic studies by supplying, upon request, H-range data from all five of their North American observatories.

Simple and readily applied units of measurement are a requisite to world-wide correlation. It was recognized that the most prolific source for short-wave transmission data would be from normal operation on commercial world-wide traffic. This requirement led to the application of a number-rating system allowing the receiving technicians to estimate transmission conditions, on each eight-hour watch, on selected circuits. The disturbance number-rating system, adopted by RCAC, and used since 1938, is shown in Table I.

TABLE I

<i>Circuit-Rating Number</i>	<i>Disturbance Condition</i>	<i>Signal Condition</i>
0	Unusually quiet	Unusual strength
1	Normal	Strength and fading normal
2	Slight	Slightly below normal
3	Moderate	Considerably below normal
4	Severe	Nearly out; but still audible
5	Complete drop-out	Inaudible

Earth-current variations at the RCAC Riverhead Recording Station are measured in hourly units of "percentage variability". This unit is an expression for the measured length of the earth-current trace per hour in terms of hourly baseline. For instance, "100 per cent variability" means that the measured earth-current trace length is twice the baseline length. Percentage variability is an expression which is proportional to the mean rate of change of the earth field during the hour.

Cheltenham magnetograms are analyzed for hourly departures of the H-intensity range by the customary procedure. A running chart is issued covering each solar rotation of 27 days. This chart divides each day into 4 six-hour periods. The sum of the H ranges in each 6-hour period is plotted as ordinates in 27-day sequences.

The Cheltenham magnetic activity chart provides for a very con-

siderable degree of circuit-condition prediction since many solar disturbances persist for 6 or more rotations of the sun. The chart is a continuous record of solar, magnetic, and ionosphere activity. The form of the chart is shown in the upper portion of Figure 10.

A reproduction to scale of Riverhead earth-current traces corresponding to RCAC circuit-disturbance rating numbers 0 to 5 is shown

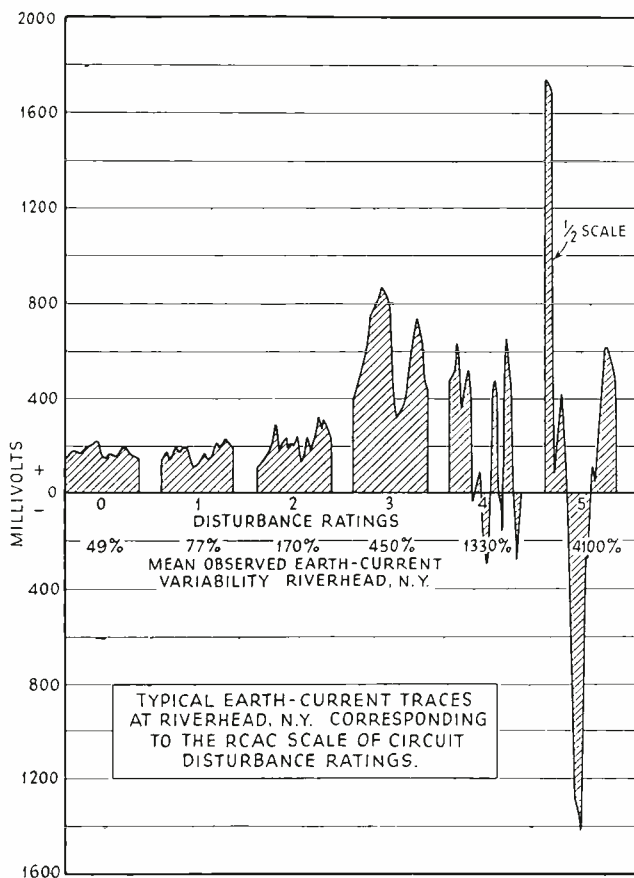


Fig. 1

in Figure 1. Under each rating number is written the observed mean percentage variability corresponding to that number. The sketch above each number illustrates one equivalent shape of the trace.

It is of interest to compare the new 3-hour K index method of magnetic rating, adopted by the U. S. Coast and Geodetic Survey, and used in Science Service Research Aid Announcements, with the equivalent RCAC circuit-disturbance ratings. This comparison is made in Figure 2. The ordinates in this figure are Cheltenham H-intensity ranges, and the abscissas RCAC disturbance and K index ratings. A

considerable band of overlap is seen to exist. The practical result of this overlap between mutual values 0 to 5 is that RCAC disturbance ratings and K values are interchangeable. All values of K above 5 will still produce RCAC rating 5—namely, complete signal drop-out or inaudibility.

It was believed that simultaneous recording of a typical North European signal, and earth-current variability during a considerably

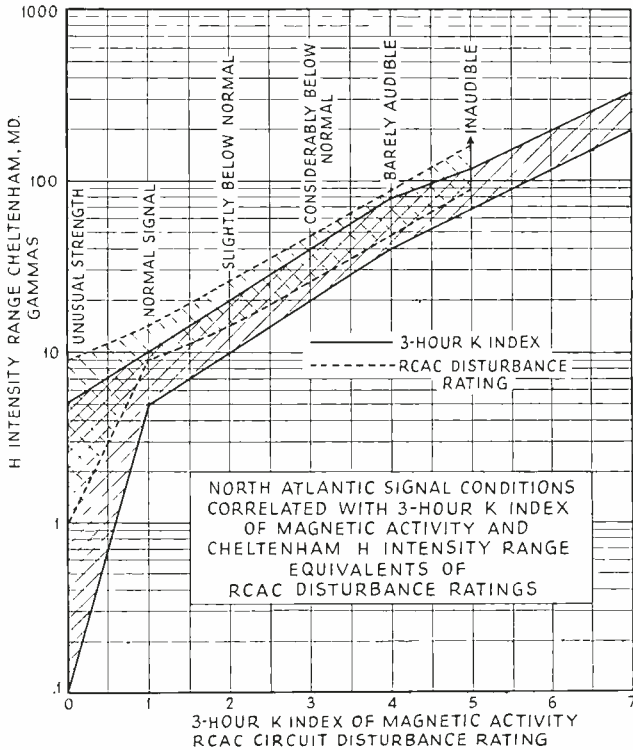


Fig. 2

disturbed month might lead to a useful relationship between magnetic variability and signal strength. Consequently, London signal "GLH", 13525 Kc, was continuously recorded during the month of April, 1936 at Riverhead, N. Y. and compared with the corresponding Riverhead earth-current trace variability. Both quantities were reduced to a mean daily figure. The result of signal-vs.-variability observations is shown in Figure 3. The days of the month are identified by numbers, and the magnetic condition of each day by the magnetic legend. Three broad types of days were segregated, namely, quiet, storm, and post-storm days. The full-line curve is the form the points would have assumed if they follow precisely the inverse-variability law. If post-

storm days are neglected, during which period the signal is controlled by absorption, the inverse-variability law is a fair mean of all observations. The decibels above and below normal signal in terms of disturbance ratings are indicated in the lower portion of Figure 3.

This signal inverse-variability relation has provided a means for computing the range of power that will permit commercial signaling

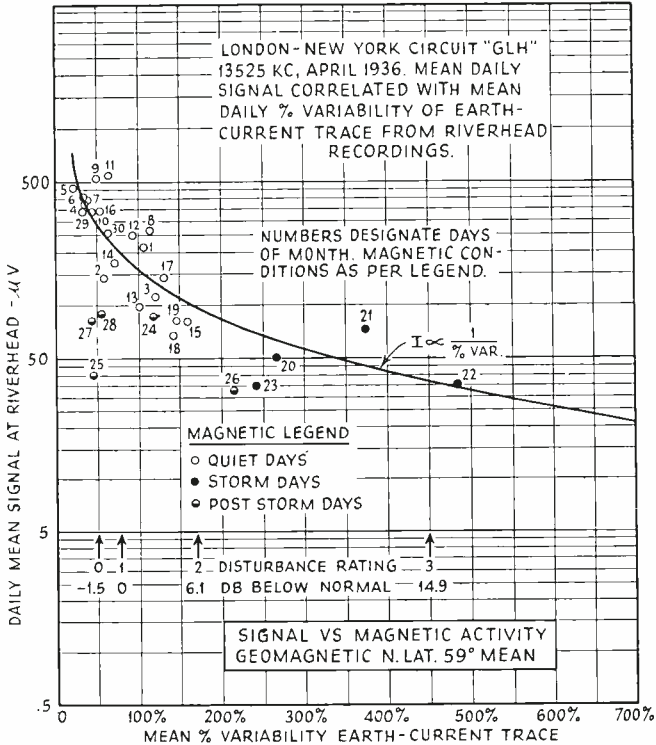


Fig. 3

across the Atlantic for various degrees of magnetic disturbance. This subject is considered in more detail in the next section.

It was indicated in Figure 3 that the order of signal level below normal for circuit rating 3 was 14.9 db. Experience has indicated that during such disturbance level over the North Atlantic the standard 20/40 kw RCA transmitter will be operating at maximum rated power, namely, 40 kw, to avoid circuit interruption. If, therefore, 40 kw, and circuit rating 3, be taken as unity, and if the power varies inversely as the earth-current variability, the power range for all disturbance ratings will vary in accordance with Figure 4.

The extreme range of power will consequently be,—

Rating	KW	Power Range
5	3460	7200
0	0.48	

The geomagnetic polar region is a zone of high magnetic activity, consequently of severe short-wave fading. The equatorial region, on

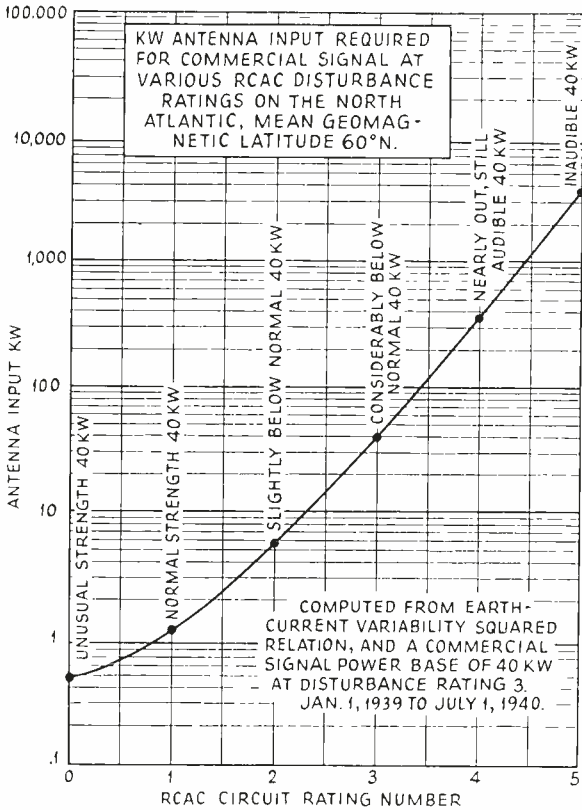


Fig. 4

the other hand, is a belt of low magnetic activity, consequently of low short-wave fading.

A short-wave radio circuit will respond to the above geophysical relation in fair agreement with its mean geomagnetic latitude, particularly during magnetic disturbances.

In Figure 5 is shown the mean daily circuit ratings observed during 16 major magnetic storms of 1939 and 1940, as well as the conditions 6 days before and after these storms on circuits having mean geomagnetic latitudes 14° N, 48° N and 59° N. The comparative

disturbances are proportional to the total indicated shaded areas at the different latitudes. This area is very much lower at 14° N than at 59° N geomagnetic latitude.

The observed relationship between earth-current variability and

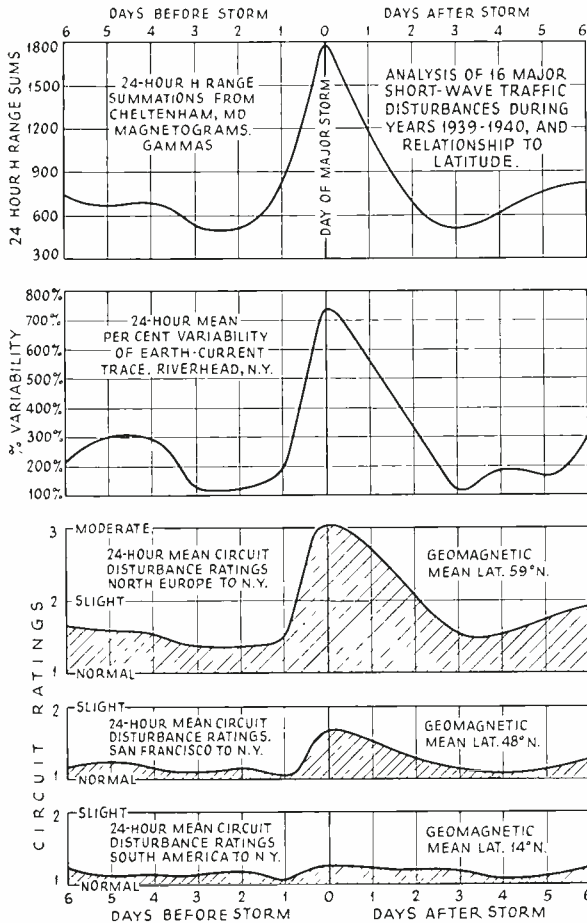


Fig. 5

“GLH” signal suggested that if, correspondingly, earth-current variability could be related to H range, it should be possible to compute transmitting power in terms of geomagnetic latitude. Cheltenham H-intensity ranges correlated with Riverhead earth-current variability have indicated that transmitting power may be related to H-intensity range by the condition that the power required at any mean latitude varies approximately as the 3.5 power of the H range at that latitude. If this relationship is applied to the H-range data of North American magnetic observatories of the U. S. Coast and Geodetic Survey for

the year 1939 there is obtained the transmitting-power-vs.-geomagnetic-latitude graph shown in Figure 6.

Comparison of the power requirements at geomagnetic latitudes 30° and 60°, from Figure 6, produces the result shown in Table II.

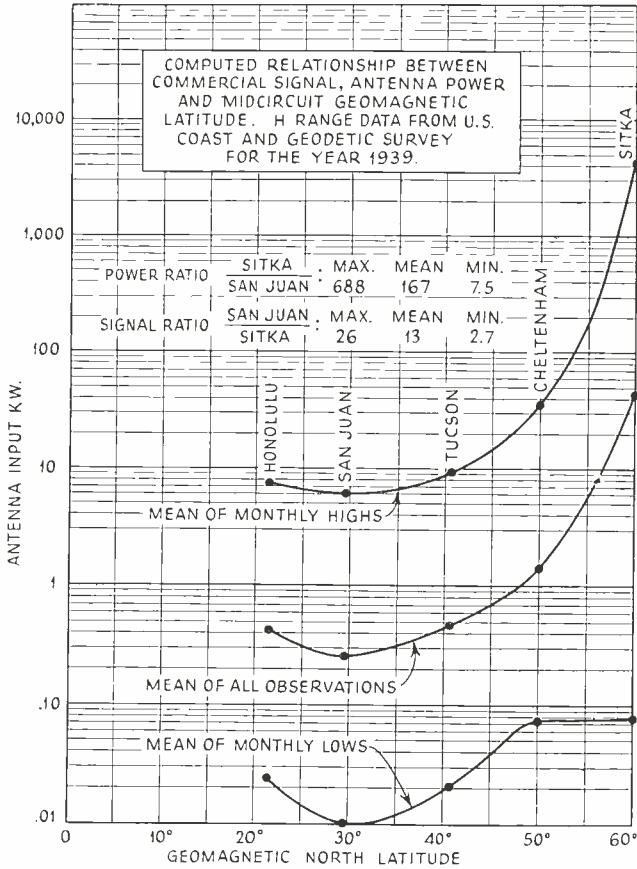


Fig. 6

TABLE II

Geomagnetic Latitude	Antenna KW for Commercial Transmission		
	Max.	Min.	Yearly Mean (1939)
30°	6.15 kw	0.010 kw	.265 kw
60°	4224	0.075	44.3
Ratio 60°/30°	688	7.5	167

It is of interest to compare these transmitting-power computations vs. geomagnetic latitude, from magnetic data, with the results of the long series of international broadcast recordings, at broadcast fre-

quencies, published by J. H. Dellinger and A. T. Cosentino in the *Proceedings of the IRE*, October, 1940.

Dellinger and Cosentino found that broadcast intensities, between North and South America, averaged 25 times those between North America and Europe, and were only 1/15 as variable.

The signal ratios at short waves, from Figure 6, will be proportional to the square roots of the power ratios. This produces the relationship for the year 1939 shown in Table III.

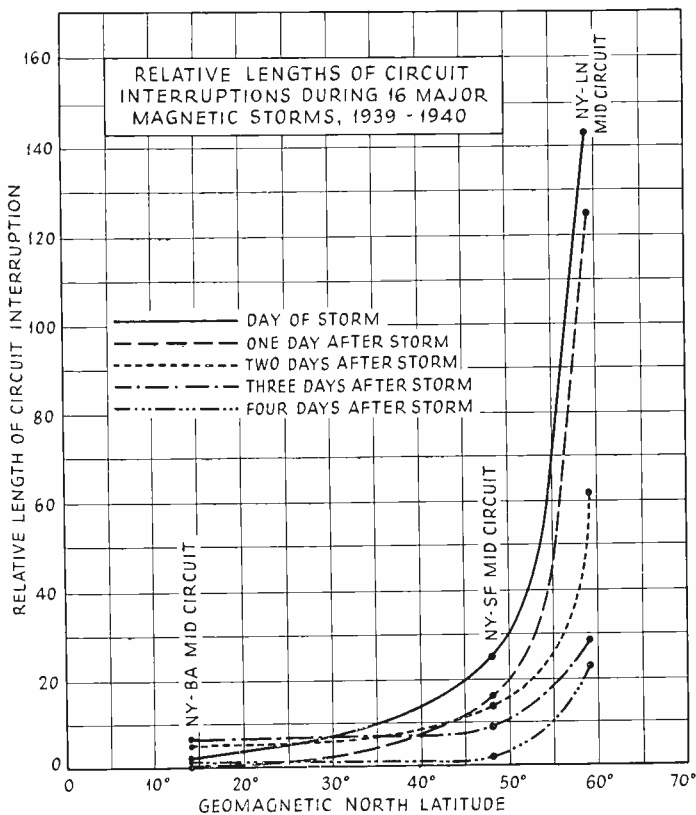


Fig. 7

These figures indicate that geomagnetic range is a major factor in international short-wave transmission. A similar conclusion was reached by Dellinger and Cosentino for international transmission at broadcast frequencies.

Circuit interruptions are definitely a function of geomagnetic latitude. Comparisons of the relative lengths of short-wave circuit interruptions, on the particular circuits used in this analysis, during and after 16 major magnetic storms of 1939 and 1940 have produced

the results shown in Figure 7. A pronounced "knee" in the interruptions vs. geomagnetic latitude graphs is seen to occur at 50° N geomagnetic latitude. The New York-San Francisco circuit (mean geomagnetic latitude 48° N) is less disturbed during the peak of the storm than is the New York-London circuit (mean geomagnetic lati-

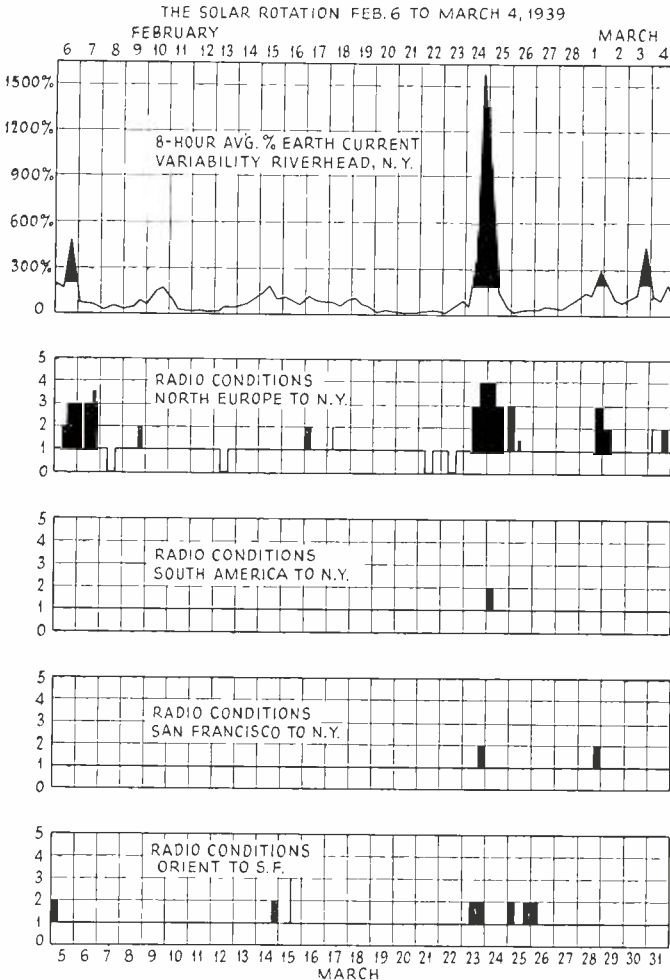


Fig. 8

TABLE III

Geomagnetic-Latitude Ratio	Signal Ratio for Equal Power		
	Max.	Min.	Yearly Mean
30°/60°	26	2.7	13

tude 59° N) 3 days following. The New York-Buenos Aires circuit (mean geomagnetic latitude 14° N) is comparatively undisturbed. There is some evidence of a slow southward disturbance filtration reaching a maximum 3 days after the storm.

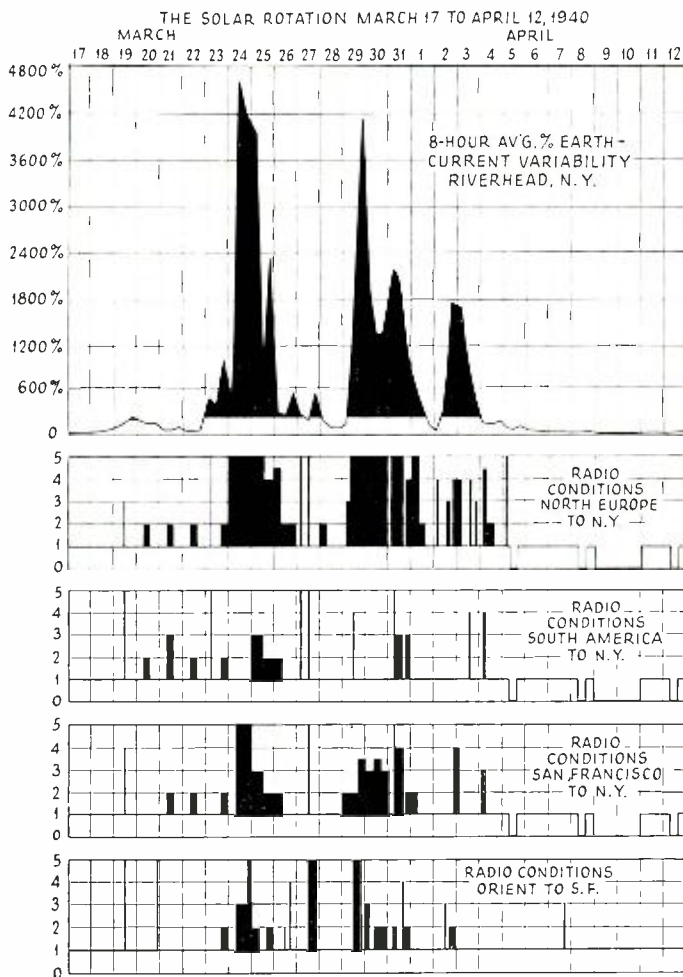


Fig. 9

It is not to be assumed that all short-wave transmission across the North Atlantic encounters the 50° N geomagnetic latitude “knee”. The records show this was true a negligible percentage of total circuit time during the peak magnetic year of 1939.

A typical RCAC circuit-disturbance rating graph is shown in Figure 8. It covers the solar rotational period of February 6 to March 4th, 1939. This period contained a wide range of magnetic disturbances over the North Atlantic circuits.

The plot at the top of Figure 8 is the 8-hour average percentage variability of the recorded earth-current trace at Riverhead, N. Y. Solid fills above 200 per cent indicate watches, or portions thereof, above the circuit-disturbance level.

The 4 plots in Figure 8 show the reported scales of radio disturbance, in order, on the following circuits,—

- a. North Europe to New York.
- b. South America to New York.
- c. San Francisco to New York.
- d. Orient to San Francisco.

Short-period disturbances are indicated by thin lines of width proportional to their durations. A solid fill for each watch indicates an average disturbance for the watch of the amplitude indicated by the rating number.

The dates at the bottom of the chart are those for the oncoming solar rotation. If the disturbance areas on the sun persist, they represent dates of probable recurrence.

The North Europe disturbances during this rotation contain two characteristics of particular interest,—

1. On February 22nd and 23rd, two days of unusual signal strength preceding the major-storm day of February 24th.
2. On February 7th and February 26th, a persistence of circuit disturbance after earth-current activity had dropped to normal.

The latitude effect, previously illustrated in Figure 7, is quite in evidence in Figure 8. The tranquility of the South America-to-New York circuit is outstanding.

Figure 9 illustrates perhaps one of the most exciting solar rotations in short-wave history. It covers the period from March 17th to April 12th, 1940. This solar rotation created aurora, abnormal power and radio-transmission disturbances, and wide comment in the public press.

The range of the percentage variability of the Riverhead earth-current trace at the top of Figure 9 has been extended to permit a visual estimate of its amplitude, above normal circuit disturbance level, particularly on March 24th and March 29th.

Features of particular interest were as follows:—

- a) A premonitory round-the-world short-period fade, 1800-1900 GMT, on March 19th.
- b) During the maximums of the disturbance peaks, March 24th and 29th, short-wave communication over the North Atlantic to Europe was completely cut off. European service was how-

ever continued without interruption by the relaying of messages to Europe via Buenos Aires.

- c) A second round-the-world fade, 1615-2000 GMT, on March 27th, preceded the second magnetic storm on March 29th.
- d) The South American circuit again has the helpful influence of low geomagnetic latitude. It was entirely normal during the storm peaks.

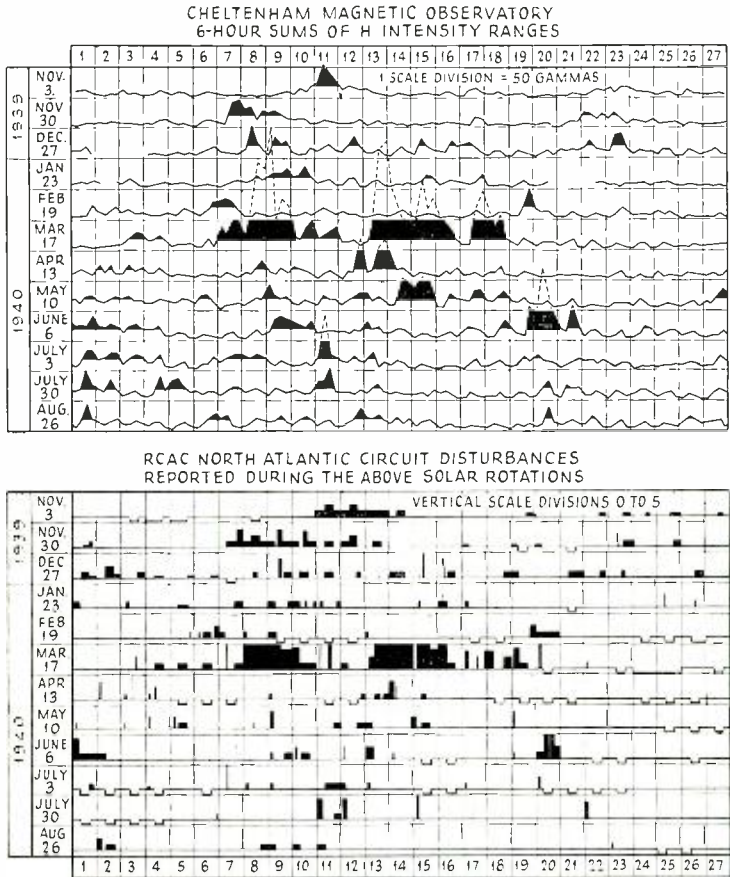


Fig. 10

North Atlantic short-wave circuit disturbances and Cheltenham H-intensity ranges are plotted in 27-day solar sequences for a period of 12-solar rotations, beginning November 3rd, 1939 and ending September 21st, 1940 in Figure 10. The date of commencement of each solar rotation is at the left of each row, and corresponds with horizontal numeral Number 1.

Cheltenham H ranges have been corrected for scale calibrations,

and each point is a six-hour sum of hourly departures. The vertical scale is 50 gammas per division. Values above 250 gammas are indicated by dotted lines.

The North Atlantic-circuit disturbances are represented by disturbance numbers 0 to 5 in accordance with Table I. The bottom line of each row represents 0 rating, the top line 5 rating.

The charted-time interval selected includes the peak of the magnetic disturbance in the current eleven-year cycle. This chart is useful for the purpose of indicating concurrent radio and geomagnetic disturbance; but may produce a misleading impression as to the value of such charts for disturbance prediction. The selection of a period of twelve solar rotations earlier would have shown repetitive disturbances for as many as ten solar rotations.

A careful study of these parallel charts in Figure 10 will reveal the persistence of radio disturbance, the repetitive property of moderate storms, and the non-repetitive property of major storms. It will bring to light one anomaly, the first to come to the author's attention, namely, the association of excellent signal conditions, in the face of considerable magnetic disturbance during the first four or five days of the sequence beginning July 30, 1940.

If the question of location of a monitoring magnetic observatory for any long-distance short-wave circuit is considered it is now evident that the ideal location for such an observatory would be at the mid-point of the circuit. Such a site selection presents practical difficulties when the application is in the mid-Atlantic. It will also be evident that the selection of any site, on land, above 60° geomagnetic latitude will provide much information of scientific value, both as to geomagnetism, and the ionosphere.

The data here presented are further evidence that short-wave radio transmission, the ionosphere, and geomagnetism are closely related to the changing rotational complexion of the solar surface.

The closer scientific correlation of geomagnetism and radio transmission, and the ionosphere, at locations more suited to bring out the latitude characteristics, will further supplement our knowledge of all these fields.

There is shown to exist during geomagnetic disturbances a short-wave communications "knee" at about 50° geomagnetic North latitude. Great-circle paths intercepting above 50° do so at the cost of increased power and circuit interruption.

On the other hand, great-circle paths that follow the lower latitudes are relatively free from circuit interruption during geomagnetic disturbances and may operate at lower power with lesser fading, in proportion to the long observed improvement in geomagnetic variability at the lower latitudes.

# VIDEO OUTPUT SYSTEMS

BY

D. E. FOSTER AND J. A. RANKIN

RCA License Laboratory, New York

*Summary*—The output stage of the video frequency amplifier of a television receiver is required to modulate the grid of the picture tube over the range of optimum contrast. In order to accomplish this purpose a relatively large output is necessary over the entire video frequency range. In addition, the output stage must reinsert the d-c component which determines the average brightness of the scene. The advantages and disadvantages of direct coupling, grid rectification, and diode rectification as a means of accomplishing d-c reinsertion are discussed. It is pointed out that d-c reinsertion tends to restore low frequencies.

The characteristics of circuits to obtain uniform high-frequency response are discussed. The circuits dealt with are shunt peaking, series peaking, series and shunt peaking, series  $m$ -derived filter sections, shunt  $m$ -derived filter sections, and two-section constant- $K$  filter sections.

The performance of typical video output tubes with the several circuit types as to gain and voltage output is shown.

## INTRODUCTION

VIDEO frequency amplifiers have been treated in radio literature generally. However, the requirements of the video amplifier used as the output stage of the television receiver to modulate the grid of the picture tube (Kinescope) with picture signals require special consideration. This article discusses the video output stage, its particular requirements, methods of d-c reinsertion, suitable circuits for use with available tubes, and typical performance characteristics.

## OUTPUT STAGE REQUIREMENTS

The video-output stage must have sufficient output to modulate the picture-tube grid over the optimum contrast range, plus additional output capability for the synchronizing pulses in order that the picture be properly reproduced. It would not be necessary to reproduce the synchronizing pulses faithfully as they occur during the blanking interval, except that the overload of the output tube is due to plate-current cut-off, so the entire video signal must be reproduced to avoid distortion of any part. Picture tubes now commonly used in this country require some 25 or 30 volts peak-to-peak for full contrast, so that with 25 per cent synchronizing pulses, the output tube must be capable of delivering at least 40 volts peak-to-peak. A higher maximum output is

desirable so that there is never any question that full contrast is achieved. It is always possible to reduce the output by means of the contrast control, so many receivers have 60 to 120 volts peak-to-peak maximum output. The situation is similar to that in radio receivers where it is desirable to have sufficient audio gain to overload the output tube even at low-modulation levels. In order to keep the number of video stages at a minimum, the gain of the output stage should be high. By careful use of the principles considered herein sufficient gain may be obtained so that the video-output stage provides all the video amplification required on practically any television receiver. The maximum output of the video stage is a function of maximum permissible plate current and the load-resistor value. The gain is a function of the effective transconductance and the load value. The load resistance for a given band width is a function of tube-output capacitance, so it may be seen that the video-output tube should have high transconductance, high plate current, and low output capacitance.

In considering circuits for video-output purposes it has been assumed in this article that the response be flat over the desired frequency range, as this is the condition generally desired. In some designs a characteristic which rises towards the high frequencies is used to compensate for loss in the high frequencies either due to picture-tube spot size or loss elsewhere in the system. This can usually be done safely to compensate to a moderate degree the effect of spot size, without introduction of undue phase distortion, but an attempt to provide more than a small amount of compensation for deficiencies elsewhere in the receiver frequently leads to phase-distortion difficulties. Therefore, for the sake of generality and because it is the most commonly used condition, it is assumed that flat response is the design criterion.

The phase shift should of course vary linearly with respect to frequency so that the time delay does not vary with frequency. However, the phase shift is not usually a serious problem in the case of a single video stage in a receiver, both because the number of reactances is relatively small, so that large phase shift does not occur, and also because the phase shift in the intermediate-frequency amplifier is ordinarily so much greater that the phase shift due to the video-output stage is of little consequence when the overall receiver-phase characteristic is considered. For these reasons the phase characteristics of the networks covered herein are not discussed. However, if the same networks are used in an application where several video stages in cascade are employed, the phase characteristics become important and must be considered in order to obtain satisfactorily uniform time delay.

The low-frequency compensation methods for video amplifiers have

been dealt with in a previous issue<sup>1</sup> so are not covered here except as the method of securing bias and the d-c reinsertion affect the low-frequency response.

### D-C REINSERTION

In a television system where the average brightness of the scene being scanned at the transmitter is transmitted as variation of the carrier level, it is the equivalent of transmitting the d-c component of the scene. Such a system is therefore called the d-c transmission type and is in use in the United States. Since the d.c. is not carried as

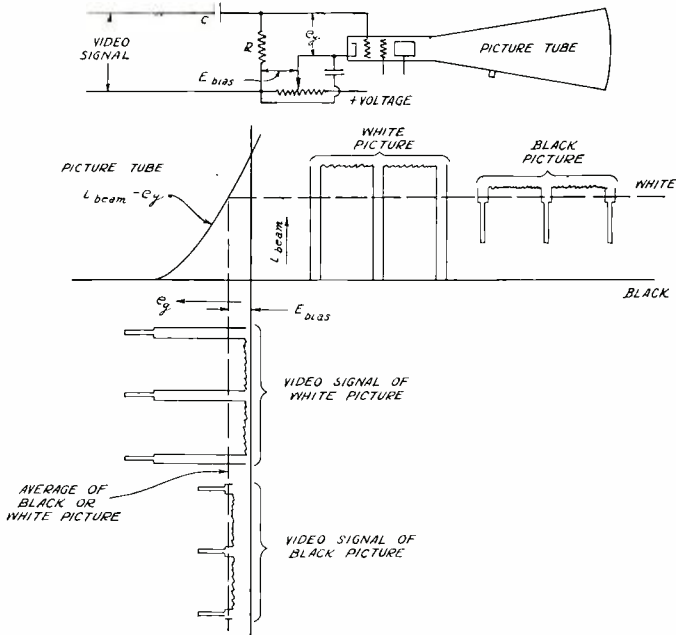


Fig. 1

such through the entire system, it is necessary to recover or to reinsert the d-c component at the receiver, this d-c reinsertion providing automatic control of the brightness of the picture tube. This restoration of the d.c. serves to fix the black level of the video signal.

The necessity for fixing the black level of the video signal appearing at the picture-tube grid is most readily appreciated by considering what conditions prevail when the black level of the video signal is not maintained at a fixed point on the operating characteristic of the picture tube.

<sup>1</sup> Analysis and Design of Video Amplifiers, S. W. Seeley and C. N. Kimball, *RCA Review*, Oct. 1937 and Jan. 1939.

The circuit of Figure 1 is that of the input of the picture tube. The picture tube in this circuit is operated at a constant grid bias indicated on the diagram as  $E_{bias}$ . The video signal is coupled to the picture-tube grid by the coupling condenser  $C$ , which coupling condenser permits the video signal appearing across the grid-leak  $R$  to swing around the average level of the particular video wave. The average level being such that the areas of the video wave on either side of the average level line are equal.

In Figure 1 a picture-tube  $i_{beam}-e_g$  characteristic is shown with two video signals applied to that characteristic. The signals are two horizontal lines with three blanking and synchronizing pulses. Considering only the video signal of a white picture, the picture-tube bias is adjusted so that the synchronizing pulses swing the picture-tube grid beyond beam current cut-off. The average level of the video signal centers about the bias and the picture portion of the video signal is near the zero-bias end of the characteristic. With this adjustment of bias, the video signal of a white picture produces a picture-tube beam current as shown on the diagram.

It is to be noted that the picture-tube beam current is at cut-off during the blanking-pulse interval and that maximum beam current occurs during the picture portion of the wave producing a white picture.

With the same bias adjustment as that for the white-picture signal, consider the reproduction of a picture that is predominantly black. As with the white-picture signal, the average level of the black-picture signal will center on the bias. The picture-tube beam current produced by the black-picture signal is shown on Figure 1 and it is to be noted that the beam current is not at cut-off during the blanking interval. This permits the scanning retrace to be visible. The picture portion of this signal represented a black picture, nevertheless the beam current produced by this signal during the picture portion of the wave is nearly as great as that produced by the previously considered white picture. It is seen that the fixed-bias operation of the picture tube is not satisfactory due to loss in contrast and to the visible presence of retrace lines on certain types of pictures. For satisfactory operation, the black level of the various video signals must be maintained at picture-tube beam current cut-off. Several methods for fixing the black level will be discussed.

#### DIRECT COUPLING

The National Television System Committee recommended type of television transmission is one in which a decrease in initial light intensity causes an increase in radiated power and the black level is

represented by a definite carrier level, independent of light and shade in the picture. By using direct coupling between the second detector and the picture-tube grid, the black level is retained and is at a fixed point on the picture-tube grid characteristic.

A circuit for direct coupling between the second detector and the kinescope is shown in Figure 2. The two section  $L-C$  filter between the diode detector and the load  $R_L$  is the conventional type of diode filter. This circuit is impractical in that high-output voltage would be

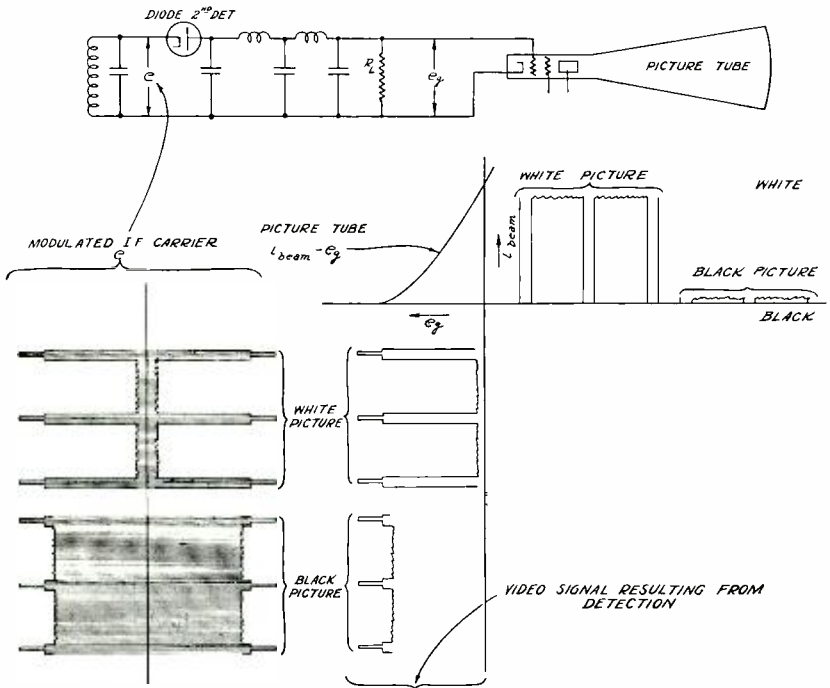


Fig. 2

required from the second detector. In a practical application of direct coupling an amplifier stage would be interposed between the second detector and the picture tube. Such an amplifier stage would require direct coupling at both input and output ends.

The modulated i-f carrier that is applied to the diode second detector is shown at "e" for two different picture signals, white and black. The video signal resulting from detection is shown applied to the picture-tube  $i_{b, cam} - e_g$  characteristic.

The detected video signal will produce a satisfactory picture because the black level of the two video signals are at the same level and may

be adjusted to fall at picture-tube beam current cut-off. The beam current produced by these two video-signal voltages is shown, and is seen to produce beam current of approximately correct contrast if the picture-tube characteristic is reasonably linear, and to cut the beam current off during the blanking pulse interval.

One of the disadvantages of this method of operation is that when the signal is removed the picture-tube screen becomes white. This is due to the fact that with no signal the picture tube is operating at zero bias, hence at maximum beam current, which may result in damaging the picture tube.

The second major disadvantage of this system lies in the action of the contrast control. Assume, for instance, that the contrast control varies the magnitude of the modulated i-f carrier. As the carrier amplitude is increased the detector-video output will also be increased. However, the white portion of the picture is at or near zero output of the detector, so that by increasing the output of the detector the white level remains approximately fixed while the grey and black portions of the picture get blacker. This is a direct opposite to normal operation.

The addition of one or more direct-coupled amplifier stages between the second detector and the picture-tube grid does not change the mode of operation of this system as regards the zero-bias condition or action of the contrast control.

This system will perform creditably if the transmission polarity is positive with the d-c component of the video signal transmitted, as in this type of transmission the black level is at minimum-carrier amplitude while white level is at maximum-carrier amplitude so the picture tube is operated with a fixed negative grid bias. As the picture signal is applied to the picture-tube grid the fixed negative bias is decreased in accordance with the amplitude of the applied signal.

#### DIODE AUTOMATIC BRIGHTNESS CONTROL

The use of a diode rectifier to bias the picture-tube grid in accordance with the video-picture signal appearing at the picture-tube grid is a method of operation with several advantages.

The circuit for this arrangement is shown in Figure 3. The video signal is coupled to the picture-tube grid by means of the coupling-condenser  $C$ . The picture-tube bias is due to a fixed-bias  $E$  and the bias developed by the diode rectifier.

The picture tube  $i_{beam}-e_g$  characteristic is shown in Figure 3 along with a diode characteristic. The diode characteristic is that of a diode as connected in the circuit and is displaced from the zero axis due to the bias  $E_{bias}$ .

Consider the application of a video signal of a white picture to

this circuit. The bias  $E$  is adjusted to be greater than the bias necessary for picture-tube beam-current cut-off. The average level (dotted line) of this video signal would center on the bias  $E$  were it not for the action of the diode which creates a bias  $i_d R$  nearly equal to the peak amplitude of the video signal in the negative direction. This action places the video wave as shown on the diagram with the negative peaks of the synchronizing pulses just drawing diode current. The beam current produced by this white-picture signal is shown with the picture

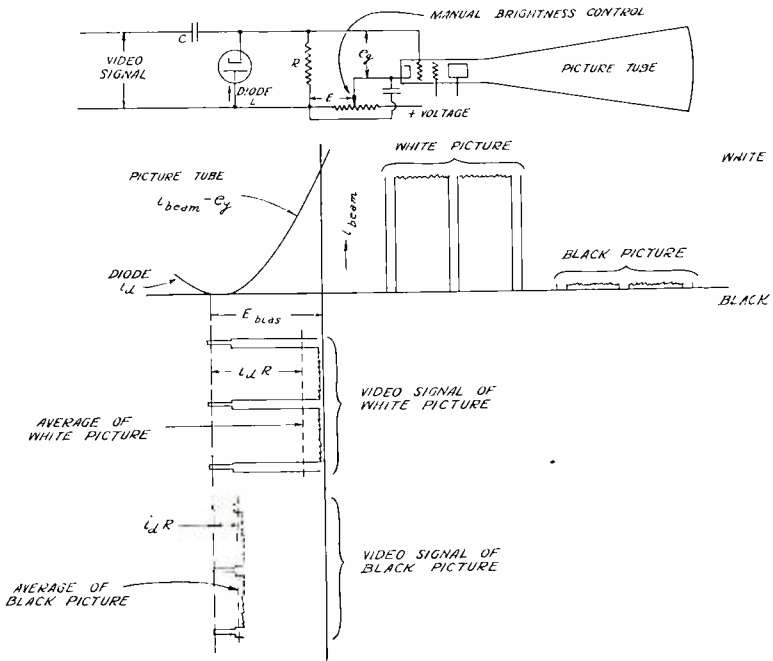


Fig. 3

portion of the wave near maximum beam current and the beam-current cut-off during the blanking-pulse interval.

With the same bias adjustment a video signal of a black picture may be applied to the circuit, again the tips of the synchronizing pulses draw diode current, but in a lesser amount than in the case of the white picture, producing a positive bias proportional to the negative-peak amplitude of the wave. The position of the black-picture wave will be as shown in Figure 3, and will produce a beam-current wave as shown, with the picture portion of the wave near black level and with the beam-current cutoff during the blanking pulse.

If the video signal is completely removed from this circuit, the bias on the kinescope will be  $E$  volts, which will cut the beam current off.

A second advantage of this circuit lies in the fact that the black level is always at a fixed point, even when the magnitude of the input-video signal is varied, so that increasing the contrast increases the brightness of the highlights.

The use of a diode as a d-c reinserter has the further advantage that with normal values of diode-leak resistance the bias developed by rectification is a linear function of the peak amplitude of the applied video signal.

#### BIAS DEVELOPED

It was pointed out above that the bias developed by the diode rectifier would be nearly equal to the peak amplitude of the wave in the negative direction. The exact amount of bias developed is dependent upon several circuit constants and may be most readily appreciated by reference to Figure 4. The circuit shown is that of the video-output stage producing a voltage " $e$ " with an equivalent internal-impedance  $R_c$ , driving the conventional diode through the coupling-network  $R_d-C$ .  $R$  is the internal resistance of the diode during the time that it is conducting. For the type 6H6 diode one plate-cathode will have a resistance of approximately 4000 ohms. During the non-conducting interval the value of  $R$  will approach infinity.

The wave shown in Figure 4 is a typical video wave representing two horizontal lines with three blanking and synchronizing pulses. The tip of the synchronizing pulse is assumed to occupy 7 per cent of the time of one complete line. The percentage indicated in Figure 4 is 8 per cent. This increase is due to the addition of six vertical pulses that occur at field frequency. In a system using 441 lines at 30 frames, the line frequency is 13,230 cycles per second which is 75.5 microseconds for one complete line. If the diode is to charge the condenser  $C$  during the time of one synchronizing pulse, the time of charge will be 8 per cent of 75.5 microseconds or 6 microseconds, while the time that the condenser discharges will be the remainder or 69.5 microseconds.

On the wave shown in Figure 4 the voltages indicated  $e_c$  and  $e_d$  represent, respectively, the voltage that contributes to charging the condenser  $C$ , and the voltage that appears across  $C$  in the form of the bias developed.

If steady-state conditions are to prevail, the quantity of electricity on charging the condenser  $C$  must equal the quantity on discharge. From this, the ratio of  $e_c$  to  $e_d$  may be determined.

In a device of his kind, if the magnitude of the time constants on charge and discharge are known to a fair degree of accuracy, the evaluation of the ratio of  $e_c$  to  $e_d$  may be readily accomplished.

If  $C(R_d + R_c)$  is of the order of 0.1 second it is very large compared to the time of discharge of the signal wave, which is 69.5 microseconds, the discharge current then may be assumed to be constant and equal to

$$\frac{e_d}{(R_d + R_c)}$$

If  $C(R_c + R)$  is of the order of 700 microseconds it is very large compared to the time of charge of the signal wave which is 6 micro-

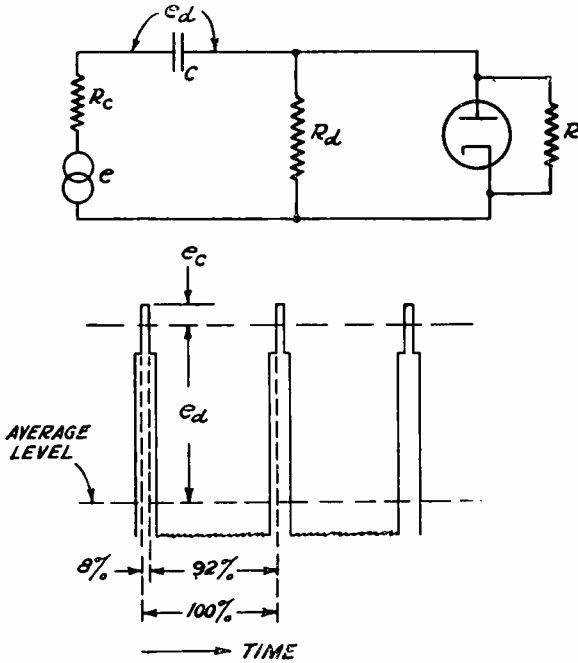


Fig. 4

seconds, and the charge current may be assumed to be constant also and equal to  $\frac{e_c}{(R_c + R)}$ .

As stated before, for steady-state conditions to prevail the quantities of electricity on charge and discharge must be equal.

The quantity of electricity  $Q$  is equal to:

$$Q = \int i dt$$

however in the case at hand the current "i" is constant so,

$$Q = i \int dt = it$$

Therefore, since the charge occupies 8 per cent of the time, and discharge 92 per cent of the time,

$$i_d \times 0.92 = i_c \times 0.08$$

where,

$$i_d = \frac{e_d}{(R_d + R_c)} \quad \text{and} \quad i_c = \frac{e_c}{(R_c + R)}$$

$$\frac{e_d}{R_d + R_c} \times 0.92 = \frac{e_c}{R_c + R} \times 0.08$$

$$\frac{e_d}{e_c} = \frac{8}{92} \times \frac{R_d + R_c}{R_c + R}$$

Previously in this discussion time constants of charge and discharge were assumed, these time constants result if the following circuit constants are chosen:

$$\begin{aligned} R_d &= 1,000,000 \text{ ohms} \\ R_c &= 3000 \text{ " "} \\ R &= 4000 \text{ " "} \\ C &= 0.1 \mu\text{f.} \end{aligned}$$

With these values of resistance the actual ratio of  $e_d$  to  $e_c$  may be calculated and equals

$$\frac{e_d}{e_c} = 12.5$$

Referring again to Figure 4 it is seen that the sum of  $e_d$  and  $e_c$  is equal to the peak amplitude of the video wave in the direction of the synchronizing pulses. From this the bias  $e_d$  may be determined in terms of the peak amplitude and is in this case 92.6 per cent of the peak amplitude.

The wave appearing in Figure 4 is that of a white picture; however, the above method of determination of bias as a function of peak amplitude applies equally well to a video signal of a black picture. A white picture might for instance have a peak amplitude of 30 volts which would produce 27.8 volts of bias, while a black picture might have a peak amplitude of 8 volts producing a bias of 7.4 volts.

#### GRID RECTIFICATION AS AUTOMATIC BRIGHTNESS CONTROL

Another satisfactory method of automatic brightness control is by the use of the circuit of Figure 5 wherein the last video amplifier tube "T" is biased by grid current and the picture-tube grid is directly connected to the video-amplifier-tube plate.

The video signal is coupled to the grid circuit of the amplifier tube by means of the coupling condenser  $C$ . The  $i_p-e_g$  characteristic of this tube is shown in Figure 5 along with the  $i_g-e_g$  characteristic of the kinescope.

The video signals appearing in the grid circuit of this tube produce grid current and bias in proportion to the peak amplitude of the video signal in the positive direction. The two video signals of a white-and-black picture illustrated in Figure 5 will assume their respective positions as shown due to grid rectification. It is seen that this method of bias fixes the black level of the picture signal at the

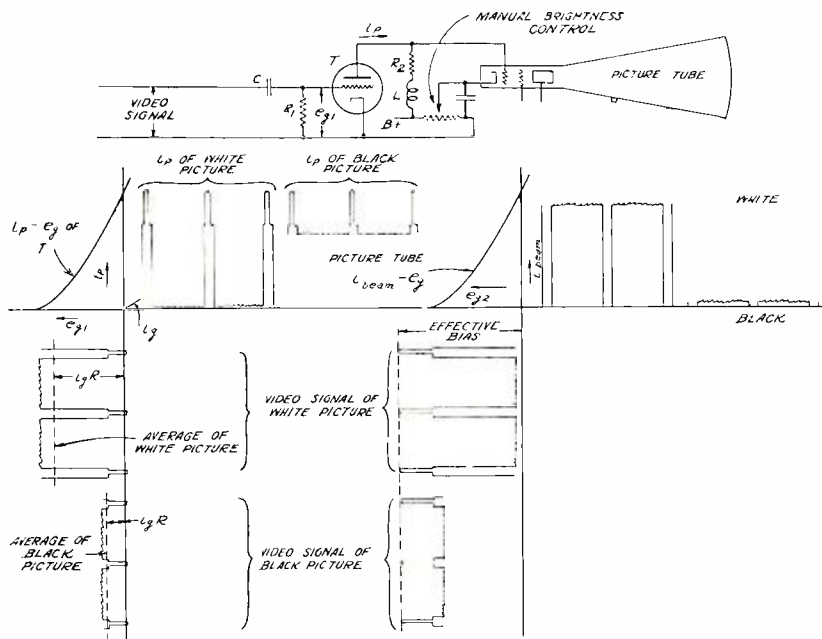


Fig. 5

amplifier-tube plate so that the tips of the synchronizing pulses just draw grid current. The actual amount of bias developed may be determined in the manner described in the previous section.

The amplifier-tube plate current produced by these two signals is as shown, which in turn produces the picture-tube grid voltage by flowing through the plate load  $R_2$  and  $L$ .

The manual-brightness control permits adjustment of the picture-tube grid bias. The bias of the picture-tube grid is due to two voltages acting in opposition—that due to the  $IR$  drop in  $R_2$  due to d-c plate current, and that between  $B+$  and the arm of the manual-brightness control. The manual-brightness control is adjusted so that the "effective bias" as indicated on the picture-tube  $i_{beam}-e_g$  characteristic of

Figure 5 is obtained with no signal applied to the amplifier tube "T". As signal is applied to the grid of "T" the picture-tube operating bias is reduced in proportion to the peak amplitude of the video signal in the negative direction due to decreased plate current flowing through  $R_p$ .

The beam currents resulting from the application of video-signal waves of white-and-black pictures are shown; the white-picture signal produces maximum-beam current, while the black-picture signal produces minimum-beam current and in both cases the picture-tube beam current is at cut-off during the blanking-pulse interval.

If the video signal is removed from the amplifier-input circuit the picture tube is biased beyond cut-off; further, as the signal amplitude is increased (increase of contrast) the picture highlights become brighter in the correct manner.

For the circuit of Figure 5 the video-output tube "T" will be a pentode or beam-power tube which necessitates screen voltage for that tube. A precaution is necessary in obtaining that screen voltage if normal operation of the automatic-brightness control system is to result. The screen voltage should be obtained from a bleeder that draws 3 to 4 times the current drawn by the screen.

The circuit of Figure 6 is that of the grid type of automatic-brightness-control system employing a pentode-amplifier tube "T". The tube "T" obtains screen voltage by means of a screen-dropping resistor  $R_s$ . This circuit, though not practical, is useful in indicating the need for a stiff screen voltage-supply source.

In the diagram of Figure 6 is shown the  $i_p-e_g$  characteristic of the amplifier-tube "T" with three different magnitudes of video signal applied to the grid. The three signals represent, as indicated, a black, grey, and white picture respectively. These three signals produce bias-voltages  $B$ ,  $G$ , and  $W$  in proportion to the peak amplitude of the respective signals.

As the bias voltage is increased from zero, the screen current decreases so that the screen-operating voltage rises, with the result that for any particular bias condition the plate current available over the cycle of grid swing will be greater than in the case of fixed screen voltage. This is shown graphically by the three dotted  $i_p-e_g$  characteristics labeled  $B'$ ,  $G'$ , and  $W'$ .

Considering again the three video waves of black, grey, and white pictures, the plate-current wave of each has a different  $i_p-e_g$  characteristic. For the black-picture wave the  $B'$  characteristic obtains, for the grey-picture wave the  $G'$  characteristic obtains, and for the white-picture wave the  $W'$  characteristic obtains. The black-level plate-current wave for each of the three waves is indicated as  $B''$ ,  $G''$ , and  $W''$ . It is evident that even though the black levels of the various picture

signals are fixed in the grid circuit of tube "T" they are not at the same level in the plate circuit. If the screen of the amplifier-tube "T" had been operated from a fixed-voltage source the plate current corresponding to black level for the three signal waves would be the same, and at point "A". In practice it has been found satisfactory to operate the screen from a bleeder that draws three to four times the current drawn by the screen.

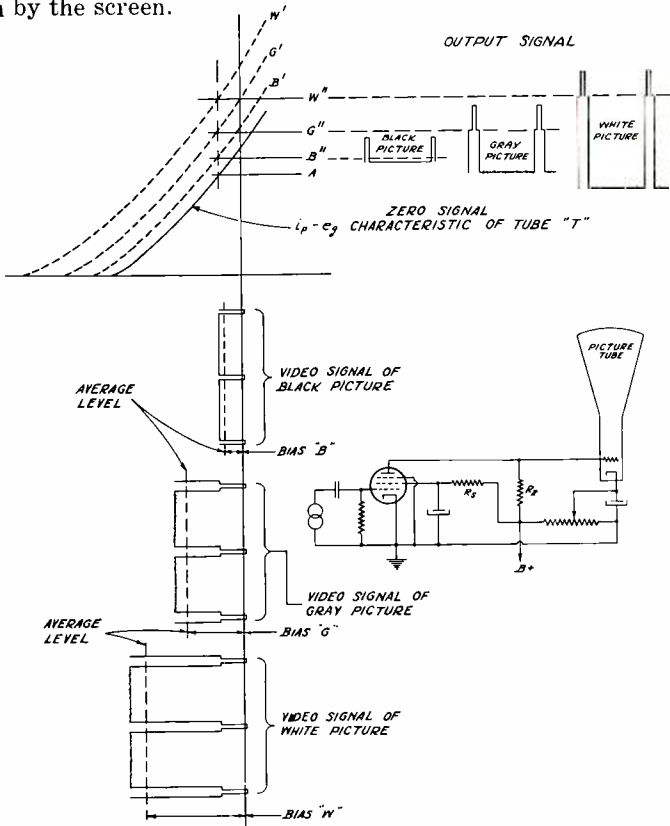


Fig. 6

Reinserting the d-c component of the video signal by grid rectification in the last video amplifier tube when a stiff screen source is used appears to perform creditably, however it has several disadvantages when compared to the diode d-c reinsertor.

When operating a tube at zero bias, such as is the case with grid-type d-c reinsertion, it is necessary to lower the screen voltage to limit the plate current with no signal input to a value such that the plate dissipation of the particular tube is not exceeded. This results in reducing the maximum output to 0.4-0.5 of that obtained with normal bias operation.

Grid reinsertion of the d.c. is usually not as linear as that obtained when a diode is used. However, the non-linearity is determined by the amplifier tube used and certain tube types may be entirely satisfactory.

The major disadvantage of this type of d-c reinsertor lies in the fact that during the warm-up period of the receiver the picture-tube grid is positive relative to the cathode. Present types of picture tubes and high-voltage rectifiers have a short warm-up time as do many of the common filament-type low-voltage rectifiers. As was stated before, the effective picture-tube bias in the circuit of Figure 5 is due to two voltages; the  $IR$  drop in  $R_2$  and the voltage between  $B+$  and the arm of the manual-brightness control. During the warm-up period tube "T" will not start drawing plate current at the instant the  $B+$  voltage is first available, which effectively returns the picture-tube grid to  $B+$  with the cathode at a lower potential. The picture-tube heater and high-voltage power-supply warm-up time is approximately equal to the low-voltage power supply which results in the picture tube operating with full voltage on the electron-gun elements and a positive potential on the grid.

The condition of positive grid during warm-up may be remedied by several expedients. A heater-type low-voltage rectifier may be used which will eliminate the positive grid during warm-up, but will permit the picture tube to operate at zero bias.

A time-delay relay might be used in series with the picture-tube heater supply so that the picture-tube heater starts warm-up after the remaining tubes in the receiver are operating properly.

The warm-up time of the picture-tube heater may be delayed by the addition of a resistance in series with the heater. The picture-tube heater has a positive-temperature coefficient of resistance so that high current is drawn at the start of warm-up. The series resistance limits the initial current and, hence, prolongs the warm-up time. The heater-transformer voltage will have to be increased to compensate for the voltage drop in the series resistance. This system has the disadvantage of impairing the regulation of the heater circuit.

With the diode type of d-c inserter the grid of the picture tube is always negative even during the warm-up period so that the above precautions are not ordinarily necessary for that circuit.

#### REINSERTION OF LOW FREQUENCIES BY AUTOMATIC-BRIGHTNESS CONTROL ACTION

Reinsertion of the direct-current component in a video signal to secure automatic brightness control may also restore low frequencies to a certain degree.

The manner in which the low frequencies are reinserted is illus-

trated in Figure 7. The circuit is that of a d-c reinsertor by grid rectification; however the diode type of d-c reinsertor performs in much the same manner in restoration of low frequencies.

The common cause for poor low-frequency transmission in a video amplifier is due to small interstage-coupling capacitors and low values of grid leaks or insufficient cathode-resistor by-passing.

The video-signal wave represented in Figure 7 is a full frame of a picture that is half black and half white. The number of horizontal blanking and synchronizing pulses per frame have been reduced from the standard for the purpose of clarity in drawing and the vertical

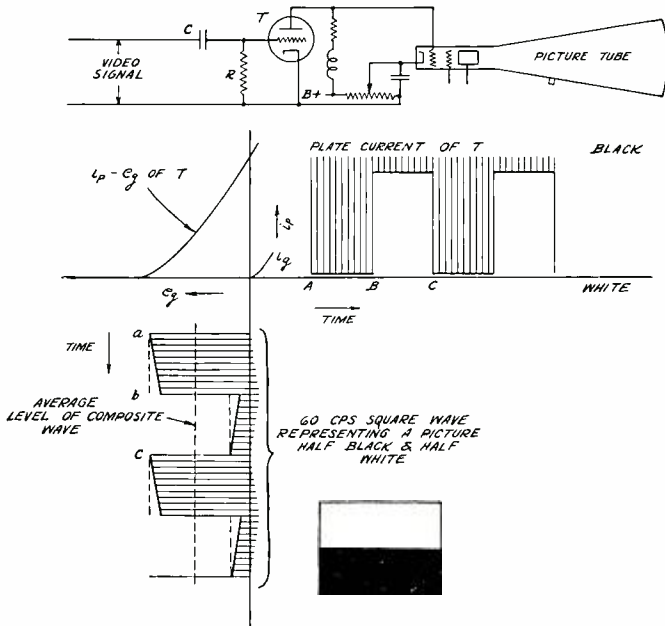


Fig. 7

synchronizing information normally present in this wave has been completely eliminated for the same reason.

The normal video wave of a picture half black and half white would be a perfect square wave of 60-cycle repetition rate. The wave shown in Figure 7 has been amplified by a video-amplifier stage that did not have perfect transmission of the low frequencies. This is evidenced by the droop of the signal wave of Figure 7. The loss in low-frequency response that this wave has suffered will be restored by the action of the automatic-brightness-control system.

Time in the diagram starts at "a". The super-sync pulse at "a" will adjust on the grid characteristic so that the tip of the pulse just draws grid current. Due to the loss in low-frequency response the

super-sync pulses that occur between "a" and "b" will progressively go further into grid current, hence produce a progressively increasing bias. The bias increases so that the tip of each super-sync pulse in the portion of the wave between "a" and "b" just draws grid current, which has the effect of restoring the low-frequency loss. The plate-current wave produced is shown and is a square wave.

The restoration of the low-frequency loss in the portion of the grid-voltage wave between "b" and "c" depends upon a factor not previously considered.

At the time when the super-sync pulse at "b" reaches the grid, the bias voltage (by the action described above) is great enough so that the super-sync pulse at *b* just draws grid current. Consider now the portion of the wave between "b" and "c". This portion of the wave slopes away from the zero-bias axis which requires that the bias progressively decrease in a discrete manner during the time interval "b" to "c" if the low frequencies are to be properly reinserted.

If the time constant  $RC$  of Figure 7 be made equal to the equivalent time constant that caused the droop in the square wave, then the bias voltage will decay at a rate equal to the slope of the signal-voltage wave. This will place the tip of each of the super-sync pulses in the "a"-*c* interval at the point of drawing grid current. The resulting plate-current wave is shown for the entire grid-voltage wave and is a perfect square wave.

If the time constant  $RC$  is less than the equivalent time constant which caused the droop, but still large compared to  $1/13230$  sec., the bias voltage could decay at a faster rate than is actually required, but it can not do so because this would cause the super-sync pulses to extend beyond zero bias so that each pulse in the "b"-*c* portion of the signal wave draws grid current and the wave is straightened in the same manner as the "a"-*b* portion of the wave.

If the time constant of  $RC$  is appreciably larger than that causing the drop, the d-c reinsertor will not restore the low frequencies and will result in poor reproduction of the picture.

There is one additional factor to consider in fixing the value of the time-constant  $RC$  and this is due to change in picture background. The time-constant  $RC$  should be short compared to the most rapid background change, which might be of the order of ten seconds. A value of  $RC$  of 0.1 sec. has been found satisfactory in practice.

The action of automatic brightness control should not be relied upon to reinsert large losses of low frequencies. If the losses of low frequencies are large, the droop of the square wave is no longer linear, but may vary in a number of ways depending upon the number of low-frequency loss circuits and upon the relative loss in each circuit, it is

therefore impossible to correctly compensate the low-frequency loss in this case by means of automatic-background-control action, because the  $RC$  time constant of the automatic-brightness-control circuit permits the bias to decay only in an exponential manner. However, the decay is practically linear if the  $RC$  time constant is large compared to the time duration of the lowest-frequency wave to be faithfully transmitted, as is the case having characteristics shown in Figure 7.

### OUTPUT TUBES

The general requirements for video-output tubes have been outlined above. Three of the tubes currently available have characteristics suitable for such use. These are the 6AC7, the 6AG7, and the 6V6. The table below shows typical operating conditions with bias supply. The permissible load resistor for a given bandwidth varies inversely as the output capacitance, so that the gain is a function of  $G_m/C_{out}$  and the maximum output is a function of  $I_p/C_{out}$ . From this table it may be seen that the 6V6 has the greatest output, but the 6AC7 has the greatest sensitivity.

TABLE I—TYPICAL OPERATION

<i>Tube</i>	<i>6AC7</i>	<i>6AG7</i>	<i>6V6</i>	
<i>E</i> plate	250	250	250	volts
<i>E</i> screen	150	140	250	volts
<i>E</i> bias	2.0	2.0	12.5	volts
$I_p$	10	33	45	ma.
$G_m$	9000	10200	4100	$\mu\text{mhos}$
$C_{out}$	5	12*	12	$\mu\mu\text{f}$
$G_m/C_{out}$	1800	850	340	$\mu\text{mhos}/\mu\mu\text{f}$
$I_p/C_{out}$	2.0	2.75	3.75	ma/ $\mu\mu\text{f}$

\* The output capacitance of the 6AG7 tube has now been reduced to 7.0  $\mu\mu\text{f}$  in place of 12  $\mu\mu\text{f}$  shown in the table. This reduction in output capacitance correspondingly increases the realizable output and gain and permits the use of this tube in types of circuits not previously suitable.

The input capacitance does not directly affect the operation as a video amplifier, but it does influence the permissible load on the preceding stage and thus the overall video gain. In addition the plate and screen-current requirements must be considered, the 6AC7 being most economical in that respect.

### BIAS SUPPLY

The foregoing section was based on ideal bias supply. In practice the bias may be "fixed", self-bias, or grid-current bias. In the case of fixed bias, the d-c grid potential is usually obtained by the drop across

a resistance in the negative end of the power supply. Bypassing this type of bias supply is not a serious problem because a resistance-capacitance filter may be used. However, tubes operating at or near maximum rating, as do video-output tubes, are more susceptible to grid-emission difficulties and premature failure under fixed than under self-bias condition, and fixed bias is more subject to voltage-supply regulation troubles, so self-bias is to be preferred.

The use of self-bias by means of a cathode resistor results in bypass problems because of the low-resistance value necessary for securing the proper bias. The use of low-frequency compensation in the plate circuit may not be as desirable a solution in this case as is the use of a large bypass or no bypass. If degeneration at frequencies down to 60 cycles is to be avoided capacitances of the order of 200 to 1000  $\mu\text{f}$  are required. With no bypass whatsoever there is no frequency discrimination, but the effective transconductance is reduced by the factor

$$G'_m = \frac{G_m}{1 + G_m R}$$

Where  $G'_m$  is effective transconductance,  $G_m$  is transconductance under d-c voltage conditions obtaining,  $R$  is cathode-resistance value. It can be seen that this degeneration may cause a loss of the order of two to one in sensitivity. Where this loss in sensitivity can be tolerated the unbypassed cathode resistor may be used for bias supply.

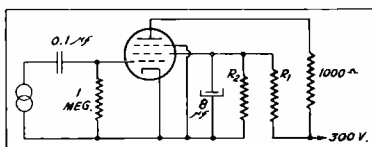
It has been pointed out under the section on d-c reinsertion that the operating bias for the video-output tube may be obtained by grid-current flow through a relatively high value of grid resistor. This method of securing bias may be used whether or not it is depended upon for d-c restoration. It has a satisfactory frequency characteristic, but does result in limitation of maximum output since the plate current can swing only towards cut-off and the maximum plate current at zero signal is limited by the safe plate dissipation of the tube used. The maximum plate current under no-signal input conditions may be held to a safe value by proper choice of screen potential.

The transconductance of a tube operating in this manner is not a constant, since the operating bias is a function of signal amplitude on the grid. The effective transconductance is therefore best given in the form of a curve of output versus input. A series of such curves for the three tube types considered is shown in Figure 8.

This series of curves is plotted with peak-to-peak output volts per 1000 ohms load resistance, against input in peak-to-peak volts. The operating and circuit conditions under which these curves were obtained are shown on the figure. The screen-bleeder values given provide

adequate stabilization of screen voltage so that the data may be used in evaluation of operation for d-c reinsertion by grid current.

The 6V6 is seen to have the highest output, but also requires the largest input and is not linear over any appreciable range. The 6AG7 has good transconductance and high output and is very nearly linear up to 2.5 volts input.



TUBE	$I_{p0}$	$I_{sc0}$	$R_1$	$R_2$	$E_{sc}$
6AC7	10ma	2.5ma	18 K $\Omega$	7.7K $\Omega$	77 V.
6AG7	30	6.4	6.4 K	3.7 K	95
6V6	45	2.8	13 K	10.7	120

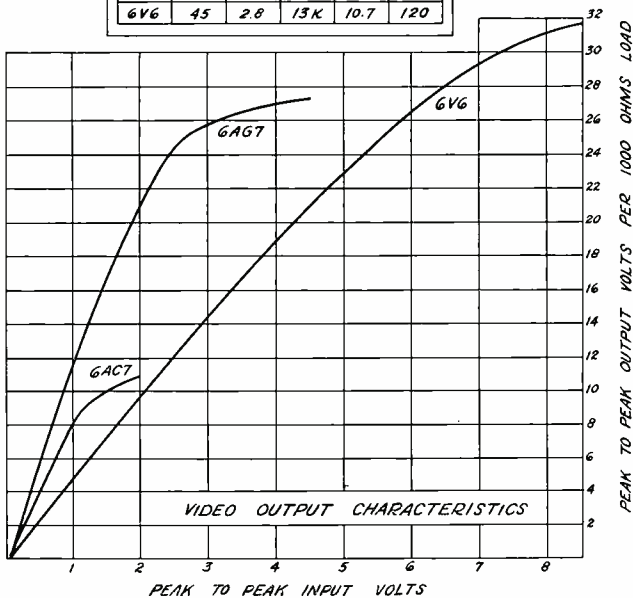


Fig. 8

The 6AC7 does not have as high transconductance, and does have materially less output voltage. It should be remembered, however, that the gain is dependent upon permissible load resistor as well as  $G_m$ , so that the performance of the 6AC7 is considerably better by comparison than would be indicated from Figure 8 because of its low-output capacitance.

In order to decide which of the three tube types considered should be employed in a given design, we must know the value of load resistor, and in order to determine the permissible-load resistor the influence

of various types of circuit must be taken into account. We shall accordingly consider circuits for these three types of tubes with both grid-current d-c reinsertion and diode d-c reinsertion.

#### HIGH-FREQUENCY COMPENSATION

Circuits used for high-frequency compensation in video amplifiers have as their aim the elimination of the effect of inherent shunt capacitance on the high-frequency response. The circuit should result in as high a value of load resistor as possible over a given band width, since, as has been mentioned above, the gain and output are dependent on the load-resistor value. The circuit capacitances are principally those of the output capacitance of the video tube and the input capacitance of the picture tube. While the performance of some types of circuit depends upon the ratios of these capacitances as well as their sum, the total capacitance may be taken for general consideration of a performance index. With this qualification, the criterion of a video circuit is  $R\omega C$ . Here  $R$  is the load resistance,  $\omega$  is  $2\pi$  times the bandwidth over which uniform response is obtained, and  $C$  is the total circuit capacitance. This criterion is not an exact one, because, as mentioned above, some circuits depend upon the way in which the circuit capacitances may be physically separated as well as on the total capacitance and in addition the obtainable detail depends not only upon the frequency range over which the response is flat, but also upon how rapidly the response decreases outside that range. For example, if we were to observe a picture on two different video amplifiers each of which had a loss of 2 db in response at 3.5 Mc, but one of which had a 10 db loss in response at 3.6 Mc and the other had a 10 db loss at 4.0 Mc, the observable-picture detail would be greater in the case of the second amplifier.

However, it is necessary, in the case of television receivers, to take into account the overall passband, and the i-f response usually drops off more sharply above the nominal cut-off frequency than does the video response so that the advantage of a video amplifier with a gradual cut-off is largely nullified from an overall television-receiver standpoint. Consequently the uniform-response band width has been chosen as the criterion in this paper.

The networks are considered to be driven from a constant-current source, as only high-plate-impedance tubes have been discussed herein.

Several circuits have been employed to obtain uniform response over the relatively great bandwidths required for television. One method of approach to the problem has been through consideration of network theory to determine what values of  $L$ ,  $R$ , and  $C$  result in uniform response over the desired bandwidth, the other method of

approach has been through consideration of the properties of wave filters.

The consideration from the network-theory standpoint has led to evolution of circuits known as shunt peaking, series peaking, and combined series and shunt peaking. The derivation of the expressions

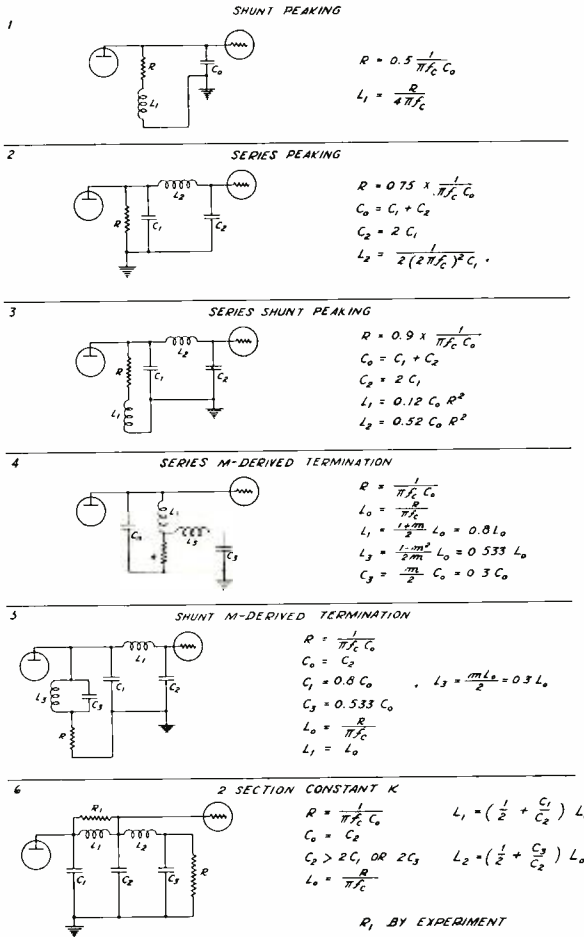


Fig. 9

applicable to these circuits has been given in detail in a previous issue<sup>1</sup> so will not be repeated. For the sake of completeness and for comparison with filter-type circuits the results of series and shunt-peaking circuits in the case of video-output circuits are considered here.

One requirement for all practical video circuits is that there be a capacitance across the points of application of voltage and a capacitance across the points at which the voltage is taken off. This require-

ment eliminates many circuits from consideration. There are six basic circuits which are to be considered; these six circuits and the design parameters are shown in Figure 9.

In that figure the d-c connections and any isolating condensers necessary are not shown. The capacitances shown are those of the input and output of the tubes. The load resistor is  $R$ , the maximum frequency of uniform response (cut-off frequency)  $f_c$ , and the nominal or determining value of capacitance  $C_p$ . The other circuit parameters are as designated on the respective diagrams.

### 1. SHUNT PEAKING

The shunt-peaking circuit is the simplest type as it uses only one inductance and does not depend upon any division of capacitance, all circuit capacitances being lumped together at one point. It has the lowest resultant load resistor of any of the circuits considered, but has the merit of permitting wide tolerances in value of circuit components with little change in performance, and has a gradual cut-off.

### 2. SERIES PEAKING

The series-peaking circuit divides the capacitance into two parts and hence permits the use of a 50 per cent higher load resistor for a given total capacitance and bandwidth than in the case of shunt peaking. Optimum results from this circuit, both as to load-resistance value and flatness of response, are obtained with a two-to-one ratio of capacitances. The method of treating the circuit when the ratio is other than two to one has been discussed by Seeley and Kimball.<sup>1</sup> The series-peaking circuit has a small number of components and permits of fairly wide tolerance of component values.

It is frequently possible to secure a higher value of load resistor than would be indicated by the design expressions for series peaking through use of a higher value of inductance. The use of this higher value of load resistance and inductance may necessitate the addition of a resistor of several thousand ohms across the inductance to secure sufficiently uniform response, but the high load-resistor value obtained is well worth while.

### 3. SERIES AND SHUNT PEAKING

The combination of series and shunt-peaking allows use of 80 per cent higher load resistance than shunt peaking, but is more critical as to component values and only allows use of maximum load-resistor value when the two-to-one capacitance ratio exists.

### 4. SERIES $m$ -DERIVED TERMINATION

In approaching video circuits from filter-theory standpoint, it is necessary to review some of the pertinent factors applying to electric-

wave filters. A number of technical articles and books have been written on the subject of wave filters and the terminology generally used therein will be followed.

In order to avoid reflections it is necessary that the filter be properly terminated and in order to join one filter section to another they must have the same image impedances. In Figure 10 are shown three half sections which may be joined together to produce a filter. There are two image impedances to consider, the mid-shunt image impedance  $Z'$  which occurs in the middle of the shunt arm, and the mid-series image impedance  $Z$ , which occurs at the middle of a series arm. We are here concerned only with low-pass filters, so that the mid-series image impedance occurs in the center of the filter inductance and the

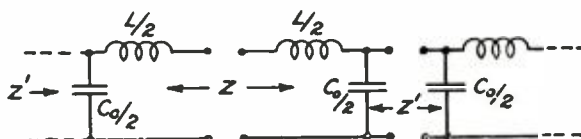


Fig. 10

mid-shunt image impedance across a filter capacitance. In video filters, experience has shown that it is readily possible to construct inductances in the form of single-layer solenoids or very narrow universal-type coils such that the  $Q$  is sufficiently high to make the dissipation effect negligible and the distributed capacitance of the coil low enough to be likewise negligible.

The mid-shunt and mid-series image impedances vary with frequency in an inverse manner. At zero frequency the image impedance of either type is  $R$ , the value of termination or effective-load resistance.

$$\text{Then } Z = R \sqrt{1 - \Delta^2}$$

$$Z' = \frac{R}{\sqrt{1 - \Delta^2}}$$

where  $Z$  is mid-series image impedance  
 $Z'$  is mid-shunt image impedance  
 $R$  is nominal or terminating resistance of the filter  
 $\Delta$  is  $f/f_c$   
 $f$  is any frequency lower than cut-off frequency  
 $f_c$  is cut-off frequency

These expressions show that the mid-series image impedance goes to zero at cut-off, whereas the mid-shunt image impedance rises to infinity.

In video amplifiers the voltage must be applied and taken off across a capacitance because of the inherent tube capacitance, which means

the voltage is taken off across a mid-shunt impedance. Now  $Z'$  rises toward infinity as cut-off is approached, but to obtain uniform voltage we should have uniform impedance. If we shunt a capacitance  $C_o/2$  across  $Z'$  this result is accomplished.

$$Z' = \frac{R}{\sqrt{1 - \Delta^2}}$$

$$X_c \text{ of shunt capacitance} = \frac{-j}{2\pi f C_o/2}$$

But by filter theory

$$R = \frac{1}{\pi f_c C_o}$$

$$\text{so } X_c = \frac{-jR}{\Delta}$$

Then  $X_c$  and  $Z'$  in parallel =  $Z''$

$$Z'' = \frac{X_c Z'}{X_c + Z'} = \frac{-jR^2}{\Delta R - jR \sqrt{1 - \Delta^2}}$$

rationalizing

$$Z'' = R(\sqrt{1 - \Delta^2} - j\Delta)$$

The absolute impedance is then

$$Z'' = R(1 - \Delta^2 + \Delta^2)^{1/2} = R$$

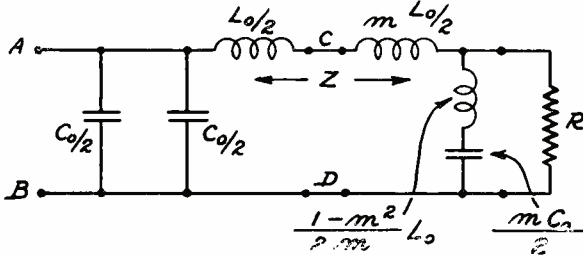


Fig. 11

so that the combination of a mid-shunt image impedance and a capacitance equal to the terminating capacitance will produce uniform impedance. It is also necessary to obtain a constant impedance equal to  $R$  in order to terminate the filter in  $R$ . This termination may be accomplished by the use of  $m$ -derived sections, specifically by terminating half-sections with an  $m$  value of 0.55 or 0.6, since such a half-section has the proper image impedance of one end to match that of a normal or constant- $K$  filter section and on the other end has an image impedance which is a pure resistance up to 80-90 per cent of the cut-off frequency. Series  $m$ -derived sections have an image impedance the

same as the mid-series impedance of a constant- $k$  section on one end and uniform impedance on the other end.

Such a terminating half-section is shown to the right of points  $C-D$  in Figure 11. To the left of  $C-D$  is a constant- $k$  half-section with added capacitance  $C_o/2$  shunted across the terminals so that the impedance across points  $A-B$  is uniform with frequency.

This type of filter permits use of twice the load impedance of the shunt-peaking circuit and does not depend upon any division of capacitance. Since the series  $m$ -derived filters require very close tolerances of components, including allowance for distributed capacitance, this circuit is critical and would probably require a small adjustable trimmer to provide for production variation.

#### 5. SHUNT $m$ -DERIVED TERMINATION

The same general principles discussed for series  $m$ -derived termination apply in the case of the shunt  $m$ -derived type, namely an  $m$  of 0.6 to secure a half-section having uniform resistance termination on one end and mid-shunt image impedance on the other end. The shunt  $m$ -derived-type filter is quite versatile, a wide range of capacitance distribution can be handled and maximum load of twice that of the shunt-peaking circuit achieved. Experience has shown that this circuit is somewhat less critical to changes in component values than is the series  $m$ -derived type, but correct evaluation of distributed circuit capacitances is required in calculating component values and an adjustable trimmer will probably be required across  $C_1$ , in this circuit. Both the series  $m$ -derived and shunt  $m$ -derived filters have sharper cut-off than other type circuits, because the 0.6  $m$  section provides a frequency of infinite attenuation 25 per cent beyond the cut-off frequency. For this reason it is desirable to assume a cut-off frequency 10 to 15 per cent higher than the desired upper frequency of uniform response in making calculations on  $m$ -derived filters.

In filters with sharp cut-off, such as the  $m$ -derived type, experience has indicated that reflection transients may be introduced into the picture by misadjustment so small that the steady-state response appears uniform and the steady-state phase shift linear. It is therefore suggested that final adjustment of these types of filters be made by observation of a test pattern.

#### 6. TWO-SECTION CONSTANT $K$

In addition to  $m$ -derived terminating sections, it is frequently possible to use two constant- $k$  filter sections to secure flat response and a load resistor of twice the value obtainable with shunt peaking. Filter sections may be joined together if they have the same image impedance

although the cut-off frequency differs. If a section with higher cut-off frequency is joined to one of lower cut-off frequency, the impedance rise of the section of higher cut-off near cut-off frequency will not affect the uniformity of response materially because it is beyond the useful range of the filter as a whole.

If the capacitances can be so divided that those on the end are less than half the value of the center capacitance satisfactorily uniform response may be secured.

In Figure 12 is shown the manner in which such a filter is constituted. The load resistor depends upon the value of  $C_2$ . The section between  $A$  and  $B$  is a full constant- $K$  section with mid-series impedance at  $A$  and  $B$  to join to the terminating half-sections. The inductances of this section are of course each half the value of those calculated for the full section. The image impedance of the end sections must be the same as that of the center section, but the cut-off is determined by the value of  $C_3$  or  $C_1$ . Since  $C_1$  and  $C_3$  are on the ends of the filter they have half the value of a constant- $K$  full-section capacitance. The load  $R$  prevents the impedance at that end of the filter from rising near

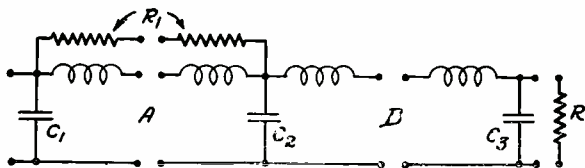


Fig. 12

cut-off of that section, but to prevent the impedance from rising near cut-off on the opposite end of the filter it is usually necessary to add dissipation by shunting a resistor  $R_1$  across the inductance on that end of the filter. The filter is then seen to be made up of a full  $T$  section in the center joined to a half-section on each end of the same image impedance, but with cut-off determined by the existing capacitance.

This type of filter has high-load impedance and is less critical than those discussed in sections 3, 4, and 5 above, but depends upon a favorable disposition of capacitance for optimum results.

#### PRACTICAL OUTPUT CIRCUIT CONSIDERATIONS

The several factors that affect the design of a video-output stage have been discussed in the preceding sections. This section is devoted to a practical application of these design considerations.

From a practical point of view, the factors that lead to the choice of the output system are: picture-tube characteristics, video band width, type of d-c inserter, gain and output required.

TABLE 2—PERFORMANCE OF SEVERAL OUTPUT SYSTEMS

Case	Video Tube	Picture Tube	Type of DC Insertion	$C_p$ $\mu\mu f$	$C_g$ $\mu\mu f$	$C_d$ $\mu\mu f$	$f_c$ Mc	Circuit	R ohms	Max. Peak to Peak Voltage Output	Gain
1	6AC7	1802	Grid	7	16		2.5	2	5500	55	40.7
2	6AC7	1804	Grid	7	20		3.8	6	3300	38	28.1
3	6AG7	1802	Grid	14	16		2.5	1	2120	53	20.9
4	6AG7	1804	Grid	14	20		3.8	4	2230	56	22.0
5	6AC7	1802	Diode	7	16	7	2.5	6	6650	166	60.0
6	6AC7	1804	Diode	7	20	7	3.8	5 or 6	3800	95	34.2
7	6AG7	1802	Diode	14	16	7	2.5	3	2730	180	27.9
8	6AG7	1804	Diode	14	20	7	3.8	5	2880	190	29.4

It is impossible to cover all combinations of output circuits, but eight cases are listed in Table 2 for illustrative purposes and it is believed will assist in making the choice of output tube and associated circuit in any particular design.

Two picture-tube types are considered, the 5BP4/1802-P4 and 9AP4/1804-P4. The type 9AP4/1804 has the same input capacitance as the types 1801, 12AP4/1803-P4, and 5AP4/1805-P4 so that as far as the video-output system is concerned they may be interchanged.

The three capacitances tabulated in Table 2,  $C_p$ ,  $C_g$  and  $C_d$ , have the following physical significance:  $C_p$  represents the output capacitance of the video-amplifier tube in the socket plus the capacitance added by the wiring.  $C_g$  represents the input capacitance of the picture tube plus wiring and socket capacitance, the wiring capacitance being perhaps higher than will be encountered in some instances, but is believed to be an average realizable condition.  $C_d$  is the capacitance added to the circuit by the diode-type d-c reinsertor which in this case was one plate-cathode of the type 6H6 plus the capacitance-to-ground of a 0.1- $\mu f$  coupling condenser and a one-megohm resistor.

The band width tabulated as  $f_c$  is the top-video frequency that is to be transmitted with no loss in fidelity. It is to be noted that only two different band widths are used namely 2.5 Mc and 3.8 Mc. The 2.5-Mc bandwidth condition is used in connection with the type 1802 picture tube because the size of the picture with this tube limits the amount of detail that may be reproduced and very little is gained by increasing the band width. The 3.8-Mc band width associated with the

larger sizes of picture tubes is felt to be a reasonable value of top frequency due to the band-width limitations of the usual i-f amplifiers.

The remaining columns have the usual significance with the exception of "circuit" which refers to the circuits of Figure 9.

#### CASE 1

In this case the circuit is that of series peaking, but the load resistance is approximately 40 per cent greater than with conventional series peaking. In raising the load resistance it is necessary to increase the series inductance to maintain the high-frequency response. This, results in more variation in gain in the pass band. With the capacities listed for Case 1 and with 5500 ohms load and 430  $\mu$ h peaking inductance the variation is  $\pm 5$  per cent. With these conditions the gain is good, but the maximum output is only about 40 per cent more than the minimum required.

#### CASE 2

This condition is not satisfactory for the reason that the maximum output is not sufficient to modulate properly the picture-tube grid. The only means of getting more output is to increase the load or plate current. The plate current is limited by plate dissipation while the circuit used results in the highest possible load for the given conditions of capacitance and bandwidth. Evidently this is not a satisfactory video-output system.

#### CASE 3

In this case the 6AG7 output tube is considered. The type 6AG7 and type 6V6 have the same output capacitance, so as far as the output circuit is concerned, the tubes are interchangeable, the only difference being in gain and maximum output. In this case, and those following, the gain when using the type 6V6 is 40 per cent of that obtained with the 6AG7 while the maximum output is 25 per cent greater with the type 6V6.

The use of circuit Number 1 results in a low value of load resistance, nevertheless, when using the type 6AG7 output tube is used, the gain is fair and the output is more than the minimum required.

#### CASE 4

The circuit (Number 4) used in this case is that of a series *m*-derived half-section terminating a half-section constant-*k* filter and results in a reasonably high value of load resistance considering the band width and total-shunt capacitance. The maximum output is adequate with fair gain. The major disadvantage in using this combination lies in the circuit. This circuit requires very close tolerances on

all of the components, particularly on the two capacitances, if uniform gain over the band is to be obtained.

## CASE 5

The gain and output for this case are excellent. However, to obtain high gain and output requires the use of a diode-type d-c reinserter which may not be justified in a receiver employing a five-inch picture tube. If the diode were eliminated and replaced by a physical capacitance the maximum output would be 67 volts with a voltage gain of 49 which would be good.

## CASE 6

Two circuits are indicated in this case. They both result in the same value of load resistance and as the gain and output are good the choice lies between the two circuits. Circuit No. 5, employing a shunt *m*-derived termination, has the disadvantage that the tolerance on the components must be close if the transmission in the passband is to be uniform. Circuit 6 does not have this disadvantage.

## CASE 7

The maximum output in this case is much more than required and the gain is reasonably good. However, the combination of tube and circuit with the addition of a diode d-c reinserter is rather expensive to use in a receiver employing a five-inch picture tube particularly in view of the good results obtained in either Case 1 or 5. Further, the circuit, which is series and shunt peaking, requires rather close tolerances of the two end capacitances.

## CASE 8

As in Case 7, the maximum output obtainable is more than ample, however the gain is lower than in Case 6 which also has sufficient output.

One point in the above discussion of the eight cases that has not been stressed is the matter of cost. Tube and component costs are always evident, but the expenditure of direct current should also be taken into account. The plate, screen, and bleeder current required by the three video-amplifier tubes considered, when operating under two conditions, are listed below.

GRID D-C REINSERTION

Tube	$I_p$	$I_{sc}$	$I_{bleeder}$	Total
6AC7	10 ma.	2.5 ma.	10 ma.	22.5 ma.
6AG7	30	6.4	25.6	62.0
6V6	45	2.8	11.2	59.0

## DIODE D-C REINSERTION

Tube	$I_p$	$I_{sc}$	$I_{bleeder}$	Total
6AC7	10	2.5	—	12.5
6AG7	33	8.5		41.5
6V6	47	6.5		53.5

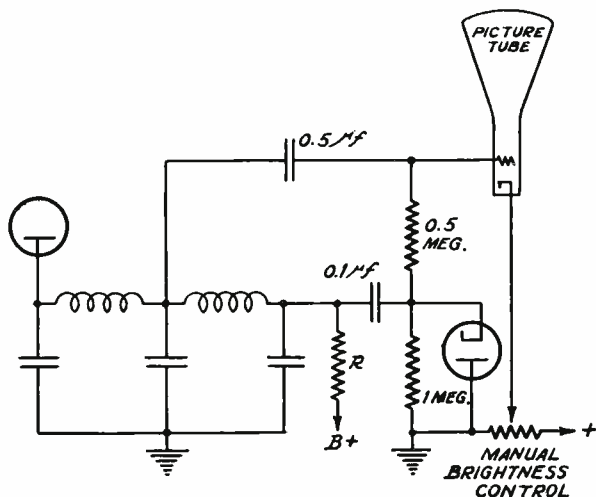


Fig. 13

On all of the circuits except Number 6 it is evident how to connect the diode to obtain d-c reinsertion. In Circuit 6 the fact that the load-resistance  $R$  is at the end opposite to the amplifier plate requires a slightly different connection as shown in Figure 13.

The eight cases considered cover the various output and picture-tube combinations, but no attempt has been made to consider each of the six filter types for each output and picture-tube combination.

The performance, as we have seen, was satisfactory in some cases and unsatisfactory in others. The principles and parameters of both output tubes and circuits have been discussed, so that the designer may calculate video-output systems other than those selected for illustration, in order to arrive at a design to meet the requirements of the particular receiver under consideration.

# DEFLECTION AND IMPEDANCE OF ELECTRON BEAMS AT HIGH FREQUENCIES IN THE PRESENCE OF A MAGNETIC FIELD

BY  
L. MALTER

Research Laboratories, RCA Manufacturing Company, Inc., Harrison, N. J.

*Summary*—A theoretical study was made of the behavior of an electron beam moving between a pair of plates across which is impressed a high-frequency signal, the entire structure being immersed in a constant magnetic field parallel to the plane of the plates.

The beam experiences an oscillatory deflection with components parallel and perpendicular to the plane of the plates. The amplitude of the deflection is dependent upon the transit time through the region between the plates and upon the strength of the magnetic field. The maximum values occur at low-frequencies and zero magnetic field.

The beam results in the impedance between the plates becoming complex. Since the resistive portion of this impedance goes through zero and negative values, there exists the possibility of generation of sustained oscillations in an external circuit.

For certain combinations of transit angle and magnetic field, considerable deflection sensitivity can be achieved while the resistive portion of the impedance due to the electron beam is small or negative. Thus, the possibility exists for the design of high-frequency amplifier tubes with negligible loading.

The same general conclusions are arrived at when the velocity components of the electron beam at the point of exit from the region between the pair of plates is considered. Deflection-type amplifier tubes can be designed which depend for their operation either upon deflecting an electron beam or giving the beam a velocity component normal to its original direction of motion.

## 1. INTRODUCTION

IN THE consideration of amplifying devices for operation at ultrahigh frequencies attention has recently been given to deflection control. In these cases, an electron beam is projected between a pair of plane-parallel plates in a direction parallel to their plane. (See Figure 1.) The application of an electric field between the plates causes the beam to suffer a displacement. This action can be taken advantage of for control of the current transmitted to an output electrode. If the applied field is alternating in nature, the deflection is correspondingly alternating with a peak value less than that occurring in the case of a steady field.

If the applied field is constant then the capacitance between the plates is decreased by the presence of the beam. When the applied field is alternating, the impedance as measured between the plates is altered from a capacitative reactance to a complex impedance consisting in part

of a resistance and in part of a capacitive reactance, different from the value for zero beam. For certain values of transit angle, since the resistance assumes negative values, the possibility for the establishment of sustained oscillations exists. In general, the solution of the problem for deflection and impedance is of value in the consideration of deflection devices for amplifiers at high frequencies. The complete solution for the case described has appeared in the literature<sup>1, 2</sup>.

If a magnetic field, parallel to the original direction of motion is introduced, the displacement is, in general, no longer solely in the direction of the electric field, but contains a component parallel to the plane of the plates (See Figure 2). The possibilities of more advantageous combinations of deflection sensitivity and electron loading (impedance due to beam only) indicated the desirability of the investigation of this more general problem.

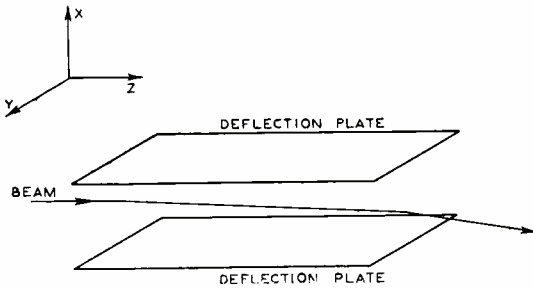


Fig. 1—Electron path in electrostatic field.

## 2. SOLUTION OF EQUATIONS OF MOTION

Notation: (See Figure 2).

$x, y, z$ —Displacements in  $X, Y,$  and  $Z$  directions respectively

$u, v, w$ —Velocity components in  $X, Y,$  and  $Z$  directions respectively

$w_0$ —Initial velocity (directed along  $Z$ )

$V_0 e^{i\omega t}$ —Voltage applied between plates

$H$ —Magnetic field strength

$d$ —Spacing between plates

$E_0 = \frac{V_0}{d}$ —Peak value of electric field

$l$ —Length of plates

$\omega$ —Angular frequency of electric field

$t_0$ —Time of entry of electrons into deflecting field

$m$ —Mass of electron

$e$ —Charge of electron

<sup>1</sup> A. Recknagel, *Zeit. f. Tech. Phys.*, 1938, No. 3, p. 74.

<sup>2</sup> Hollmann and Thoma, *Ann. der Physik*, Vol. 32, p. 459 (1938).

The equations of motion are

$$m\ddot{x} = eH\dot{y} + eE_0e^{i\omega t} \tag{1}$$

$$m\ddot{y} = -eH\dot{x} \tag{2}$$

$$m\ddot{z} = 0 \tag{3}$$

It is assumed that the field between the plates is terminated abruptly at both ends, so that the time of entry ( $t_0$ ) and the transit time ( $\tau$ ) of the electron through the region between the plates are sharply defined.

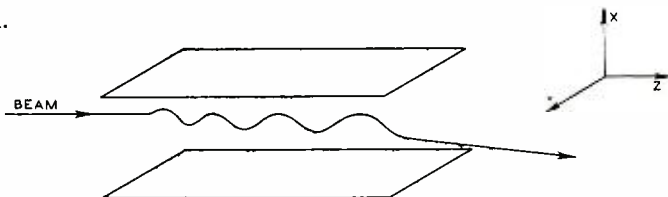


Fig. 2—Electron path in combined electrostatic and magnetic field.

A—VELOCITY COMPONENTS

If one sets  $a = e/mH$  and  $b = e/mE_0$  the solutions of (1), (2), and (3) for velocity components are

$$u = -i \frac{b\omega}{\omega^2 - a^2} e^{i\omega t} \left[ 1 - \left( \frac{\omega + a}{2\omega} \right) e^{-i(\omega + a)T} - \left( \frac{\omega - a}{2\omega} \right) e^{-i(\omega - a)T} \right] \tag{4}$$

$$v = \frac{ba}{\omega^2 - a^2} e^{i\omega t} \left[ 1 + \left( \frac{\omega - a}{2a} \right) e^{-i(\omega + a)T} - \left( \frac{\omega + a}{2a} \right) e^{-i(\omega - a)T} \right] \tag{5}$$

$$w = w_0 \tag{6}$$

where  $i = \sqrt{-1}$  and  $T = t - t_0$

If  $T = \tau$ , then (4), (5), and (6) represent the exit conditions for the electron beam.

For small transit angles, (4), (5), and (6) become

$$u_{\tau \rightarrow 0} = bT \left( \frac{\sin aT}{aT} \right) e^{i\omega t} \tag{7}$$

$$v_{\tau \rightarrow 0} = -bT \left( \frac{1 - \cos aT}{aT} \right) e^{i\omega t} \tag{8}$$

$$w_{\tau \rightarrow 0} = w_0 \tag{9}$$

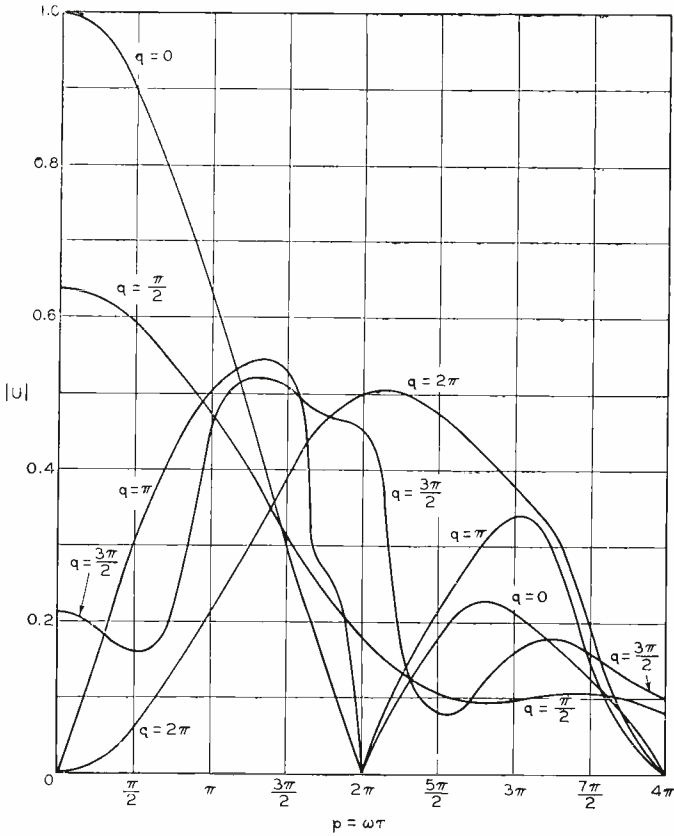


Fig. 3—Velocity in X direction acquired in combined fields.

Finally, for small transit angles and zero magnetic fields, the velocity components are

$$\frac{u_{\tau \rightarrow 0}}{H=0} = bTe^{i\omega t} = \underline{u} e^{i\omega t} \tag{10}$$

$$\frac{v_{\tau \rightarrow 0}}{H=0} = 0 \tag{11}$$

$$\frac{w_{\tau \rightarrow 0}}{H=0} = w_0 \tag{12}$$

where  $\underline{u}$  is the transverse velocity acquired in time  $T$  by an electron traversing a constant electric field of intensity  $E_0$ .

Then  $U = |u/\underline{u}|$  and  $V = |v/\underline{u}|$  represent the ratio of the maximum exit velocity in the case of the alternating field (with magnetic field present) to the velocity in the purely constant electrostatic field of intensity equal to the peak value of the alternating field.

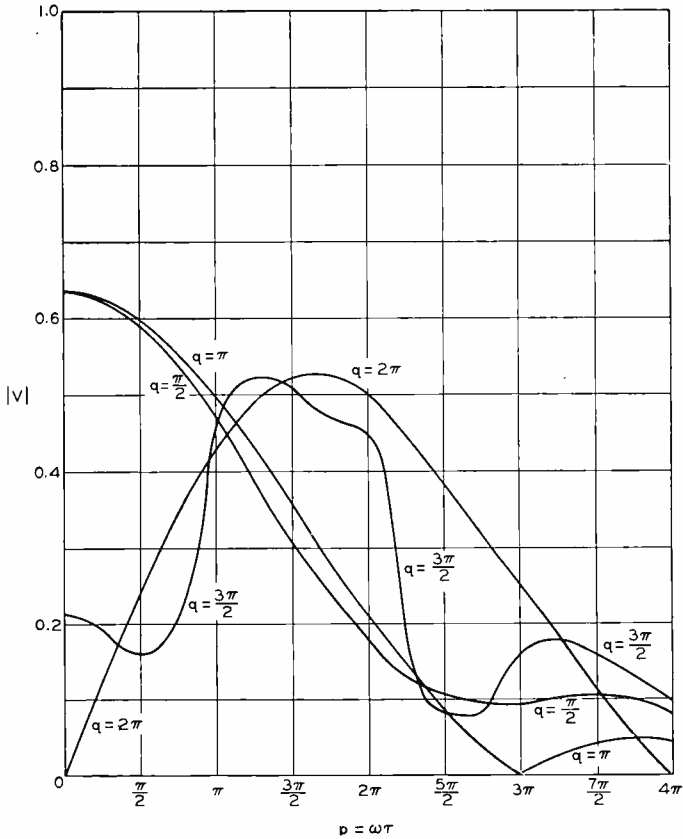


Fig. 4—Velocity in Y direction acquired in combined fields.

Setting  $\omega T = p$  and  $aT = q$ , (4), (5), and (6) can be recast into the more useful forms:

$$U = \frac{p}{p^2 - q^2} \left| 1 - \left( \frac{p + q}{2p} \right) e^{-i(p + q)} - \left( \frac{p - q}{2p} \right) e^{-i(p - q)} \right| \quad (4')$$

$$V = \frac{q}{p^2 - q^2} \left| 1 + \left( \frac{p - q}{2q} \right) e^{-i(p + q)} - \left( \frac{p + q}{2q} \right) e^{-i(p - q)} \right| \quad (5')$$

$$W = w_0 \quad (6')$$

For small transit angles (4') and (5') reduce to

$$U_{\tau \rightarrow 0} = \frac{\sin q}{q} \quad (7')$$

$$V_{\tau \rightarrow 0} = \frac{1 - \cos q}{q} \quad (8')$$

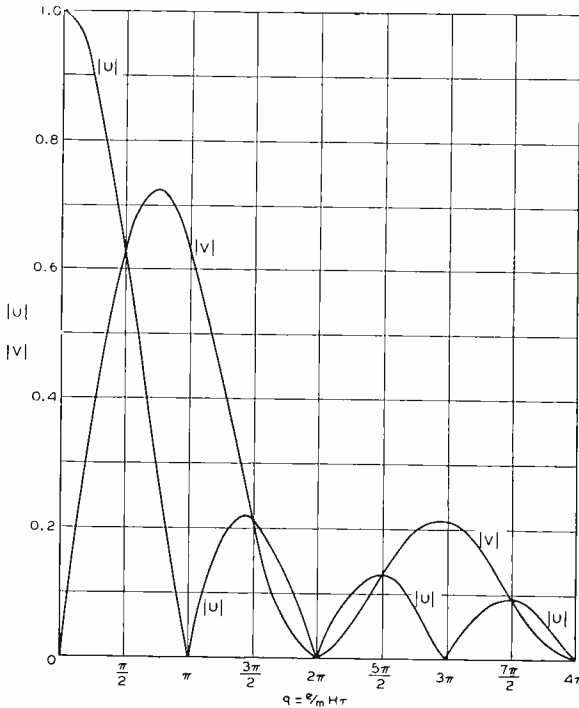


Fig. 5—Velocities for small transit angles.

Values of  $U$  and  $V$  as a function of  $p$  for various values of  $q$  as obtained from (4') and (5') are plotted on Figures 3 and 4. Values as a function of  $q$  for small transit angles as obtained from (7') and (8') are plotted on Figure 5.

B—DISPLACEMENT COMPONENTS

In the case of displacements, too, it is desirable to express the results in terms of the displacement occurring in a constant electric field of intensity  $E_0$ . The displacement in a constant field of intensity  $E_0$  is given by

$$\bar{x} = \frac{bT^2}{2}$$

One now sets

$$X = \left| \begin{array}{c} x \\ - \\ x \end{array} \right| \text{ and } Y = \left| \begin{array}{c} y \\ - \\ x \end{array} \right| \tag{10}$$

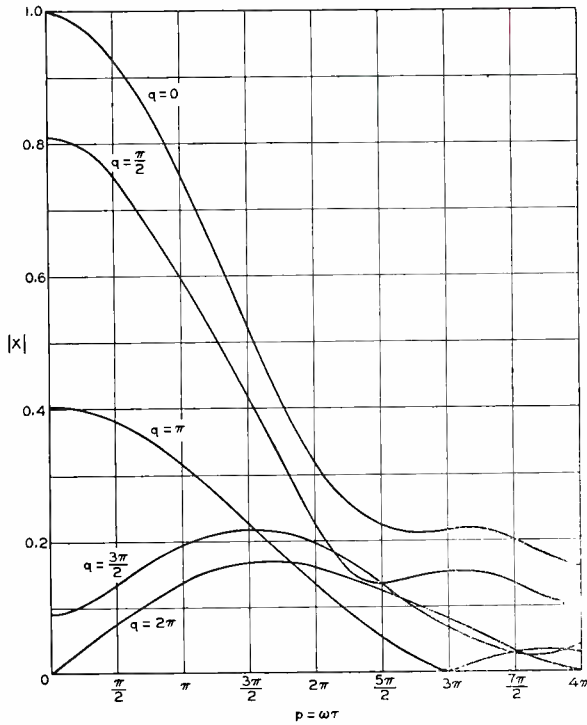


Fig. 6—Displacement in X direction for combined fields.

where  $x$  and  $y$  represent the displacements in the general case of combined magnetic field and alternating electric field. A further integration of (4) and (5) in terms of (10) yields

$$X = \frac{2}{p^2 - q^2} \left| 1 - \left( \frac{p + q}{2q} \right) e^{-i(p - q)} + \left( \frac{p - q}{2q} \right) e^{-i(p + q)} \right| \quad (11)$$

$$Y = \frac{2}{p^2 - q^2} \left| \frac{q}{p} \left( \frac{p - q}{2q} \right) e^{-i(p + q)} - \left( \frac{p + q}{2q} \right) e^{-i(p - q)} + \left( \frac{p^2 - q^2}{pq} \right) e^{-ip} \right| \quad (12)$$

$$Z = w_0 T$$

For small transit angles, these become

$$X_{\tau \rightarrow 0} = \frac{2(1 - \cos q)}{q^2} \quad (13)$$

$$Y_{\tau \rightarrow 0} = \frac{2(q - \sin q)}{q^2} \quad (14)$$

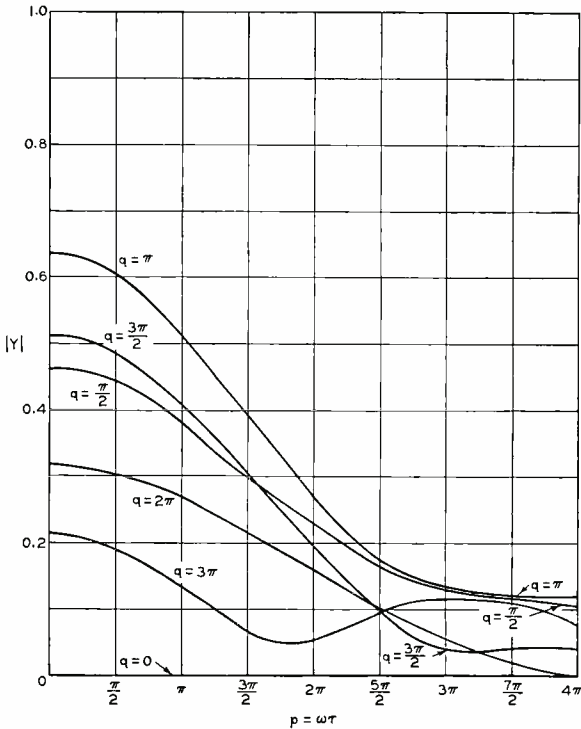


Fig. 7—Displacement in Y direction for combined fields.

Values of  $X$  and  $Y$  as computed from (11), (12), (13), and (14) are plotted on Figures 6, 7, and 8.

### 3. ELECTRON LOADING

When the electron beam is in the deflecting field it induces positive charges in each of the pair of plates. Since the beam describes a varying path, the induced charges in the pair of plates will not, in general, be equal or constant. As a consequence, a net current will flow in the deflecting-plate circuit in addition to the capacitive displacement current itself. The difference between the total current flowing in the deflecting-plate circuit when the electron beam is present and the displacement current which flows when the beam is absent, will be referred to as the *loading current*. The ratio of the loading current to the voltage applied to the plates will be known as the *loading admittance*. In general, this admittance will be complex, being composed of both conductance and susceptance.

The portions of the loading admittance and loading current due to the varying path of the electrons *within* the deflecting field will be designated as the *velocity components*.

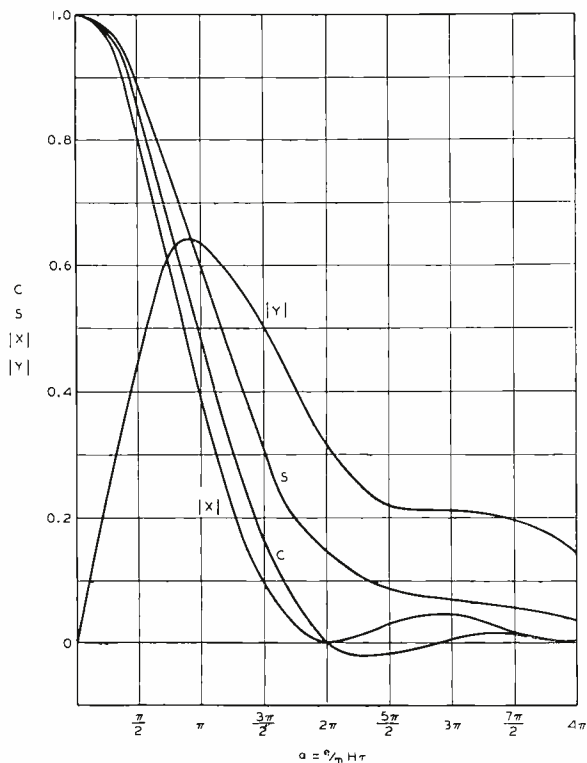


Fig. 8—Displacements for small transit angles.

In addition to the velocity components, another arises, due to the removal of the electron from the deflecting field. As the electron approaches the exit edge of the field, it has, in general, been displaced transversely from its entrance position (assumed to be midway between the plates). As a consequence the induced positive charges on the pair of plates when the electron is at the exit position are no longer equal. As the electron emerges from the field these positive charges must disappear, thus entailing a current flow in the external circuit. (No such flow occurred at the entrance to the deflecting field due to the fact that the positive charges were balanced.) As the beam position at the exit varies, a net current will flow in the external circuit which provides an additional component to the loading current, and will be known as the *displacement component of loading current*. The corresponding admittance component is similarly designated.

#### A. VELOCITY COMPONENTS OF LOADING CURRENT AND ADMITTANCE

Consider a charge  $e$  located in the region between the deflecting plates as shown in Figure 9. The current flowing between plates  $A$  and  $B$  as a result of the total motion of the charge is shown directly

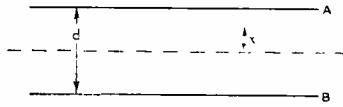


Fig. 9—Electron-electrode configuration.

from image theory to be  $\frac{e}{d} \frac{dx}{dt} = -\frac{e}{d} u$  where  $x$  is the displacement from the median plane. The current between  $A$  and  $B$ , due to the charge in length  $dz$  of the beam moving with velocity  $\omega_0$  in the  $Z$  direction, is  $dI_u = -j_0/w_0 d u dz$ . Since  $w = w_0 = \text{constant}$ ,  $\tau$  is independent of either  $t$  or  $t_0$ . Consequently  $dz/w_0 = dt_0$ , and

$$dI_u = j_0/d u dt_0$$

and the total current between the deflecting plates due to the transverse motion of the beam is

$$I_v = -\frac{j_0}{d} \int_0^\tau u dt_0$$

where  $j_0$  is beam current.

### B. DISPLACEMENT COMPONENTS OF LOADING CURRENT AND ADMITTANCE

It is assumed that the pair of plates are long compared to the distance between them. As a consequence, the fringing field is sufficiently thin so that the electron may be assumed to go from the uniform field condition to zero field instantaneously.

Referring once again to Figure 9, we find that the difference between the charge induced on plates  $A$  and  $B$  by the charge  $e$  is

$$Q_A - Q_B = 2e x/d$$

When  $e$  emerges from between the plates the charge difference must vanish. As a consequence a charge  $Q = e x/d$  must flow from one plate to the other. A beam current  $j_0$  emerging from between the plates will give rise to a current  $I_x = \frac{j_0}{d} x$  flowing between the plates.

The total loading current is, therefore,

$$I = I_u + I_x = \frac{j_0}{d} \left( x - \int_0^\tau u dt_0 \right) \tag{10}$$

where  $x$  is the transverse displacement at the exit position. For static fields, since  $x = \int_0^\tau u dt_0$ ,  $I = 0$  as it should.

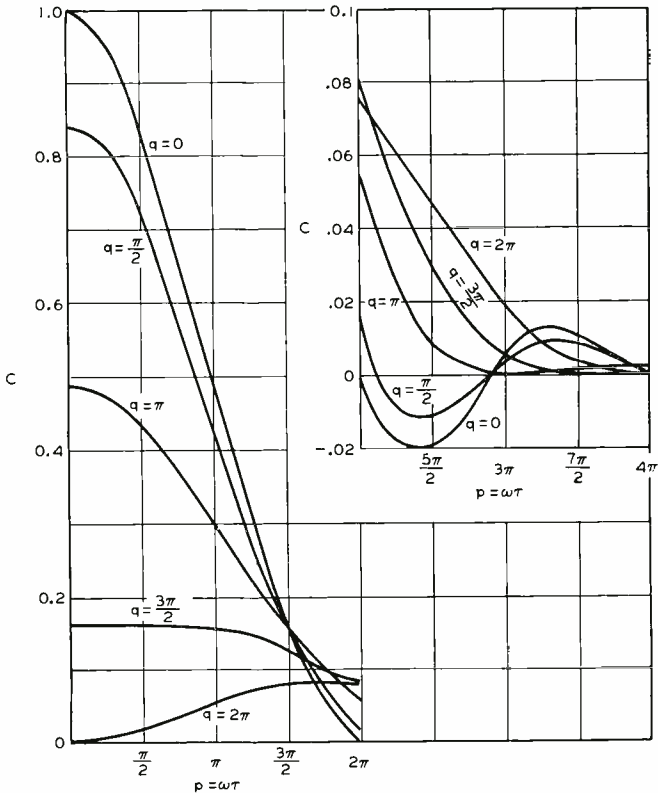


Fig. 10—Conductance due to electron beam in combined fields.

A more formal derivation of (10) has been carried out by Recknagel<sup>1</sup>.

The loading current can now be evaluated by substituting in (10) the previously derived values for  $x$  and  $u$ . There results

$$I = \beta \tau^2 \frac{j_o}{d^2} V_o e^{i\omega t} \frac{1}{p^2 - q^2} \left[ -1 + ip + \frac{1}{2} \frac{p}{q} \left( \frac{p+q}{p-q} \right) e^{-i(p+q)} - \frac{1}{2} \frac{p}{q} \left( \frac{p-q}{p+q} \right) e^{-i(p+q)} - \frac{p^2 + q^2}{p^2 - q^2} \right] \quad (11)$$

where  $\beta = e/m$

Now let  $\underline{A} = \frac{I}{V_o e^{i\omega t}} = \underline{C} + i\underline{S}$  be the loading admittance

where  $\underline{C}$  is the loading conductance

and  $\underline{S}$  is the loading susceptance

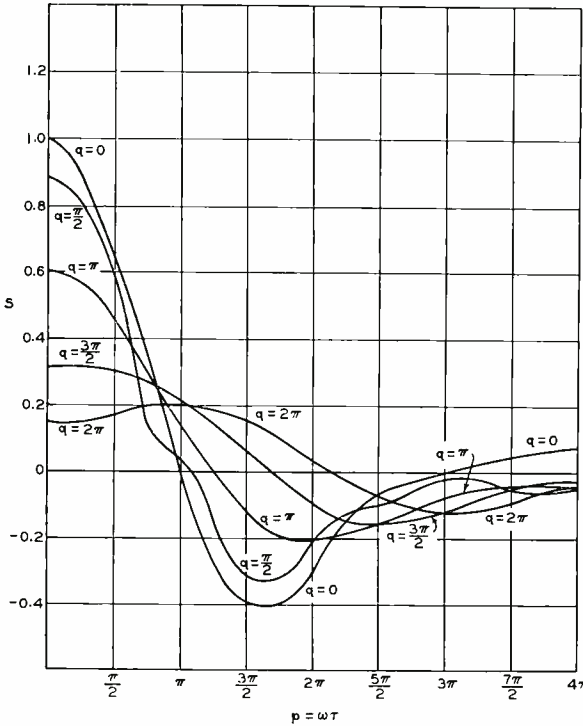


Fig. 11—Susceptance due to electron beam in combined fields.

then for  $H = 0$

$$A_{H=0} = \frac{\beta\tau^2}{p^2} \frac{j_0}{d^2} \left[ -2 + ip + (2 + ip)e^{-ip} \right] \tag{12}$$

This formula is contained in Recknagel's paper<sup>1</sup>.

For  $H = 0$  and small  $p$

$$\frac{C}{\left(\frac{H=0}{p \rightarrow 0}\right)} = \beta\tau^2 \frac{j_0}{d^2} \left( \frac{p^2}{12} \right) \tag{13}$$

$$\frac{S}{\left(\frac{H=0}{p \rightarrow 0}\right)} = -\beta\tau^2 \frac{j_0}{d^2} \left( \frac{p}{6} \right) \tag{13a}$$

To permit of plotting conductance and susceptance, it is convenient to define the quantities  $C$  and  $S$  as

$$C = \frac{\underline{C}}{\underline{C}\left(\frac{H=0}{p \rightarrow 0}\right)} \tag{14}$$

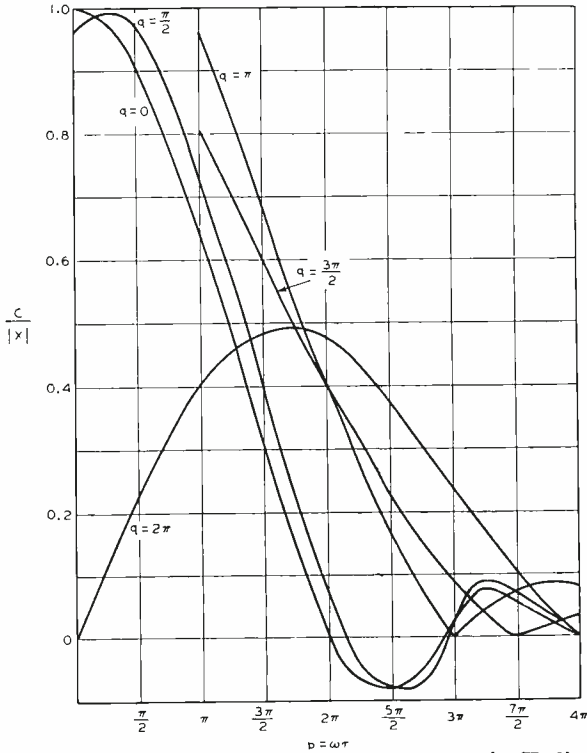


Fig. 12—Ratio of conductance to displacement in X direction.

$$S = \frac{\underline{S}}{\underline{S}\left(\frac{H=0}{\nu \rightarrow 0}\right)} \tag{15}$$

Applying (14) and (15) to (10) and separating the real and imaginary parts, there results

$$C = \frac{12}{p^2(p^2 - q^2)} \left[ -1 + \frac{1}{2} \frac{p}{q} \left( \frac{p+q}{p-q} \right) \cos(p-q) - \frac{1}{2} \frac{p}{q} \left( \frac{p-q}{p+q} \right) \cos(p+q) - \left( \frac{p^2+q^2}{p^2-q^2} \right) \right] \tag{16}$$

$$S = \frac{6}{p^2 - q^2} \left[ 1 - \frac{1}{2q} \left( \frac{p+q}{p-q} \right) \sin(p-q) + \frac{1}{2q} \left( \frac{p-q}{p+q} \right) \sin(p+q) \right] \tag{17}$$

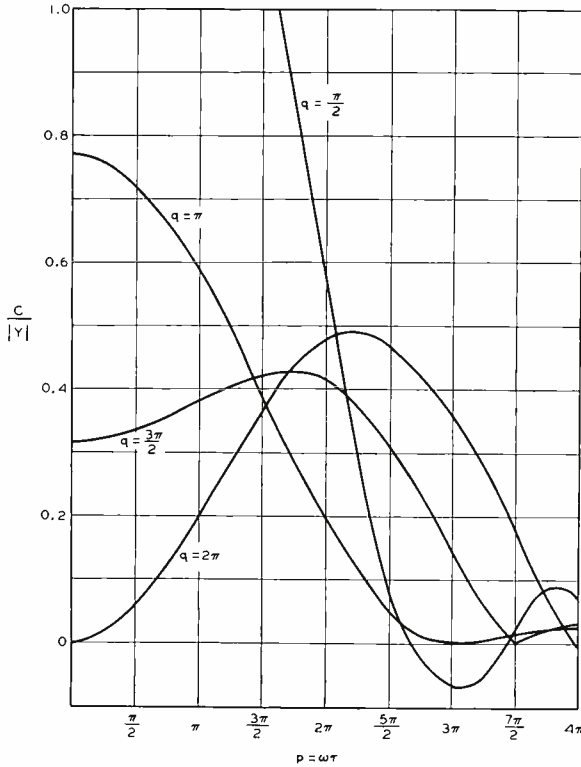


Fig. 13—Ratio of conductance to displacement in Y direction.

C and S as a function of  $p$  for several values of  $q$  are plotted in Figures 10 and 11.

For small transit angles

$$C_{p \rightarrow 0} = \frac{12}{q^4} (2 - 2 \cos q - q \sin q) \tag{18}$$

$$S_{p \rightarrow 0} = \frac{6}{q^3} (q - \sin q) \tag{19}$$

These are plotted in Figure 8.

DISCUSSION

An examination of Figures 3 to 8 indicates that under no conditions can deflections or transverse-velocity components be obtained which exceed the value for the case of a constant electrostatic field. However, although the deflection is always decreased by the magnetic

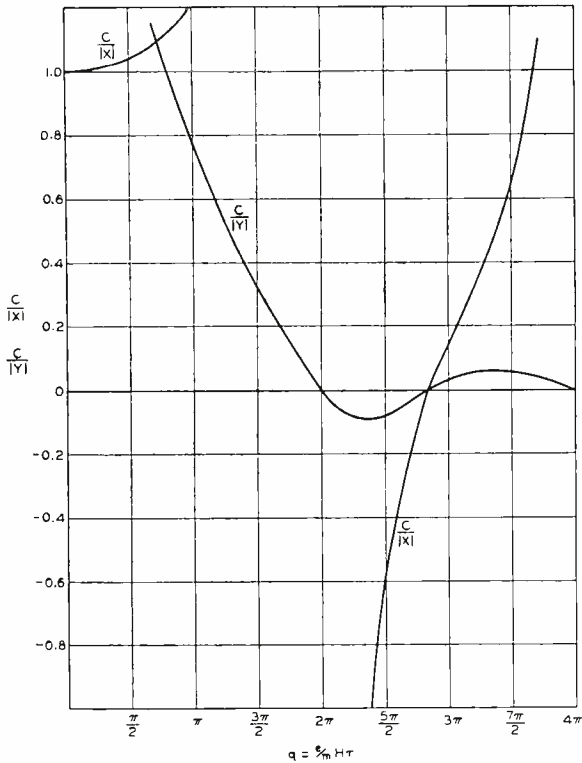


Fig. 14—Ratios of conductance to displacement for small transit angles.

field, the loading too, is decreased for certain conditions of operation. The actual decision as to whether any advantage exists in the employment of a magnetic field can be determined by plotting the ratio of

conductance to deflection, i.e.,  $\frac{C}{X}$ , and  $\frac{C}{Y}$ . This is done in Figures 12, 13, and 14. These curves reveal at once that there are large ranges of  $q$  over which both of these quantities are decreased below the values for zero magnetic field. Thus, the addition of the magnetic field results in an effectively lower electron loading for the same deflection sensitivity.

Figure 6 shows that for certain values of  $\omega\tau$ , the electron loading conductance is negative. This fact presents the possibility for the use of these devices as oscillators; it merely being necessary that the negative conductance exceed in value the positive conductance of the external circuit. For small transit angles, values of  $q$  between  $2\pi$  and about  $9$  also result in negative loading conductance. Negative-conductance conditions reoccur at higher values of  $q$ , but with diminishing

magnitude. In fact, there are certain conditions of field and transit angle for which the ratios  $\frac{C}{X}$  and  $\frac{C}{Y}$  vanish. Thus, it is possible to secure deflection control with zero electron loading. The same conclusions apply to the quantities  $\frac{C}{U}$  and  $\frac{C}{V}$ .

Equation (13a) indicates that the change in susceptance at low frequencies is negative. Since susceptance  $= \omega c$ , the capacitance change at low frequencies is negative and is given by  $e/m \frac{\tau^3}{6} \frac{j_0}{d^2}$ , a quantity which is independent of frequency. This change is analogous to the "dynamic capacitance" of space currents in diodes<sup>3</sup>.

I am indebted to D. O. North for very helpful discussions.

---

<sup>3</sup> Benner—*Annalen der Physik*, Vol. 3, No. 7, p. 993 (1929).

## ENGINEERING FACTORS INVOLVED IN RELOCATING WEAF

BY

RAYMOND F. GUY

Radio Facilities Engineer, National Broadcasting Company, Inc., New York

*Summary*—An exhaustive search for the best location of a new 50-kw WEAF transmitter indicated that it was to be found on the Sands Point-Port Washington peninsula. A new WEAF transmitting plant was built there in 1940 and the predicted results were fully realized. The population provided with 25-millivolt service was increased 450 per cent, to a total of about ten million, and the population provided with 50-millivolt service was increased 2900 per cent, to about five million.

Considering all factors, the Port Washington site appears to be the nearest possible approach to ideal for a station designed to serve the Greater New York area with 50 kw power.

IN 1927 the 5-kw WEAF plant was superseded by a new 50-kw transmitter at Bellmore, L. I., the first 50-kw broadcasting station on the Atlantic Seaboard and one of the few in existence anywhere in the world.

Many other stations in New York and elsewhere have followed NBC's example. Unfortunately, however, pioneers and leaders are often penalized by rapid technical developments and changes in standards and it became evident with the passing years that WEAF was not an exception to this generality. The end result of this series of events was the abandonment of the Bellmore station on November 8, 1940 and the placing into service of a complete new plant with the same power, but a much more favorable location at Port Washington, Long Island. This new station is but 14.5 miles from Columbus Circle, instead of 23, and serves that central point over a predominantly salt-water path having a conductivity of  $50,000 \times 10^{-15}$  electromagnetic units instead of over earth having a conductivity of from 10 to  $50 \times 10^{-15}$  electromagnetic units. As a result the number of persons provided with 25-millivolt service was increased four and one-half times to a total of ten million and the number provided with 50-millivolt service was increased 29 times to five million. Increased Bellmore antenna efficiency, or the use of a directive antenna, would not have provided the degree of improvement desired. The use of powers in excess of 50 kw is still prohibited, and in no event would it have been installed at Bellmore because of the high earth attenuation toward New York. It may be of interest to see how much power would have been required to produce the desired result. The field intensity was 10 millivolts in upper western Manhat-



tan and 75 millivolts intensity was desired. The desired field-intensity gain was thus 7.5 times. Since the field intensity varies as the square root of the power ratio, the power required would have been  $(7.5)^2 \times 50 = 2812.5$  kw.

The WEAF move was delayed for some time because of the confused situation with respect to clear-channel station-maximum powers. When it became evident that the Class 1A channels, earmarked by international agreement for 500 kw, would not be licensed for more than 50 kw for an indefinite time to come, the Port Washington project was undertaken.

The conventional method of investigating potential radio-station sites, and the one used by NBC, is to select promising locations and plot by calculation 8 to 10 field-intensity radials from which the various contours may be drawn on suitable maps. From these the populations within the important contours are tabulated, using the Federal census and other sources of population data. An engineer experienced in this work can do this quite accurately. From the most promising group of prospective sites a few are selected for further examination. This often consists of a site survey using a low-powered transmitter and temporary antenna on, or very close to, the exact site. This was done at Port Washington North, and one alternate site at New Milford, New Jersey.

What constitutes the ideal radio station site? There are many desirable features. But the most desirable is that as many persons as possible be provided with satisfactory field intensity, and as few as possible with too little or too much. 75 Millivolts is considered about ideal for such densely populated areas as Manhattan. 25 millivolts is excellent for the fringes of such areas. A principal requirement is that the population within the 250-millivolt contour be as limited as possible, because higher field intensities produce rapidly increasing difficulties with radio receivers lacking good selectivity.

An inspection of Figure 1 will show the somewhat startling fact that there appears to be, by modern standards, a good specific transmitter location having definite and valuable advantages over any other ones and that is the Sands Point-Port Washington peninsula where the new WEAF plant is located. Those advantages may be listed as follows:

1. It is very close to the center of population of Greater New York.
2. The center of population is slowly moving in the direction of the new site.
3. The 250-millivolt contour is distributed in such a way that the population within it is the lowest of any of the satisfactory sites. It may be seen on Figure 1 that this contour barely reaches the shoreline of the heavily populated Westchester side of Long Island Sound. The

contour skirts this shoreline, barely reaches the shoreline of the White-stone peninsula and also barely reaches the shoreline of the Glen Cove-Sea Cliff areas. The 250-millivolt population increases rapidly as the transmitter location is moved toward Westchester, reaching very high



Fig. 2

values at the Westchester shoreline. Similarly, moving inland to the southeast or the southwest also results in an increase.

4. Service to the Newark area is provided by the direct route over the center of Long Island Sound, thus giving the highest possible ratio of salt water to other less desirable terrains. It may be seen on Figure 1 that the Newark area is served with 35 millivolts. It may also be seen that moving only a few miles to either the northwest or

the southeast, but particularly the northwest, would introduce a greater proportion of highly attenuating terrain, thus reducing the

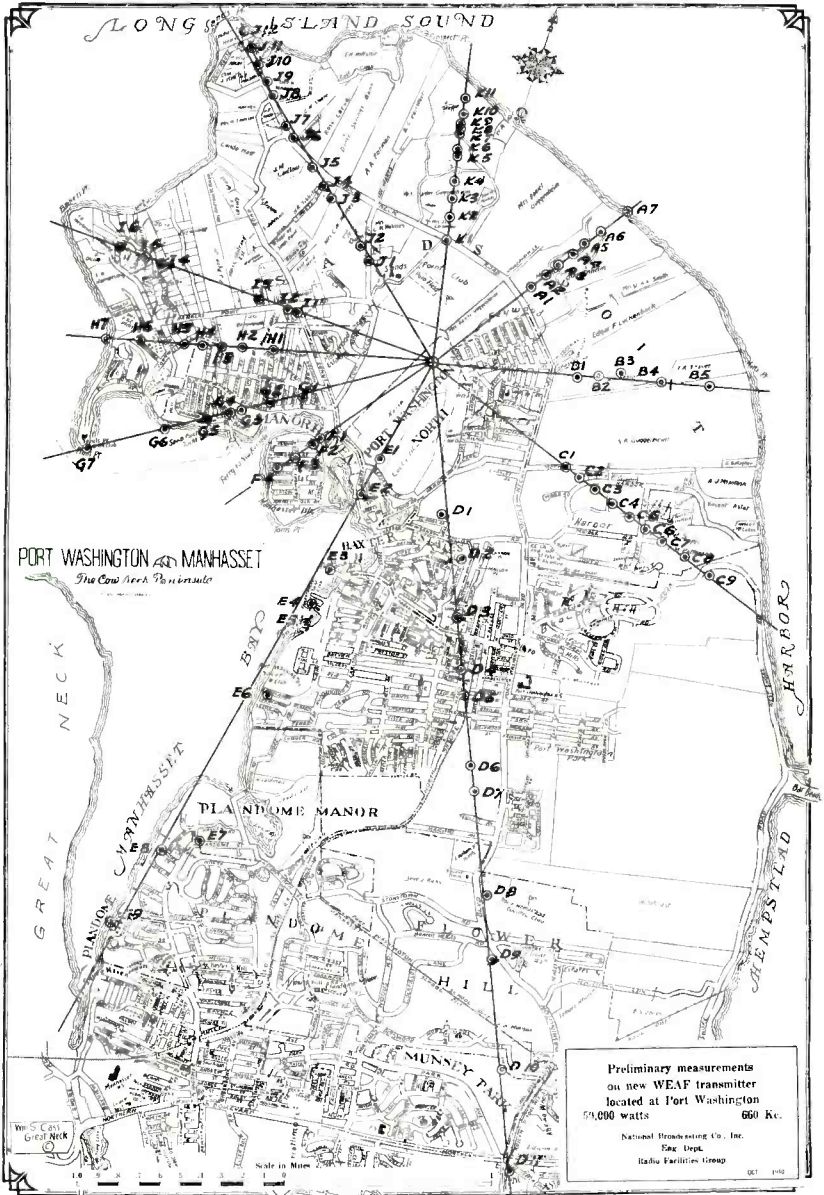


Fig. 3

field intensity in the Newark sector. This area is very important since it is the largest concentration of population and the choicest market

area of Northern New Jersey. The very short distance from the WEA F antenna to the beginning of the salt-water path is not significant so far as attenuation is concerned.

5. The new transmitter location is in a comparatively isolated por-

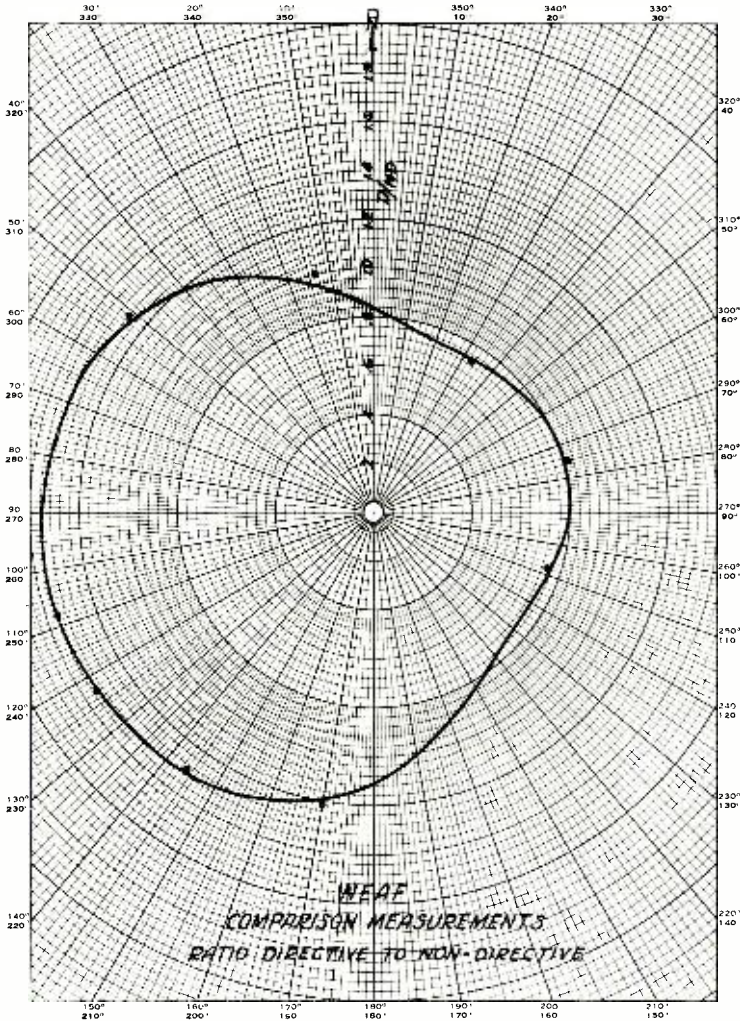


Fig. 4

tion of the Port Washington-Sands Point area, but despite this isolation it is served by good highways, good transportation, water, telephone and power facilities, is isolated from any threat of floods, and is close to attractive residential areas for the staff.

6. The location is east of New York City, making possible the use of some desirable antenna directivity to the west where both primary and secondary coverage are most important.

7. No other station is located in that area and as long as this is the case cross modulation will not be a problem.

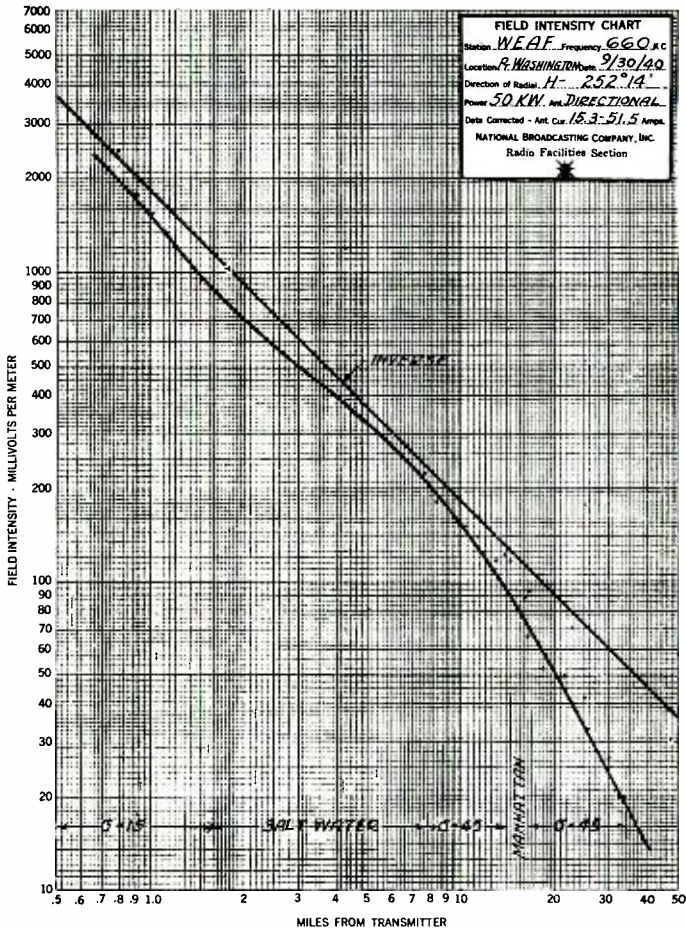


Fig. 5

In addition to other desirable features listed, the Port Washington site had very high soil-load-bearing capacity, which greatly simplified foundation designs and construction. At normal footing depths the load-bearing capacity was at least 10,000 pounds per square foot.

Figure 2 shows the population per square mile in the area of Greater New York and its environs according to the U. S. Census of

1930. It may be seen on Figures 1 and 2 that no area of 50,000 persons per square mile is served by less than 35 millivolts and, with the excep-

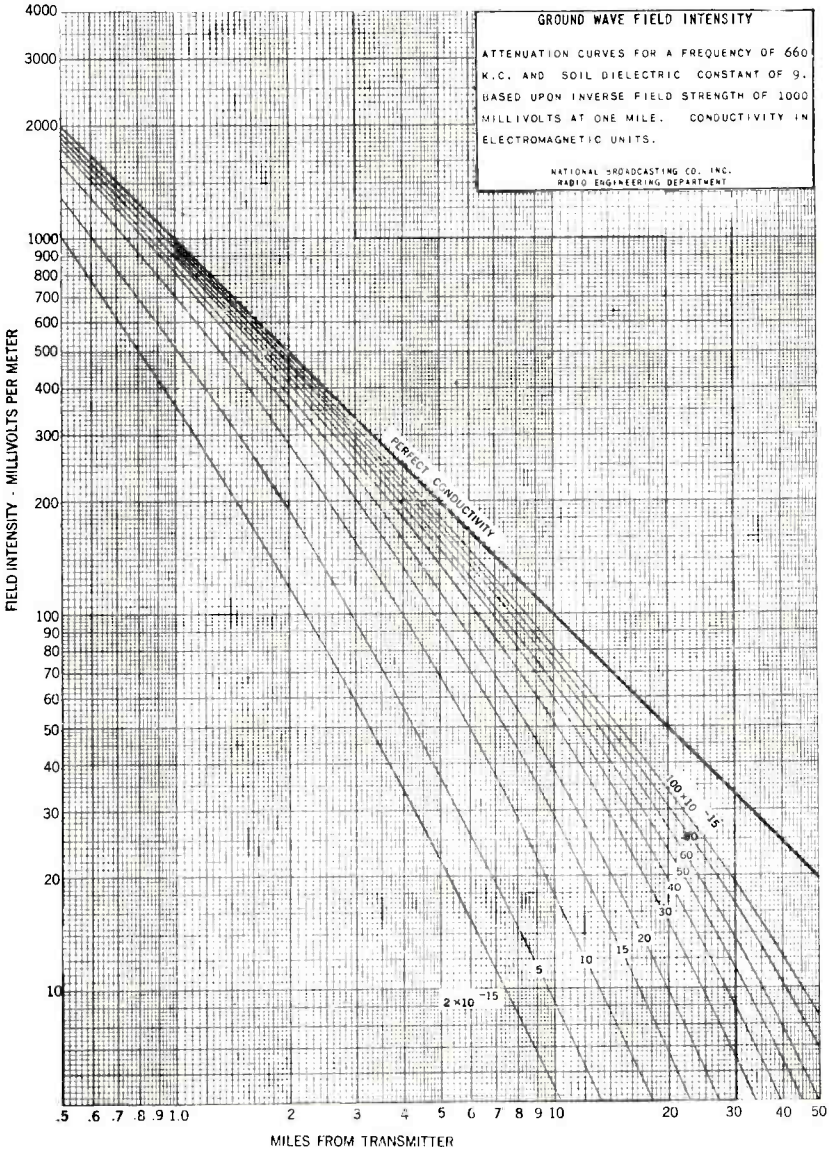


Fig. 6

tion of two small isolated sections which are in Newark, all such areas are served with from 60 to 150 millivolts. The average for all such areas is roughly 80 millivolts, which is ideal.

Figure 2 shows the boundaries of the area known as Greater New York. It may be seen that WEAFF serves substantially all of this great area with a signal intensity well in excess of 5 millivolts per meter.

Twenty engineer-weeks of personnel time and five weeks of elapsed time were devoted to the study of the external performance of the new station out to the 25-millivolt contour. In making such a study, which is a normal part of such a project and a requirement of the FCC, 19 days were devoted to the selection and staking out of suitable locations for the subsequent accurate field measurements. Approxi-



Fig. 7

mately 50,000 linear feet of radial distance were chained off to establish accurately the distances to the nearby measuring points, and many other points at slightly greater distances were measured by triangulation, using a transit. Beyond the first few miles the distances were scaled off of maps. Since all field measurements had to be made between 1:00 and 6:30 A.M. when the old Bellmore transmitter was not in operation, it obviously was necessary to select the approximately 100 nearby measuring points in advance during daylight.

Figure 1 shows, by serial number, the more distant field measuring locations and Figure 3 shows those within the first few miles.

## THE ANTENNA

In selecting a transmitter location for a seaboard city, it is obviously desirable to locate to the seaward of such a city and thus be able to moderately concentrate the field away from the ocean wastes and toward the useful primary and secondary service areas inland. Were WEAJ located inland from New York City, as in Northern New Jersey, it would have been most undesirable to weaken the primary service over Long Island by directionalizing to the west. Without such directivity the night-time easterly skywave power would have been largely wasted spraying the Atlantic Ocean. WEAJ, being a Class 1A clear-channel station, can provide night-time service over a vast area extending as far as western Indiana. It can provide it better if the field is concentrated in that direction instead of to the ocean wastes. For these

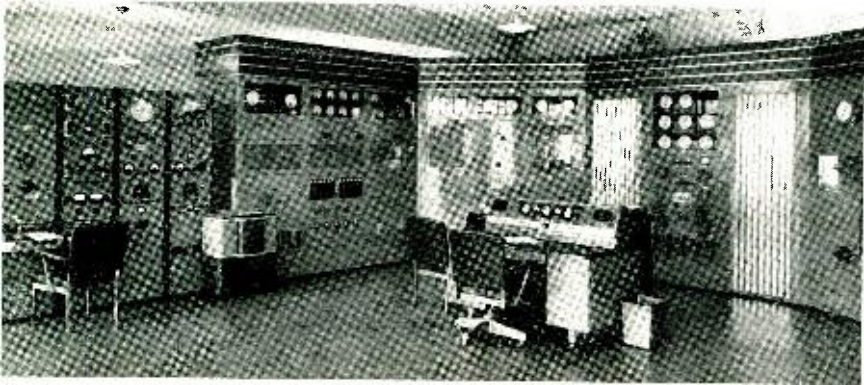


Fig. 8

reasons the WEAJ radiating system was made directive to a moderate degree, as shown on Figure 4. This, however, was not the only reason for locating east of New York City. The New Jersey location tested compared rather poorly with Port Washington with respect to the interference problem, and also with respect to the proportion of the population receiving the optimum field intensities as against those receiving too little or too much.

The antenna system consists of two separately-excited towers spaced 400 feet, or 97 degrees. They are excited by currents having a phase displacement of 115 degrees and an amplitude ratio of 3.33. The true bearing of the tower line is north 75 degrees east. The field is reduced to only a moderate degree and this occurs largely over unpopulated salt water wastes and adjoining thinly populated areas not requiring very high field intensities.

Figure 4 is the result of field measurements in which the ratios of directive to nondirective field intensities were compared. By this method of directivity measurement the effects of fixed-instrument inaccuracy or local-field distortion are automatically cancelled out.

Figure 5 is of interest since it shows the measurements on the N. 252° E. Newark, N. J. radial from Port Washington. The following table compares the field at various distances on this radial with the field on the N. 153° 54' E. radial toward Bellmore. The latter radial



*McLaughlin Aerial Photos*

Fig. 9

is typical of the terrain formerly traversed from Bellmore to New York City. The effects of directivity have been omitted by correcting to make the 1-mile fields equal.

Figures 1 and 3 show all of the radials followed and the measuring points on each.

Figure 6 is a family of curves of ground-wave field intensity plotted against distance and drawn on the same coordinate paper as is used for plotting the various radials. The conductivity of a given radial is determined by superimposing Figure 6 upon the plot for the radial and noting which conductivity curve fits the slope of the radial.

FIELD-INTENSITY TABLE

Miles	Field-Intensity Bellmore Radial	Field-Intensity Newark Radial
3	405	500
5	190	325
10	67	160
15	30	83 (Columbus Circle)
20	18	50 (Jersey City)
25	7	35 (Newark)

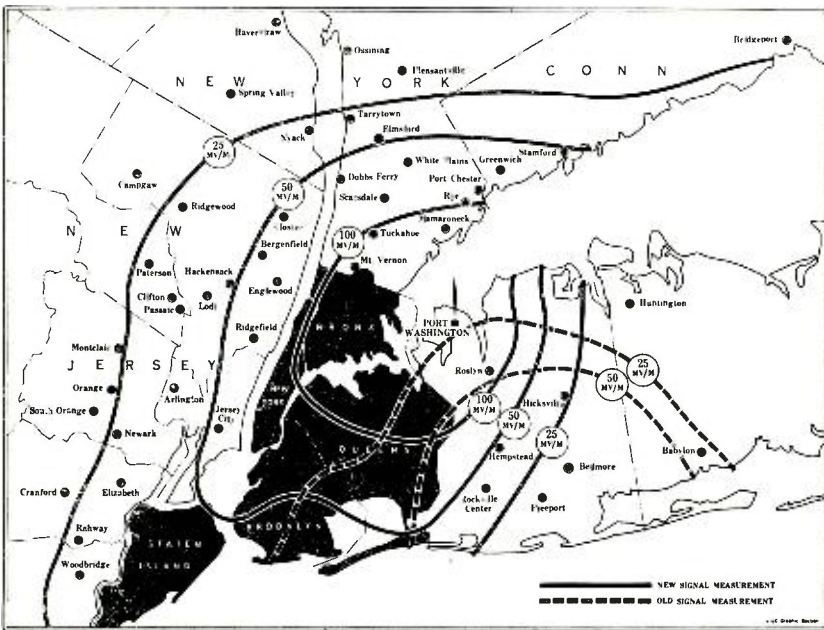


Fig. 10

Figure 7 is an aerial photograph which graphically illustrates the advantageous location of WEAJ with respect to the salt water path. Figures 8 and 9 are photographs of the new station.

Figure 10 shows a comparison of the 25 and 50-millivolt coverage of the Bellmore and Port Washington stations.

The operating characteristics of the transmitting equipment are representative of the best modern practice. The frequency response of the transmitter is uniform within a range of 30 to more than 15,000 cycles, and the Radio City studios have an equally excellent range. The duplicate connecting telephone circuits are uniform in response

from 30 to 10,000 cycles and could be extended if there were anything to be gained by doing so. The signal-to-noise ratio on the combined telephone circuits and transmitting plant is 63 db, equivalent to about 1250 in voltage. The distortion is maintained at about 1 per cent at full modulation over the frequency range where the normal amplitudes are greatest. 32-db of overall inverse feedback is used in the transmitter. These standards which have been maintained by NBC at all its stations for many years, may be taken for granted, and do not warrant further description herein.

Duplicate power lines enter the station over separate routes and duplicate program lines enter through separate cables over separate routes. The station is equipped with a receiver suitable for high-fidelity program relaying, and in the remote event of failure of both program lines, the programs may be relayed to the station without loss of fidelity, through W51NY, NBC's frequency-modulation station in the Empire State Building.

# FREQUENCY MODULATION

BY

S. W. SEELEY

RCA License Laboratory, New York

*Summary*—This paper, which contains generalized theory of the principal characteristics of frequency-modulation systems, is purposely made broad in its attack in order to achieve simplicity of presentation of fundamentals. Detailed treatment of specific problems associated with this type of modulation is given in the articles listed in the appended bibliography.

## I. FREQUENCY AND PHASE MODULATION

COMBINATION of discussions of frequency modulation and phase modulation into one treatment may seem improper, at first glance, when the subject to be treated is frequency modulation alone. It has been done in this section of the paper because the two are so related that an understanding of both is necessary for a true picture of either.

The simplest conception of a frequency-modulated wave is of one with unvarying amplitude whose frequency is altered cyclically above and below its mean unmodulated value. However, if we consider phase modulation in its simplest form, it can be seen that frequency modulation also results therefrom. Consider the case of Figure 1, in which a carrier wave of unvarying amplitude  $A$  has its phase advanced and retarded sinusoidally between values of  $+\phi$  and  $-\phi$ , with respect to its unmodulated phase. In this case the peak-to-peak phase modulation is, of course,  $2\phi$ . At the end of its excursions at either  $+\phi$  or  $-\phi$  the frequency of the wave is identical to that of its unmodulated value. However, as it progresses from  $-\phi$  toward  $+\phi$  and back again, its frequency is alternately increased and decreased, with frequency maxima and minima occurring at the point  $P$ . Thus it can be seen that the instantaneous periods of maximum phase displacement and maximum frequency deviation are misplaced from each other by  $90^\circ$  at the modulating frequency. In other words, if the phase modulation is assumed to be a cosine function, the frequency modulation is inherently the rate of change of phase, which is the first derivative of that cosine function and thus is a sine function. This assumed example is of the simplest case where the modulating component is a pure sinusoidal frequency. If the modulating frequency is raised, but the amount of

phase modulation maintained constant (deviation between  $+\phi$  and  $-\phi$  maintained) the rate of rotation of the vector  $A$  as it passes point  $P$  will be increased, which means that the maximum and minimum frequencies occurring when the vector is at point  $P$  are also increased. Thus constant phase modulation at all modulating frequencies results in more frequency modulation when higher modulating frequencies are used than for lower ones.

Figure 2 shows another simple relation between frequency and phase modulation. In the upper plot the frequency is shown to vary as a square wave, first above and then below its mean value. As long as the frequency remains at its increased value, the phase must be advancing, as shown in the plot immediately beneath. Then when the frequency is reduced on the other part of the square wave, the phase

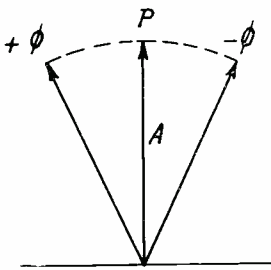


Fig. 1

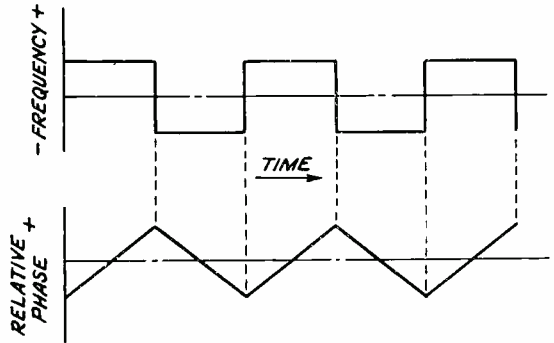


Fig. 2

is progressively retarded. The square wave will be instantly recognized as the first derivative of the triangular wave below. This is another simplified means of illustrating the fact that frequency modulation is a function of the first derivative or rate of change of any existing phase modulation.

From these considerations it is evident that if an end product is to consist of a frequency-modulated wave whose frequency deviation is proportional to the instantaneous amplitudes of a complex modulating wave, and if that frequency modulation is to be derived from a phase-modulating process, the complex modulating wave must first be integrated. In other words the applied modulating components must have amplitudes inversely proportional to their frequency, since a small amount of phase modulation at a high modulating frequency will result in the same amount of frequency modulation as a greater phase displacement at a lower modulating frequency.

## II. DEVIATION AND BAND WIDTH

The simple conception of a frequency-modulated wave, in which the frequency of a carrier wave of unvarying amplitude is altered cyclically about its mean value, is sufficiently adequate if the maximum frequency excursions of the carrier-wave frequency are large compared to the modulating frequency, for example, in the case of a wave being varied between limits separated by, say, 150 kc with the variation occurring sinusoidally at a 100-cycle per second rate.

If, however, the maximum frequency excursion is of the same order of magnitude, or equal to, or less than the frequency of change, the case is not so simple. It has often been proposed in all good faith that a communication channel could be narrowed by the use of frequency modulation in which the deviation in cycles per second is less than the modulating frequency. However, it is axiomatic that any side-band energy (and consequently the necessary intelligence component) in any type of modulation, whether frequency, phase, or amplitude, will not approach the carrier closer than a frequency interval equal to the modulating frequency. Therefore, if a narrow-band receiver is used to intercept a small deviation frequency-modulated wave whose modulating frequency is greater than one-half of the band width of the receiver, none of the modulation will be received. If we assume the case of a frequency-modulated wave with a modulating frequency of 10,000 cycles per second, which causes a deviation of + and - 10,000 cycles in the frequency of the carrier, a receiver with theoretically perfect band pass in its r-f and i-f circuits 19.9 kc wide with perfectly perpendicular sides, tuned with the carrier at the center of the band to receive that frequency-modulated wave, would not give any evidence of what modulating frequency was being used. A pure unvarying carrier with neither frequency, phase, nor amplitude modulation would be applied to its demodulating detector. It is true that in the example cited the received carrier would be somewhat decreased in value (actually to about 76 per cent) from its unmodulated amplitude, but this need not concern us for the moment. The example is cited simply to emphasize the fact that in frequency and phase modulation, as well as in amplitude modulation, the intelligence components are carried in side-band energy, and that that side-band energy must be received in order to interpret or reproduce the original modulation.

In the example cited above, side bands will exist not only at frequencies of + and - 10 kc with respect to the carrier, but also at + and - 20 kc, as well as at 30 kc, etc.<sup>1</sup> If the theoretically perfect

---

<sup>1</sup> See publications listed in the bibliography for more complete explanation of this characteristic.

band pass of our receiver were just sufficiently wide to pass only those side components at + and - 10 kc, we would have the condition shown in Figure 3A. In this figure the first three side bands are shown with their relative amplitudes when the peak frequency excursion divided by the modulating frequency is equal to unity. The theoretically perfect pass band is shown just including the carrier and the first two side bands. The resultant wave is as represented vectorially in Figure 3B, with the upper and lower side bands revolving about the point *P*, first causing a phase displacement to point *P'* and then to *P''*.

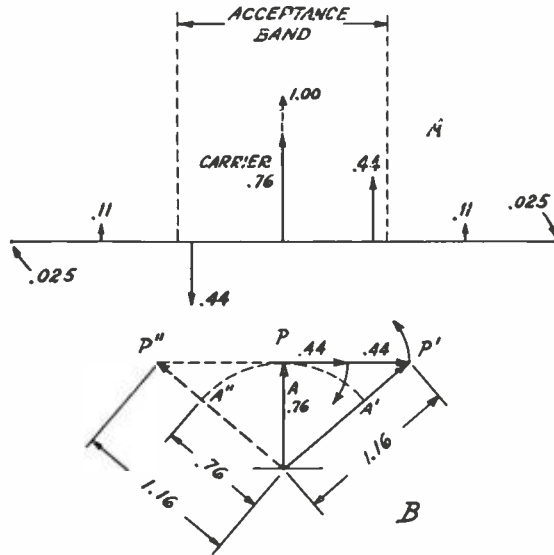


Fig. 3

Under these conditions it can be seen that the resultant instantaneous scalar magnitude of the carrier will vary between .76 and 1.16. In other words, amplitude modulation at twice the modulating frequency has resulted from deletion of all but the first side bands. This amplitude modulation contains no components at the 10,000-cycle frequency, is chiefly second harmonic, and contains small amounts of other even harmonics.

If now this wave shown emerging from our perfect 20-kc band pass filter is passed through a limiter stage which denudes the carrier of any amplitude modulation, the vector *A* will oscillate between the point *A'* and *A''*, which means that additional side bands have been recreated to cancel the amplitude modulation. It so happens that all of the even harmonic side bands are reinserted by a limiter stage, but that the odd harmonic side bands are not so reinserted, and thus a

small amount of distortion (principally third harmonic) in a demodulated wave which had been subjected to the process above described would result.

### III. NOISE REDUCING PROPERTIES OF FREQUENCY MODULATION

If a single, sharp, interfering impulse is applied to a band pass receiver, the resultant wave train which ensues is a function of the upper and lower frequencies of the pass band, and, for purposes of this discussion, can be assumed to be at one frequency only, namely that at the center of the pass band. An idealized mathematical expression for the wave train takes the form of

$$\frac{A \cos (w_1 - w_2) t}{t} \cos \frac{(w_1 + w_2) t}{2}$$

where  $A$  is a coefficient and  $w_1$  and  $w_2$  correspond to the upper and lower limits of the pass band. The expression of the form  $\frac{\cos x}{x}$  (similar to the first part of the above expression) indicates a falling amplitude of wave envelope for positive and negative values of " $t$ " as shown in Figure 4. Most of the energy of this wave train is, of course, under the large middle portion of the envelope, but the significant point is that for purposes of analysis the frequency can be assumed to be constant and equal to the mean frequency of the pass band, as shown by the second portion of the expression. Thus if this peak of interference, emerging from the pass band filters, is applied to a perfectly balanced back-to-back frequency-modulation detector or discriminator, its effect on both halves of that circuit is identical, and the net result is zero output.

If, however, a carrier wave at the mean frequency of the pass band is also present, the instantaneous phase of the interference energy and of the steady state carrier may take on any random value. Thus if the phase of the wave train due to the interfering impulse is, say  $90^\circ$  ahead of the carrier-wave phase and the interfering impulse is much stronger than the carrier wave, the instantaneous phase of the resultant of the two is altered considerably during the transmission of the interfering pulse. Therefore, even though the two waves together are passed through a limiter stage, the output of which is unvarying in amplitude, a certain amount of phase modulation (and consequently frequency modulation as well) has been developed, and the frequency modulation detector interprets it in the form of an output voltage or current. The same phenomenon may occur if recurrent interfering pulses overlap.

## IV. INTERFERENCE BETWEEN CARRIERS

If two transmitted carriers are received at one time and the beat between the two is at audible frequency, the sum of the two produces both amplitude and phase (or frequency) modulation. If one is twice the amplitude of the other, the resultant phase modulation amounts to  $\pm 26.5$  degrees regardless of the frequency of separation.

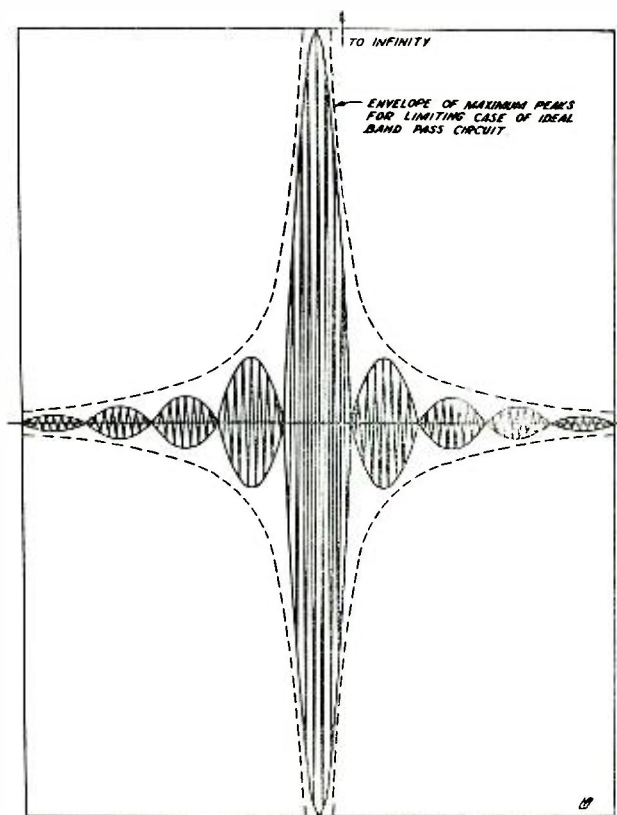


Fig. 4

This is shown in Figure 5. However, as pointed out in the first part of this discussion, the amount of frequency modulation resulting from a given amount of phase modulation is a function of the modulating frequency, which in this case can be assumed to be the frequency of separation of the two waves. Thus if the two frequencies are separated by 15,000 cycles, the equivalent frequency deviation of the frequency modulation amounts to approximately 7000 cycles per second. However, if the frequency of separation is only 100 cycles, the same

amount of phase modulation produces a frequency excursion or deviation of only 45 cycles per second.<sup>2</sup> Since the output of the frequency-modulation detector of a frequency-modulated wave receiver is dependent only upon the deviation, or excursion, from the mean frequency, it can be seen that the output will be 150 times greater when the carriers are separated by 15,000 cycles than when the separation is only 100 cycles. It is for this reason that the beat note between two frequency-modulated carrier wave stations becomes inaudible as the frequencies are brought closer and closer together.

### V. FREQUENCY-MODULATION METHODS

A frequency-modulated wave transmitter should emit a wave of

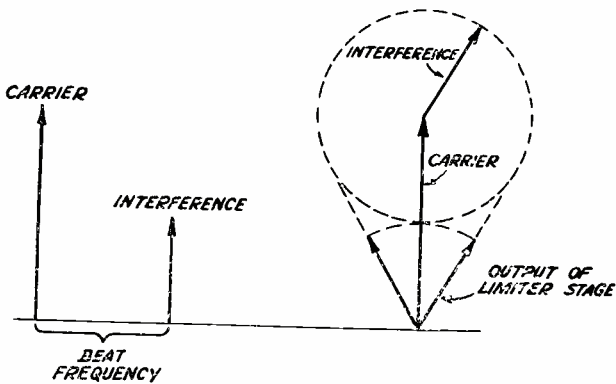


Fig. 5

unvarying amplitude with a frequency deviation about its mean (carrier) frequency in perfect conformity with the speech or program modulation. This neglects the matter of high-frequency pre-emphasis which will be discussed shortly.

There are two basic methods of producing this desired result. In either case, however, and unlike amplitude-modulated wave transmitters, the modulation takes place at the source of the transmitter frequency-determining circuits. Thereafter, the original oscillator-frequency energy may be amplified, multiplied in frequency, or heterodyned to any other frequency without altering the modulating components except to the extent that any multiplication of the source

<sup>2</sup> Actually when a single side component "phase modulates" an existing carrier, as in this case, the frequency modulation is not symmetrical. However, with a two to one ratio of original amplitude the "peak to peak" frequency shift is nearly equal to the values which the above figures would indicate.

frequency increases the deviation by an equal factor. Thus a doubler stage not only doubles the carrier frequency but also doubles the deviation width.

## VI. MODULATION OF PHASE TO PRODUCE FREQUENCY MODULATION

One means of producing frequency modulation is first to "integrate" the program material and then phase modulate some low-frequency source of energy; subsequent frequency multiplication can increase the resulting frequency deviation to any desired amount. After the desired band width has been obtained, the carrier with its modulating components can be heterodyned either directly to the transmitter frequency or to some sub-multiple thereof. In the latter case, additional deviation and band width are obtained by the subsequent multiplication to the transmitter frequency.

The integrating process usually consists of obtaining the potentials across a pure capacitive reactance in the plate circuit of a high impedance vacuum tube whose grid is supplied with the normal audio components. This causes a phase delay of  $90^\circ$  at all modulating frequencies and gives the program material an amplitude characteristic which is inversely proportional to frequency. If high-frequency pre-emphasis is to be used, the plate circuit may have a resistance in series with the capacitance with the output potentials taken across both. This allows more of the high-frequency components to enter the modulating circuit than would otherwise be the case. Present-day practice in pre-emphasis of both amplitude and frequency-modulated wave transmitters is to use a pre-emphasizing circuit equivalent to a series  $L/R$  network having a time constant of about 100 microseconds. Therefore, if the program integrating circuits for a phase-modulating frequency-modulated wave transmitter are to perform the pre-emphasis function also, the  $CR$  series combination must have a time constant of that value. Of course, the integration and pre-emphasis functions may be performed in separate stages, but it seems desirable to combine the two and thus prevent the extremely wide discrepancies between the levels of the low-frequency and high-frequency components of the program material at any point in the preparatory networks.

If the original frequency which is to be phase modulated by the prepared (integrated) program is produced by a crystal oscillator or other stable source of oscillations, the usual method of procedure is to amplitude modulate some of the energy at that frequency in a balanced modulator and then to re-insert carrier energy with an exactly  $90^\circ$ -phase rotation. The result is the same vectorially as is shown in Figure 6. The output contains both phase and amplitude modulation.

The amplitude modulation has little or no significance since it is always "limited" off in subsequent stages, but it is interesting to note that at least with sine-wave modulation, all amplitude modulation is at even harmonics of the modulation frequency without any of the fundamental being present. This is shown by the fact that the vector representing the carrier maximizes at each end of its phase excursion or twice each modulating cycle.

The developed phase modulation can be seen to be a function of the amplitudes of the horizontal vectors in Figure 6, which have been derived from the balanced modulator. As long as the angle, whose tangent is equal to the sum of the modulating vectors divided by the carrier vector, does not exceed 30° (the range through which the

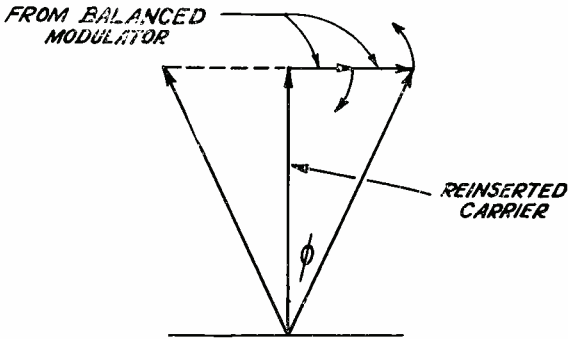


Fig. 6

tangent is approximately equal to the angle) the phase modulation can be said to vary linearly with the modulating components.<sup>3</sup>

The peak-frequency deviation of a frequency-modulated wave is related to the peak-phase deviation by the expression

$$\phi = -\frac{360}{2\pi} \times \frac{\text{Frequency Deviation}}{\text{Modulating Frequency}}$$

in which  $\phi$  is the peak-phase deviation in degrees.

If it is desired to produce a frequency deviation of  $\pm 75,000$  cycles with a 50-cycle modulating frequency, the phase displacement would amount to  $\pm 86,000$  degrees. If the assumption of 30 degrees for the

<sup>3</sup> Actually 30° phase modulation by this process results in nearly 10 per cent harmonic distortion, but since the resulting frequency modulation is a function of the product of the phase deviation and the modulating frequency the maximum phase displacement is required only for full modulation at the lowest modulating frequency.

maximum permissible-source modulation is divided into 86,000, the required carrier-frequency multiplication is seen to approach a value of 3000 times. If the original phase-modulated frequency is, say, 200 kc, eight "doubler" stages, providing a multiplication of 256 times, would give an output frequency of 51.2 megacycles. This frequency might then be heterodyned down to one-twelfth of the desired final-transmitter frequency. Two additional doubler stages and a tripler stage would then provide the correct carrier-output frequency and an overall multiplication of 3072. Obviously the heterodyning process has no effect on the absolute frequency deviation.

A system for phase modulation capable of producing phase deviations of several hundred degrees was described by Mr. R. E. Shelby of the National Broadcasting Company in a paper presented at the annual meeting of the Institute of Radio Engineers in New York in July, 1939. This system utilizes a cathode-ray tube of special design having a spiral target, which is scanned by a circularly deflected beam rotating at the carrier frequency or some sub-multiple thereof. The diameter of the circular pattern is varied in accordance with the desired modulation, and thereby alters the phase of the cycle at which the beam strikes the spiral anode. Output circuits connected to the spiral electrode can then extract the phase-modulated energy. This energy requires less frequency multiplication to produce a desired frequency deviation.

## VII. DIRECT FREQUENCY MODULATION

A more direct system for producing frequency modulation utilizes a "reactance tube", similar to those used for automatic-frequency control, directly across the tank circuit of an oscillating vacuum tube. With this arrangement the transmitter-output frequency may be modulated directly without the need for frequency multiplication. However, it is usually convenient and desirable to use some doubler or tripler stages similar to those employed in a high-frequency amplitude-modulated wave transmitter. Of course, the source frequency cannot be crystal controlled directly, but carrier-frequency control can be maintained by heterodyning the carrier wave with a crystal-controlled oscillator to some low value, which is caused to operate a sensitive discriminator circuit. The output of the discriminator in turn affects the d-c bias of the original reactance control tube in the proper manner to correct for mistuning or frequency drift of the source oscillator. Carrier-wave stability within the limits of a few hundred cycles, even for a 40-Mc transmitter, can be maintained in this manner.

### VIII. GENERALIZED FREQUENCY-MODULATED-WAVE RECEIVER CONSIDERATIONS

The radio frequency, first detector and intermediate frequency circuits of a frequency-modulated-wave receiver are identical basically with those in an amplitude-modulated-wave receiver. The only important difference is in the width of the pass band, which is generally several times greater in the frequency-modulated-wave receiver.

A detector of amplitude modulation, of and by itself, is immune to variations in the frequency of the applied wave. There can be no exact counterpart in the form of a frequency-modulation detector immune to amplitude variations. Zero amplitude is bound to produce zero output from any detector, so the output of all detectors must be some function of amplitude.

For this reason the second detector of a frequency-modulated-wave receiver is usually preceded by a limiter stage whose output is constant for wide variations in the amplitude of the applied signal. However, this is necessary only because of the inherent limitations of the detector and thus it might properly be considered as an integral part of the detection circuit.

Another characteristic of the usual frequency-modulation detector still further reduces its output response to amplitude variations. This is occasioned by the common practice of using so-called back-to-back or "push-pull" detectors. These are so arranged that a frequency deviation in a given direction causes an increase in the current or voltage output of one, while simultaneously causing a decrease in the output of the other. Both detectors, however, respond similarly to changes in amplitude of the applied wave. Thus with the output circuits of the two connected in series opposition, amplitude variations can act *only* to increase or decrease the "sensitivity" of the combination to frequency modulation, and cannot produce output in the absence of frequency deviations.

#### FREQUENCY-MODULATION BIBLIOGRAPHY

Notes on the Theory of Modulation—J. R. Carson. *Proc. I.R.E.*, February 1922, p. 57.

The Reduction of Atmospheric Disturbances—J. R. Carson. *Proc. I.R.E.*, July 1928, p. 967.

Über Frequenzmodulation—H. Roder. *Telefunken-Zeitung*, No. 53, 1929, p. 48.

Frequency Modulation—J. Harmon. *Wireless World*, January 22, 1930, p. 89.

A Study of the Frequency-Modulation Problem—A. Heilman. *E.N.T.* (*in German*), June 1930, p. 217.

Frequency Modulation—B. Van der Pol. *Proc. I.R.E.*, July 1930, p. 1154.

Frequency Modulation and Distortion—T. L. Eckersley. *Experimental Wireless & Wireless Engineer*, Sept. 1930, p. 482.

Note on Relationships Existing Between Radio Waves Modulated in Frequency and in Amplitude—C. H. Smith. *Experimental Wireless & Wireless Engineer*, Nov. 1930, p. 609.

Amplitude, Phase and Frequency Modulation—Hans Roder. *Proc. I.R.E.*, Dec. 1931, p. 2145.

The Reception of Frequency-Modulated Radio Signals—V. J. Andrew. *Proc. I. R.E.*, May 1932, p. 835.

Phase Shift in Radio Transmitters—W. A. Fitch, *Proc. I.R.E.*, May 1932, p. 863.

A New Electrical Method of Frequency Analysis and Its Application to Frequency Modulation—W. S. Barrow. *Proc. I.R.E.*, October 1932, p. 1626.

Frequency Modulation and the Effects of a Periodic Capacitance Variation in a Non-dissipative Oscillatory Circuit—W. L. Barrow. *Proc. I.R.E.*, Aug. 1933, p. 1182.

High-Frequency Measurements—August Hund. (*A book*) McGraw-Hill Co., 1933.

Transmission Lines as Frequency Modulators—A. V. Eastman and E. D. Scott. *Proc. I.R.E.*, July 1934, p. 873.

Theoretical and Experimental Investigation of Frequency and Phase-Modulated Oscillators—F. Lautenschlager. *E.N.T.*, October 1934, p. 357.

The Detection of Frequency-Modulated Waves—J. G. Chaffee. *Proc. I.R.E.*, May 1935, p. 517.

Phase-Frequency Modulation—D. G. Fink. *Electronics*, November 1935, p. 431.

Frequency Modulation on Ultra-Short Waves—D. Pollack. *Radio News*, February 1936, p. 458.

A Method of Reducing Disturbances in Radio Signalling by a System of Frequency Modulation—E. H. Armstrong. *Proc. I.R.E.*, May 1936, p. 689.

Frequency-Modulation Propagation Characteristics—M. G. Crosby. *Proc. I.R.E.*, June 1936, p. 898.

A Study of the Characteristics of Noise—V. D. Landon. *Proc. I.R.E.*, Nov. 1936, p. 1514.

Frequency-Modulated Generators—A. W. Barber. *Radio Engineering*, Nov. 1936, p. 14.

Frequency-Modulation Noise Characteristics—M. G. Crosby. *Proc. I.R.E.*, April 1937, p. 472.

Communication Engineering—W. L. Everitt. (*A book*) McGraw-Hill Co., 1937, p. 408 (2nd edition).

Radio Engineering—F. E. Terman. (*A book*) McGraw-Hill Co., 1937, p. 380.

Noise in Frequency Modulation—H. Roder. *Electronics*, May 1937, p. 22.

Application of the Autosynchronized Oscillator to Frequency Demodulation—J. R. Woodyard. *Proc. I.R.E.*, May 1937, p. 612.

Variable-Frequency Electric Circuit Theory with Application to the Theory of Frequency Modulation—Carson and Fry. *Bell System Technical Journal*, October 1937, p. 513.

Effects of Tuned Circuits on a Frequency-Modulated Signal—Hans Roder. *Proc. I.R.E.*, December 1937, p. 1617.

Armstrong's Frequency Modulator—D. L. Jaffe. *Proc. I.R.E.*, April 1938, p. 475.

Carrier and Side-Frequency Relations with Multi-Tone Frequency for Phase Modulation—M. G. Crosby. *RCA Review*, July 1938, p. 103.

Reduction of Interference by Frequency Modulation—E. H. Plump. *Hochfrequenztechnik und Electroakustik*, Sept. 1938, p. 73.

Communication by Phase Modulation—M. G. Crosby. *Proc. I.R.E.*, Vol. 27, No. 2, Feb. 1939, p. 126.

The Application of Negative Feedback to Frequency-Modulation Systems—J. G. Chaffee. *Bell System Technical Journal*, Oct. 1937, p. 404. *Proc. I.R.E.*, May 1939, p. 317.

A Receiver for Frequency Modulation—J. R. Day. *Electronics*, June 1939, p. 32.

A Noise-Free Radio Receiver for the Reception of Frequency-Modulated Ultra-Short Waves—G. W. Fyler and J. A. Worcester. *Gen. Electric Review*, July 1939, p. 307.

Frequency Modulation—C. H. Yocum. *Communications*, Nov. 1939, p. 5.

Frequency-Modulated Transmitters. *Electronics*, Nov. 1939, p. 20.

# CASCADE AMPLIFIERS WITH MAXIMAL FLATNESS

BY

V. D. LANDON

RCA Manufacturing Company, Inc., Camden, N. J.

(Continued from January, 1941 RCA REVIEW)

## PART II

### APPENDIX 1—PERFORMANCE OF CIRCUITS OF FIGURE 1

The performance of Figure 1-a is

$$\begin{aligned}\frac{E_1}{E_o} &= \frac{r}{j\omega L + r} \\ &= \frac{r/L}{j\omega + r/L}\end{aligned}$$

Letting  $\beta = r/L$

and  $A = \text{gain at zero frequency} = \text{unity}$

$$\begin{aligned}\frac{E_1}{E_o} &= A \frac{\beta}{j\omega + \beta} \\ \left| \frac{E_1}{E_o} \right| &= A \frac{\beta}{\sqrt{\omega^2 + \beta^2}}\end{aligned}$$

The performance of Figure 1-b is:

$$\begin{aligned}\frac{E_1}{E_o} &= g_m \frac{1}{j\omega C + 1/R} \\ &= g_m \frac{1}{RC} \\ &= g_m \frac{1}{j\omega + \frac{1}{RC}}\end{aligned}$$

$$\text{Letting } \beta = \frac{1}{RC}$$

and  $A = \text{gain at zero frequency} = g_m R$

$$\frac{E_1}{E_o} = A \frac{\beta}{j\omega + \beta}$$

$$\left| \frac{E_1}{E_o} \right| = A \frac{\beta}{\sqrt{\omega^2 + \beta^2}}$$

#### APPENDIX 2—PERFORMANCE OF CIRCUITS OF FIGURE 2

The performance of Figure 2-a is:

$$\frac{E_1}{E_o} = \frac{\frac{R}{1 + jR\omega C}}{r + j\omega L + \frac{R}{1 + jR\omega C}}$$

$$= \frac{R}{r - \omega^2 RLC + j\omega(rRC + L) + R}$$

$$= \frac{1}{LC} \frac{1}{-\omega^2 + j\omega \left( \frac{1}{RC} + \frac{r}{L} \right) + \frac{r+R}{R} \frac{1}{LC}}$$

$$= \frac{R}{r+R} \left( \frac{r+R}{R} \frac{1}{LC} \right) \frac{1}{-\omega^2 + j\omega \left( \frac{1}{RC} + \frac{r}{L} \right) + \frac{r+R}{R} \frac{1}{LC}}$$

$$\text{Letting } \alpha = \frac{1}{RC} + \frac{r}{L} \quad (\text{the damping factor})$$

$$\beta = \sqrt{\frac{r+R}{R} \frac{1}{LC}} \quad (\text{the nominal cut-off frequency})$$

$$A = \frac{R}{r+R} \quad (\text{the gain at zero frequency})$$

$$\frac{E_1}{E_o} = A \frac{\beta^2}{-\omega^2 + j\omega\alpha + \beta^2}$$

$$\left| \frac{E_1}{E_o} \right| = A \frac{\beta^2}{\sqrt{\omega^4 + \omega^2(\alpha^2 - 2\beta^2) + \beta^4}}$$

The performance of Figure 2-b is:

$$\begin{aligned} \left| \frac{E_1}{E_o} \right| &= \frac{g_m}{j\omega C + \frac{1}{R} + \frac{1}{j\omega L + r}} \frac{r}{j\omega L + r} \\ &= g_m r \frac{R}{-\omega^2 LCR + j\omega CrR + j\omega L + r + R} \\ &= g_m r \frac{1}{LC} \frac{1}{-\omega^2 + j\omega \left( \frac{1}{RC} + \frac{r}{L} \right) + \frac{r+R}{R} \frac{1}{LC}} \\ &= g_m \frac{rR}{r+R} \left( \frac{r+R}{R} \frac{1}{LC} \right) \frac{1}{-\omega^2 + j\omega \left( \frac{1}{RC} + \frac{r}{L} \right) + \frac{r+R}{R} \frac{1}{LC}} \\ &= A \beta^2 \frac{1}{-\omega^2 + j\omega\alpha + \beta^2} \\ \left| \frac{E_1}{E_o} \right| &= A \frac{\beta^2}{\sqrt{\omega^4 + \omega^2(\alpha^2 - 2\beta^2) + \beta^4}} \end{aligned}$$

These are the same expressions as those obtained for Figure 2-a, but it must be remembered that  $A$  had the value  $\frac{R}{r+R}$  there, while for Figure 2-b,  $A$  has the value  $g_m \frac{rR}{r+R}$ .

APPENDIX 3

The derivative of  $\left| \frac{E_1}{E_o} \frac{E_2}{E_1} \dots \right|$  with respect to  $\omega^2$  is

$$\begin{aligned} \frac{d}{d\omega^2} \left| \frac{E_1}{E_o} \frac{E_2}{E_1} \dots \right| &= (A_1 A_2 \dots) (\beta_1 \beta_2^2 \dots) \\ &= \frac{n\omega^{2n-2} + (n-1)C_{n-1}\omega^{2n-4} + (n-2)C_{n-2}\omega^{2n-6} \dots + C_1}{(\omega^{2n} + C_{n-1}\omega^{2n-2} + C_{n-2}\omega^{2n-4} \dots + C_1\omega^2 + \beta_1\beta_2^2 \dots)^{3/2}} \end{aligned}$$

If above equals zero, then

$$n\omega^{2n-2} + (n-1)C_{n-1}\omega^{2n-4} + (n-2)C_{n-2}\omega^{2n-6} \dots + C_1 = 0$$

Setting  $\omega = 0$

$$C_1 = 0$$

Setting successively higher derivatives equal to zero at  $\omega = 0$  makes other coefficients go to zero up to the  $(n-1)$ th derivative which makes  $C_{n-1}$  go to zero.

#### APPENDIX 4

The values of the  $n$ th root of  $(-1)$ .

From the standpoint of the theory of the complex variable,

$$\begin{aligned} -1 &= e^{j\pi} \quad (\text{where } j = \sqrt{-1}) \\ &= e^{j\pi} e^{j2\pi(m-1)} \quad \text{where } m \text{ is any integer} \\ &= e^{j\pi(1+2m-2)} \\ &= e^{j\pi(2m-1)} \\ (-1)^{1/n} &= e^{j\pi/n(2m-1)} \\ &= \cos \left[ \frac{\pi}{n} (2m-1) \right] + j \sin \left[ \frac{\pi}{n} (2m-1) \right] \end{aligned}$$

$m$  may be taken as any integer, but the roots start to repeat if values of  $m$  are chosen larger than  $n$ . Therefore, all the roots are found by assigning successive values to  $m$  from 1 to  $n$ .

The geometric interpretation of the roots, for  $n$  equals 8, is shown in Figure 3. The relationship between conjugate roots is also shown.

#### APPENDIX 5

Proof that if  $\omega = p - \frac{p_o^2}{p}$ , then  $\omega$  is the width of the band between frequencies of equal attenuation.

If  $p_1$  is any fixed value of the angular frequency  $p$  and if  $p_2$  is a value giving equal and opposite reactance to that at  $p_1$ , (in a circuit resonant to  $p_o$ ) then

$$\begin{aligned} \omega &= p_1 - \frac{p_o^2}{p_1} = -p_2 + \frac{p_o^2}{p_2} \\ p_1 + p_2 &= \frac{p_o^2(p_1 + p_2)}{p_1 p_2} \end{aligned}$$

Therefore,  $p_o = p_1 p_2$

Then if 
$$\omega = p_1 - \frac{p_o^2}{p_1}$$

$$\begin{aligned} \omega &= p_1 - \frac{p_1 p_2}{p_1} \\ &= p_1 - p_2 \end{aligned}$$

Hence, the logical interpretation of  $\omega$  is the band width between any two points of equal attenuation on the performance curve.

APPENDIX 6—THE PERFORMANCE OF THE CIRCUIT OF FIGURE 7-a

In Figure 7-a, the coefficient of coupling is  $K = \frac{M}{\sqrt{L_p L_s}}$ . The whole

primary circuit is resonant below  $p_o$ . It is resonant to  $p_o$  if a portion of the inductance equal to  $L_p K^2$  is omitted. If  $L_p$  could be replaced by two inductors, one having no coupling to  $L_s$  and the other coupled 100 per cent, the portion coupled 100 per cent would have to have an inductance equal to  $L_p K^2$  in order for the mutual inductance between primary and secondary circuits to be unchanged.

In a transformer having 100 per cent coupling and no internal resistance, impedances may be changed from one winding to another by multiplying the impedance by the square of the turns ratio. The only effect on the signal in the impedance is to multiply the voltage by the turns ratio. The effective turns ratio is  $L_s/M$  (because  $L_s M^2/L_s^2 = M^2/L_s = L_p K^2$ ).

Thus  $C_s \frac{L_s^2}{M^2}$  and  $R \frac{M^2}{L_s^2}$  may be considered to be shunted across

$L_p K^2$  in Figure 7-a, thus giving the band-pass analogue of Figure 2-a. However, the actual output voltage of Figure 7-a is larger than that of the equivalent circuit just described, by the ratio  $L_s/M$ .

In view of this equivalence, it can be seen that the performance of Figure 7-a is:

$$\frac{E_1}{E_o} = A \frac{\beta^2}{\sqrt{\omega^4 + \omega^2 (\alpha^2 - 2\beta^2) + \beta^4}}$$

where  $A = \text{gain at } p = p_o \quad (\text{or } \omega = 0)$

$$= \frac{R \frac{M^2}{L_s^2} L_s}{r + R \frac{M^2}{L_s^2} M}$$

For Figure 2-a

$$\beta^2 = \frac{r + R}{R} \frac{1}{LC}$$

Hence, for Figure 7-a

$$\begin{aligned} \beta^2 &= \frac{r + R \frac{M^2}{L_s^2}}{R \frac{M^2}{L_s^2}} \frac{1}{L_p (1 - K^2) C_s \frac{L_s^2}{M^2}} \\ &= \frac{r L_s^2}{R M^2} \frac{1}{L_p (1 - K^2) C_s \frac{L_s^2}{M^2}} + \frac{1}{L_p (1 - K^2) C_s \frac{L_s^2}{M^2}} \\ &= \frac{r}{L_p (1 - K^2)} \frac{1}{R C_s} + \frac{1}{L_s C_s \frac{L_p L_s}{M} (1 - K^2)} \\ &= \alpha_p \alpha_s + p_o^2 \frac{K^2}{(1 - K^2)} \end{aligned}$$

If  $\alpha_p = \alpha_s = \alpha/2$

then  $\alpha_p \alpha_s = \alpha^2/4 = \beta^2 \sin^2 \left[ \frac{\pi}{2n} (2m - 1) \right]$

Substituting this for  $\alpha_p \alpha_s$  in above equation for  $\beta^2$ .

$$\beta^2 = \beta^2 \sin^2 \left[ \frac{\pi}{2n} (2m - 1) \right] + p_o^2 \frac{K^2}{1 - K^2}$$

then  $p_o^2 \frac{K^2}{1 - K^2} = \beta^2 \left( 1 - \sin^2 \left[ \frac{\pi}{2n} (2m - 1) \right] \right)$

$$= \beta^2 \cos^2 \left[ \frac{\pi}{2n} (2m - 1) \right]$$

Letting  $b = \beta/p_o \cos \left[ \frac{\pi}{2n} (2m - 1) \right]$

$$K^2 = b^2 - b^2 K^2$$

$$K^2 = \frac{b^2}{1 + b^2}$$

$$K = \frac{b}{\sqrt{1 + b^2}}$$

Of course, if  $b$  is small,  $b^2$  may be neglected and  $K \approx \beta/p_o \cos$

$$\left[ \frac{\pi}{2n} (2m - 1) \right] \text{ (the symbol } \approx \text{ means "is approximately equal to.")}$$

It should be remembered that this is only for equal damping factors in primary and secondary circuits. If all the damping can be concentrated in one circuit, then:

$$\beta^2 = p_o^2 \frac{K^2}{1 - K^2}$$

$$K = \frac{\beta/p_o}{\sqrt{1 + (\beta/p_o)^2}} \text{ if } (\beta/p_o)^2 \text{ can be neglected}$$

$$K \approx \beta/p_o$$

#### APPENDIX 7—THE GAIN OF FIGURE 7-b

The gain of Figure 7-b at  $p = p_o$  may be calculated approximately as follows:

The ideal condition of  $R_p = \infty$  is assumed.

The primary resonant impedance is

$$Z_p = \frac{p_o^2 L_p^2}{R_s \frac{M^2}{L_s^2}} \quad \text{(See Appendix 6)}$$

The ratio of the voltage across  $L_p$  to that across the reflected resistance  $\left( R_s \frac{M^2}{L_s^2} \right)$  is approximately

$$\frac{R_s \frac{M^2}{L_s^2}}{p_o L_p}$$

The step-up ratio from the voltage across  $R_s \frac{M^2}{L_s^2}$  to the output voltage is  $\frac{L_s}{M}$ .

Then, the gain is

$$A \approx g_m \frac{p_o^2 L_p^2}{R_s \frac{M^2}{L_s^3}} \frac{R_s \frac{M^2}{L_s^2}}{p_o L_p} \frac{L_s}{M}$$

the symbol  $\approx$  means, "is approximately equal to."

$$\begin{aligned} A &\approx g_m p_o L_p \frac{L_s}{M} = g_m \frac{1}{p_o} \frac{1}{\sqrt{L_p C_p}} \frac{1}{\sqrt{L_s C_s}} \sqrt{L_p L_s} \frac{\sqrt{L_p L_s}}{M} \\ &= g_m \frac{1}{p_o} \frac{1}{\sqrt{C_p C_s}} K \\ &\approx g_m \frac{1}{\beta \sqrt{C_p C_s}} \end{aligned}$$

It should be noted that the gain is independent of  $\alpha$  and, hence, independent of  $m$ .

APPENDIX 8—BAND-PASS CHARACTERISTICS FROM A CASCADE AMPLIFIER EMPLOYING A SINGLE RESONANT CIRCUIT IN EACH STAGE

(A) Direct method.

In the following,  $n$  stages are assumed to be operated in cascade. If  $n$  is odd, one stage is tuned to  $p_o$ , the mean pass-band angular fre-

quency. The remainder of the stages are considered in pairs. If  $n$  is even, all the stages are considered in pairs. In each pair of stages, one is tuned to a higher frequency  $p_a$  and one to a lower frequency  $p_b$  in such a manner that  $p_a p_b = p_o^2$ .

The value of  $p_a$  (and of  $p_b$ ) is different for each pair.

The circuit of each stage is assumed to be that of Figure 8. The performance of the stage resonant to  $p_o$  is:

$$\begin{aligned} \frac{E_1}{E_o} &= g_m \frac{1}{jpC + \frac{1}{j\omega L} + \frac{1}{R}} \\ &= g_m R \frac{1}{p_o C R} \\ &\quad \frac{1}{j(p/p_o - p_o/p) + \frac{1}{p_o C R}} \\ &= A \frac{1/Q}{j(p/p_o - p_o/p) + 1/Q} \end{aligned}$$

where  $Q = RCp_o$ . (The distinction between  $Q$  and  $q$  should be noted. The value of  $q$  is  $RC\beta$ .)

$$\left| \frac{E_1}{E_o} \right| = A \frac{1/Q}{\sqrt{(p/p_o - p_o/p)^2 + 1/Q^2}}$$

Similarly, the performance of one of the detuned stages is:

$$\left| \frac{E_a}{E_o} \right| = A_a \frac{1/Q_a}{\sqrt{(p/p_a - p_a/p)^2 + 1/Q_a^2}}$$

where  $A_a = g_m R_a =$  gain at  $p = p_a$

$$Q_a = R_a C p_a$$

The performance of the other stage is:

$$\left| \frac{E_b}{E_o} \right| = A_b \frac{1/Q_b}{\sqrt{(p/p_b - p_b/p)^2 + 1/Q_b^2}}$$

now  $p/p_a - p_a/p = p/p_o \cdot p_o/p_a - p_o/p \cdot p_a/p_o$

Letting  $x = \ln p/p_o; y = \ln p_b/p_o = \ln p_o/p_a$

$$e^x = p/p_o; e^y = p_b/p_o$$

$$2 \sinh x = p/p_o - p_o/p; 2 \sinh y = p_b/p_o - p_o/p_b$$

$$2 \sinh(x+y) = p/p_o \cdot p_o/p_a - p_o/p \cdot p_a/p_o$$

$$= p/p_a - p_a/p$$

$$2 \sinh(x-y) = p/p_o \cdot p_o/p_b - p_o/p \cdot p_b/p_o$$

$$= p/p_b - p_b/p$$

$$\left| \frac{E_a}{E_o} \right| = A_a \frac{1/Q_a}{\sqrt{4 \sinh^2(x+y) + 1/Q_a^2}}$$

$$\left| \frac{E_b}{E_a} \right| = A_b \frac{1/Q_b}{\sqrt{4 \sinh^2(x-y) + 1/Q_b^2}}$$

$$\left| \frac{E_a}{E_o} \frac{E_b}{E_a} \right| = A_a A_b \frac{1/Q_a \cdot 1/Q_b}{\sqrt{(4 \sinh^2(x+y) + 1/Q_a^2)(4 \sinh^2(x-y) + 1/Q_b^2)}}$$

Letting  $Q_a = Q_b = Q$  the portion under the radical becomes:

$$16 \sinh^2(x+y) \sinh^2(x-y) + 4/Q^2$$

$$[\sinh^2(x+y) + \sinh^2(x-y)] + 1/Q^2$$

Now  $\sinh^2(x+y) \sinh^2(x-y)$

$$= [\sinh^2 x \cosh^2 y - \cosh^2 x \sinh^2 y]^2$$

$$= [\sinh^2 x (1 + \sinh^2 y) - (1 + \sinh^2 x) \sinh^2 y]^2$$

$$= [\sinh^2 x - \sinh^2 y]^2$$

$$= \sinh^4 x + \sinh^4 y - 2 \sinh^2 x \sinh^2 y$$

And  $\sinh^2(x+y) + \sinh^2(x-y)$

$$= [\sinh x \cosh y + \cosh x \sinh y]^2$$

$$+ [\sinh x \cosh y - \cosh x \sinh y]^2$$

$$= 2 \sinh^2 x \cosh^2 y + 2 \cosh^2 x \sinh^2 y$$

$$= 2 \sinh^2 x (1 + \sinh^2 y) + 2 \sinh^2 y (1 + \sinh^2 x)$$

$$= 4 \sinh^2 x \sinh^2 y + 2 \sinh^2 x + 2 \sinh^2 y$$

So that

$$\left| \frac{E_a}{E_o} \frac{E_b}{E_a} \right| = \frac{A_a A_b 1/Q^2}{\sqrt{16[\sinh^4 x + \sinh^4 y - 2 \sinh^2 x \sinh^2 y] + 4/Q^2[4 \sinh^2 x \sinh^2 y + 2 \sinh^2 x + 2 \sinh^2 y] + 1/Q^4}}$$

Letting  $2 \sinh x = w$ ;  $2 \sinh y = s$

$$\left| \frac{E_a}{E_o} \frac{E_b}{E_a} \right| = \frac{A_a A_b 1/Q^2}{\sqrt{w^4 - w^2[2s^2 - s^2/Q^2 - 2/Q^2] + [s^2 + 1/Q^2]^2}}$$

If  $n$  stages are placed in cascade the performance of the overall amplifier is:

$$\left| \frac{E_n}{E_o} \right| = (A_1 A_2 \dots) \frac{(1/Q_1^2 1/Q_2^2 \dots)}{\sqrt{w^{2n} + w^{2n-2} C_{n-1} \dots - w^2 C_1 + C_o^{2n}}}$$

where  $A_1$  is the value of  $A_a A_b$  for the first pair of stages,  $A_m$  is the value of  $A_a A_b$  for the  $m$ th pair of stages.

$Q_1 Q_2 \dots Q_m$  are the various values of  $Q$  for the various pairs of stages.

Setting the first  $(n - 1)$  derivatives of  $\left| \frac{E_n}{E_o} \right|$  (with respect to  $w^2$ ) equal to zero at the point  $w = 0$  gives the flattest curve. This makes

$$C_{n-1} = C_{n-2} \dots = C_1 = 0 \quad \text{so that}$$

$$\left| \frac{E_n}{E_o} \right| = (A_1 A_2 \dots) \frac{(1/Q_1^2 1/Q_2^2 \dots)}{\sqrt{w^{2n} + C_o^{2n}}}$$

$w^{2n} + C_o^{2n}$  may be factored into  $n$  factors of which the  $m$ th factor is:

$$w^2 - C_o^2 \left[ \cos \left[ \frac{\pi}{n} (2m - 1) \right] + j \sin \left[ \frac{\pi}{n} (2m - 1) \right] \right] \quad (\text{see Appendix 4})$$

the conjugate is  $w^2 - C_o^2 \left[ \cos \left[ \frac{\pi}{n} (2m - 1) \right] - j \sin \left[ \frac{\pi}{n} (2m - 1) \right] \right]$

the product is  $w^4 - 2w^2 C_o^2 \cos \left[ \frac{\pi}{n} (2m - 1) \right] + C_o^4$

For maximal flatness in the overall curve, this expression is set equal to the trinomial under the radical in the general performance equation for the  $m$ th pair of stages.

$$\begin{aligned} w^4 - 2w^2 C_o^2 \cos \left[ \frac{\pi}{n} (2m - 1) \right] + C_o^4 \\ = w^4 - w^2 [2s^2 - s^2/Q^2 - 2/Q^2] + [s^2 + 1/Q^2] \end{aligned}$$

Then

$$C_o^2 = s^2 + 1/Q^2$$

and

$$\begin{aligned} -2 C_o \cos \left[ \frac{\pi}{n} (2m - 1) \right] &= -2s^2 + s^2/Q^2 + 2/Q^2 \\ &= -2s^2 + (s^2 + 2)(C_o^2 - s^2) \end{aligned}$$

$$s^4 + s^2(2 - C_o^2 + 2) - C_o^2 \left( 2 \cos \left[ \frac{\pi}{n} (2m - 1) \right] + 2 \right) = 0$$

$$\begin{aligned} s^2 &= \frac{C_o^2 - 4}{2} \pm \sqrt{\left( \frac{C_o^2 - 4}{2} \right)^2 + C_o^2 \left( 2 \cos \left[ \frac{\pi}{n} (2m - 1) \right] + 2 \right)} \\ &= -\frac{4 - C_o^2}{2} + \sqrt{\left( \frac{4 + C_o^2}{2} \right)^2 - C_o^2 \left( 2 - 2 \cos \left[ \frac{\pi}{n} (2m - 1) \right] \right)} \end{aligned}$$

$$1/Q^2 = C_o^2 - s^2$$

$$= \frac{C_o^2 + 4}{2} - \sqrt{\left( \frac{4 + C_o^2}{2} \right)^2 - C_o^2 \left( 2 - 2 \cos \left[ \frac{\pi}{n} (2m - 1) \right] \right)}$$

The last two equations are equivalent to a pair of equations given by Von Rudolph Schienemann in *Telegraphen Fernsprech—Funk—Und Fernseh Technik*, January, 1939.

This can be simplified considerably if it is assumed that  $C_o^2$  is quite small.

$$s^2 = \frac{C_o^2}{2} - 2 + \sqrt{4 + 2C_o^2 + C_o^4/4 - 2C_o^2 - 2C_o^2 \cos \left[ \frac{\pi}{n} (2m - 1) \right]}$$

neglecting  $C_o^4$

$$\begin{aligned}
 s^2 &\approx \frac{C_o^2}{2} - 2 + 2 \sqrt{1 + \frac{C_o^2}{2} \cos \left[ \frac{\pi}{n} (2m - 1) \right]} \\
 &\approx C_o^2/2 - 2 + 2 \left( 1 + \frac{C_o^2}{4} \cos \left[ \frac{\pi}{n} (2m - 1) \right] \right) \\
 &= C_o^2/2 \left( 1 + \cos \left[ \frac{\pi}{n} (2m - 1) \right] \right) \\
 &= C_o^2 \cos^2 \left[ \frac{\pi}{2n} (2m - 1) \right] \\
 s &\approx C_o \cos \left[ \frac{\pi}{2n} (2m - 1) \right]
 \end{aligned}$$

At the point where the overall response drops to  $1/\sqrt{2}$ ;  $w^{2n} = C_o^{2n}$ , or  $w = C_o$ . But  $w = p/p_o - p_o/p = 1/p_o (p - p_o^2/p) = \beta/p_o$ . Therefore  $C_o = \beta/p_o$  where  $\beta$  is the band width at  $1/\sqrt{2}$  response.

$$s = p_o/p_a - p_a/p_o = \frac{p_b - p_a}{p_o} \approx \pm \beta/p_o \cos \left[ \frac{\pi}{2n} (2m - 1) \right]$$

$$p_a - p_b \approx \beta \cos \left[ \frac{\pi}{2n} (2m - 1) \right]$$

similarly,

$$1/Q \approx \beta/p_o \sin \left[ \frac{\pi}{2n} (2m - 1) \right]$$

It should be noted that although

$$Q_a = Q_b$$

$$Q_a = RC_a p_a, \text{ while } Q_b = R_b C p_b$$

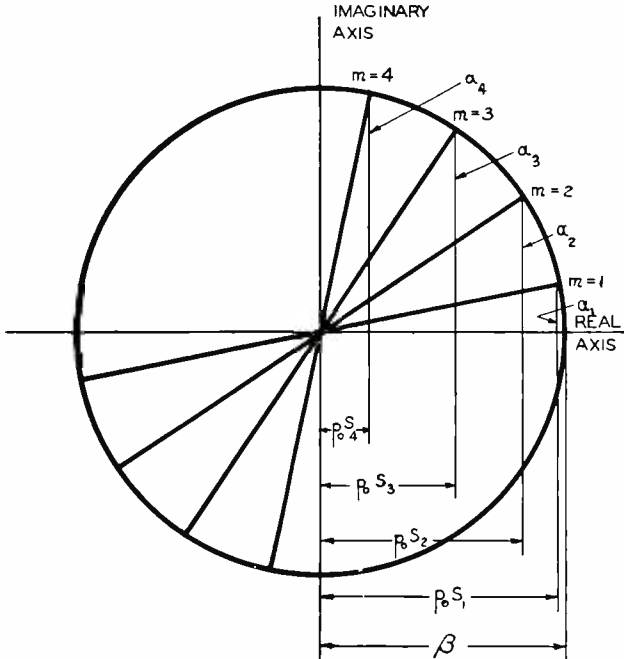
so that  $R_a = R_b p_b/p_a$ .

However, if  $\beta$  is small so that  $p_b/p_a \approx 1$  then  $R_a \approx R_b$  making this assumption:

$$1/Q = \frac{1}{RC p_a} \approx \alpha/p_o$$

$$\alpha \approx \frac{1}{RC} \approx \beta \sin \left[ \frac{\pi}{2n} (2m - 1) \right]$$

$$R \approx \frac{1}{C\beta \sin \left[ \frac{\pi}{2n} (2m - 1) \right]}$$



GEOMETRICAL INTERPRETATION OF  $\alpha = \beta \sin \left[ \frac{\pi}{2n} (2m-1) \right]$  AND  $p_b S = \beta \cos \left[ \frac{\pi}{2n} (2m-1) \right] = p_b - p_a$  FOR  $n = 8$  (8 STAGES WITH ONE TUNED CIRCUIT PER STAGE)

Fig. 11.

A geometrical interpretation of  $\alpha$  and of  $p_b - p_a$  is shown in Figure 11.

THE GAIN PER STAGE

The performance of a single stage is:

$$\left| \frac{E_a}{E_o} \right| = g_m \frac{A_a}{Q_a} \frac{1}{\sqrt{(p/p_a - p_a/p)^2 + 1/Q_a^2}}$$

Letting  $p = p_o$ .

$$\begin{aligned} \left| \frac{E_a}{E_o} \right| &= g_m \frac{R_a}{R_a C p_a} \frac{1}{\sqrt{s^2 + 1/Q_o^2}} \\ &= g_m \frac{1}{C p_a} \frac{1}{C_o} \\ &= \frac{g_m}{C p_a} \frac{p_o}{\beta} \\ &\approx \frac{g_m}{\beta C} \end{aligned}$$

The gain of a pair of stages is accurately:

$$\frac{g_m}{C p_a} \frac{p_o}{\beta} \frac{g_m}{C p_b} \frac{p_o}{\beta} = \left( \frac{g_m}{\beta C} \right)^2$$

because  $p_o^2 = p_a p_b$ .

(B) Indirect Method.

As a check on the algebra, it is interesting to note that the same result may be obtained from the solution for Figure 7-a described in Appendix 6.

Identical circuits coupled together, as in Figure 7-a, may be replaced, from a selectivity standpoint, by the same circuits cascaded and mistuned by plus and minus  $M$ .

The frequency of resonance of one circuit becomes

$$p_a = \frac{1}{\sqrt{CL(1-k)}} = \frac{p_o}{\sqrt{1-k}} \approx p_o(1+k/2)$$

$$p_b \approx p_o(1-k/2) \quad \text{(for the second circuit)}$$

$$p_a - p_b \approx p_o K$$

$$\approx \beta \cos \left[ \frac{\pi}{2n} (2m-1) \right] \quad \text{(from Appendix 6)}$$

$$\alpha_a \approx \alpha_b \approx \frac{1}{2} \alpha = \beta \sin \left[ \frac{\pi}{2n} (2m-1) \right]$$

APPENDIX 9—COMPARISON TO CONVENTIONAL FILTERS

For maximal flatness in a cascade low-pass amplifier, when  $n = 3$ , two stages are required, a single-element stage (like those in Figure 1) and a two-element stage (like one of the circuits of Figure 2). In the latter,

$$\alpha/\beta = 2 \sin \left[ \frac{\pi}{2n} (2m - 1) \right] = 2 \sin \frac{\pi}{6} = 1. \text{ Thus, if the circuit of Figure 2-a is chosen and } r = 0, \text{ then } \alpha/\beta = \frac{1}{RC\beta} = 1.$$

$$R = \frac{1}{\beta C}$$

It will be shown that a one-section low-pass filter is equivalent to the above. This circuit is given in Figure 9.

If the circuit is broken at the point  $P$ , the voltage to ground of the point at the left of the break will double. This is true because of the impedance match at  $P$ . The circuit is symmetrical about this point. If the two circuit fragments are operated separately, the product of the two curves divided by two is the curve of the original circuit. Since the first half, works into an open circuit, the inductance  $L/2$  may be neglected. The circuit has now become the same as Figure 1-b.

For the circuit of Figure 1-b,  $\beta = \frac{1}{RC}$ . Due to labeling, the condenser  $C/2$  in Figure 9, this becomes:

$$\beta = \frac{1}{R C/2} = \frac{2}{\sqrt{L/C C}} = \frac{2}{\sqrt{LC}}$$

The cut-off angular frequency of the low-pass filter is also  $\frac{2}{\sqrt{LC}}$ .

The second fragment of the circuit can be seen to be the same as Figure 2-a (with  $r = 0$ ) except for labeling. For Figure 2-a ( $n = 3, m = 1$ ).

$$\beta = \frac{1}{\sqrt{LC}}$$

$$\alpha = \frac{1}{RC}$$

$$\alpha/\beta = 1.$$

For the fragment of Figure 9, under discussion, the corresponding values are (due to labeling the elements  $L/2$  and  $C/2$ ).

$$\beta = \frac{1}{\sqrt{L/2 C/2}} = \frac{2}{\sqrt{LC}} = \text{cut-off of filter.}$$

And 
$$\alpha = \frac{1}{RC/2} = \frac{1}{\sqrt{L/C C/2}} = \frac{2}{\sqrt{LC}}$$

$$\alpha/\beta = 1$$

The circuit of Figure 9 is thus seen to be equivalent in selectivity to a maximally flat cascade amplifier with  $n = 3$ .

It may be noted in passing, that if resistance is present in series with the inductance, the circuit may be readjusted for maximal flatness anyway, unless the resistance exceeds a certain critical value. The solution is to use unequal terminal resistors of critical values determined experimentally.

#### THE TWO-SECTION LOW-PASS FILTER

A two-section low-pass filter is shown in Figure 10. If this circuit is bisected by breaking the circuit at  $P$ , the two fragments may be operated separately. The product of the two curves divided by two is the same as the curve on the original circuit. In the fragment on the right, the first capacitor is shorted by the generator. The circuit is thus seen to be equivalent to Figure 2-a (with  $r = 0$ ).

The parameters are:

$$\beta = \frac{1}{\sqrt{LC/2}} = \frac{\sqrt{2}}{\sqrt{LC}} \neq \text{cut-off frequency of low-pass filter}$$

$$\alpha = \frac{1}{RC/2} = \frac{1}{\sqrt{L/C C/2}} = \frac{2}{\sqrt{LC}}$$

$$\beta/\alpha = \frac{\sqrt{2}}{2}$$

This does not correspond to any of the values of  $\beta/\alpha$  tabulated for a maximally flat amplifier with  $n = 5$ .

Therefore, the two-section low-pass filter of Figure 10 does not have the flattest performance curve that may be obtained with 5 reactance elements.

# A NEW SERIES OF INSULATORS FOR ULTRA-HIGH-FREQUENCY TUBES

By

L. R. SHARDLOW

Research and Engineering Department, RCA Manufacturing Company, Inc., Harrison, N. J.

*Summary*—The electrical properties of power factor and dielectric constant, and the physical properties of porosity and firing shrinkage have been determined on an alumina-talc-silica series of ceramic bodies. The effect of body composition and firing temperature on the above properties is shown, and some theoretical considerations of these are discussed. It is shown that while small amounts of flux may be advantageous, large amounts are detrimental to the electrical properties. On the other hand large amounts of flux may be beneficial in the production of the desirable physical properties.

UNTIL the past few years, designers of transmitting tubes to be used at high frequencies have depended almost entirely upon natural silicates or fused silica as sources of insulation. The cost and difficulty of fabricating fused silica into complicated shapes have been its chief disadvantages. Among the natural materials, acid magnesium metasilicate, commonly known as soapstone or massive talc, has been widely used. It has one advantage not found in other high-frequency insulators in that it is easily machined to shape in the raw state before being hardened by firing to approximately 1100°C. However, as conditions of use became more exacting because of trends to higher frequencies and higher temperatures of operation, the insulating qualities of this natural material proved to be inadequate.

When the development of high-frequency tubes having close-spaced electrodes began to show the faults of the natural silicate, the ceramists manufactured a material composed of approximately 80 per cent talc. This material, which was better in general than the natural silicate because of a lower percentage of impurities, filled a need at the time, but it was not long before it was judged to be unsatisfactory for the insulation requirements of the newer high-frequency tubes. The demand for better insulation finally became so acute that it was found necessary to develop material especially for this application.

Aluminum oxide was chosen by the author as the base material for the developmental program because of its known electrical characteristics at the frequencies of interest. The use of this material alone, however, presented several disadvantages, chief of which were, (1) relatively low mechanical strength for firing temperatures below 1600°C, and (2) extreme abrasive action on dies used for forming the

insulators. To overcome this first disadvantage, it was necessary to add a flux to the base oxide. If possible this flux should be non-abrasive. Talc and feldspar were the only two fluxing agents that offered possibilities of meeting these requirements, but feldspar had previously shown poor results when used in the high-frequency field. Talc had the desired properties of having a relatively low melting point (approximately 1300°C) and of being non-abrasive (hardness of 1 on the Moh scale). Previous tests had demonstrated that when talc was used with a refractory material such as aluminum oxide, it had a tendency to "drain", or melt and flow to the bottom of the specimen. This action resulted in a non-homogeneous insulator, or spacer. To overcome this disadvantage, it was found expedient to add some oxide which would not interfere with the bonding action of the fused talc, but would react with it to make the resulting flux viscous enough to prevent "draining". For this material, silica (ground quartz) was chosen because of its good electrical properties at high frequencies. A mixture having a ratio of three parts talc to two parts silica showed promising results as a flux for alumina.

On this basis as a starting point, the following series of ceramic bodies was made:

TABLE 1

<i>Body No.</i>	<i>Percentage of Materials in Body</i>		
	<i>Al<sub>2</sub>O<sub>3</sub></i>	<i>Talc</i>	<i>SiO<sub>2</sub></i>
1 .....	100%	0%	0%
2 .....	90%	6%	4%
3 .....	80%	12%	8%
4 .....	70%	18%	12%
5 .....	60%	24%	16%
6 .....	50%	30%	20%
7 .....	40%	36%	24%

To obtain intimate mixtures of these materials, it is important that the individual grain sizes of the components be as small as possible. It was found that when 90 per cent of the material was 2 microns or less in diameter with no particle larger than 70 microns, a mixture permitting economic operation was obtained. These oxides were blended with an organic binder, crushed, and pressed under pressure of 5000 pounds per square inch into the desired shapes for testing. These test pieces were fired in an air atmosphere at temperatures of 1300°C and 1400°C, in a firing cycle of six hours, the top temperatures being held for 1½ hours.

The desired electrical and physical characteristics of a high-fre-

quency insulator for vacuum tubes are: (1) low power factor, (2) low dielectric constant, (3) high mechanical strength, (4) high porosity or zero porosity, and (5) low linear firing shrinkage. Zero porosity is difficult to obtain except with a perfect glass, such as fused quartz.

Table 2 shows power factor and dielectric-constant measurements for 60 megacycles per second at 25°C and 400°C for fused quartz, magnesium metasilicate, and some of the glasses used in vacuum tubes.

TABLE 2

(Measurements made at 60 megacycles per second)

<i>Material</i>	<i>Power Factor</i> $\times 10^4$		<i>Dielectric Constant</i>	
	25°C	400°C	25°C	400°C
Fused Quartz (milky) . . . . .	3	5	3.5	3.4
Fused Quartz (clear) . . . . .	3	6	3.8	3.6
Magnesium metasilicate—				
Italian origin . . . . .	13	62	4.7	4.7
Glass 707 (Borosilicate) . . .	12	103	3.7	3.7
Glass 772 (Nonex) . . . . .	28	286	4.2	4.4
Glass 774 (Pyrex) . . . . .	54	679	4.1	4.6
Glass 008 (Soda lime) . . . . .	106	*	6.1	—

\* Power factor too large to be measured with available equipment.

Figures 1 and 2 show similar data on specimens of this series fired at both 1300°C and 1400°C. These measurements, as well as those in Table 2, were made by Dr. J. M. Miller, formerly of this laboratory.<sup>1</sup> Although measurements were made at 60 megacycles and 120 megacycles, the results corresponded so closely that only one curve plot for the series was considered necessary.

From the data in Figures 1 and 2 it appears that Body No. 2 has the best electrical properties at elevated temperatures, and that when fired at 1400°C it is slightly better than when fired at 1300°C. On the other hand, Body No. 3 fired at 1400°C is indicated as the best material when measured at room temperature. The difference in power factor at 400°C and 25°C is outstanding, and while all of these compositions might be considered good for use at low temperatures, elevated-temperature application limits the materials to the first three bodies.

It can be said, in general, that a ceramic body containing a mixture of crystalline material in a glassy matrix possesses poorer electrical properties at high frequencies than those compositions composed en-

<sup>1</sup> J. M. Miller and B. Salzberg. "Measurements on Resistors and Insulators at Ultra-High Frequencies, RCA REVIEW, Vol. III, No. 4, pp. 486-504 (1939).

tirely of crystalline or crypto-crystalline materials.<sup>2</sup> There are two methods of obtaining this latter condition: (1) the development of a glassy matrix composed of readily combining oxides, and the cooling of the matrix so slowly that it devitrifies or crystallizes during the cooling period, or (2) the use, in the original composition, of an extremely high percentage of crystalline material with small amounts of flux, which functions only to cement the particles of crystalline material together. The first method is difficult to control since its whole success

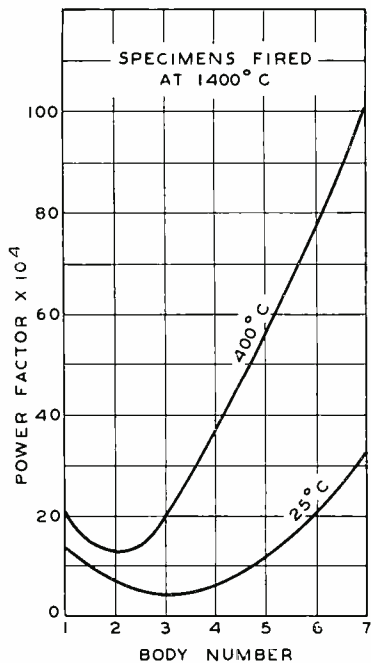


Fig. 1A

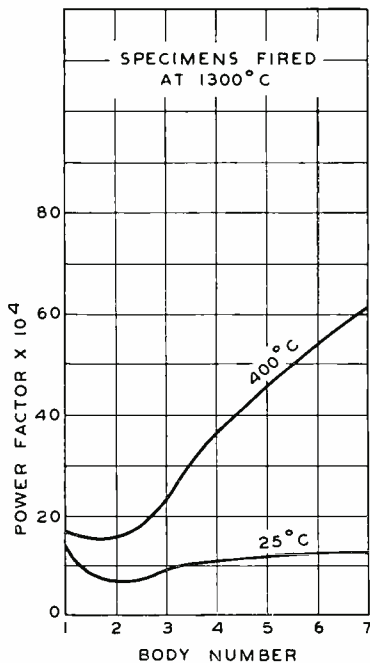


Fig. 1B

depends on two separate reactions, the correct combination of which results in good recrystallization, but slight deviations from the ideal conditions result in poor devitrification and a consequent non-homogeneous specimen. The second method is easier to control, particularly when the crystalline material is not easily soluble in the flux. Since some devitrification can be expected on cooling, the resultant percentage of glassy bond is usually lower than the percentage of flux used. The amount of flux that can be used depends, to some extent, on the nature and chemical properties of the inactive material. This, it is believed, explains the good high-frequency properties of Bodies No. 1, No. 2, and No. 3.

<sup>2</sup>H. Thurnauer. "Review of Ceramic Materials for High-Frequency Insulation". *Jour. Amer. Cer. Soc.*, 20, 11 (1937).

As the percentage of flux is increased, more of the non-glassy material will be taken into solution, and the conditions outlined under Method 1 will be approached. It will be noted that the active flux content (talc) of Body No. 3 is only 12 per cent (the actual amount of  $SiO_2$  taken into solution is difficult to determine), and that those bodies containing larger amounts have a rapidly increasing power factor (as measured at  $400^\circ C$ ) with increasing flux content.

Flux content also affects the mechanical strength, porosity, and firing shrinkage. As the flux content is increased, the mechanical strength increases, unless the firing temperature is high enough to

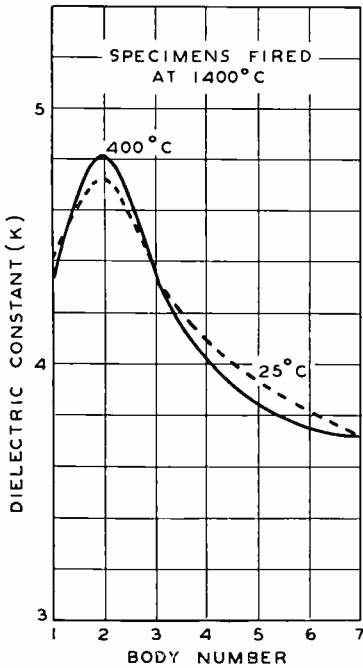


Fig. 2A

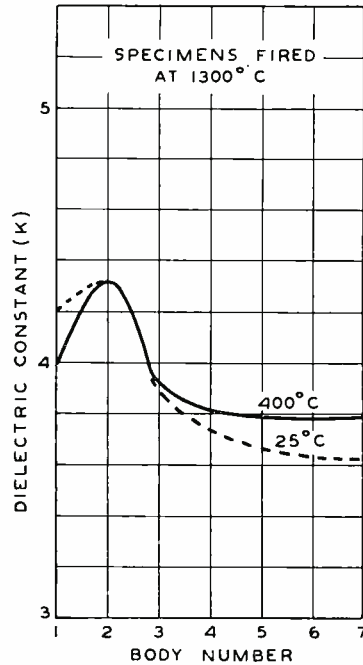


Fig. 2B

cause a vitreous vesicular structure. If the fired material is cooled too rapidly, however, the material will show the usual properties of glasses (weak in tension and strong in compression). Of the compositions investigated here, suffice it to say that Bodies No. 2 and No. 3 fired at  $1400^\circ C$  and Bodies No. 4, No. 5, No. 6, and No. 7 fired at  $1300^\circ C$  are sufficiently strong to answer the mechanical requirements necessary for vacuum tubes. Body No. 1 contains no flux and is consequently mechanically weak at these temperatures.

It is to be expected that as the glassy content increases the porosity will decrease. However, the flux content cannot be used as a direct indication of the amount of glassy material that will be present in the

final product, because the amount of devitrification depends on the composition of the glass formed during firing and the rate of cooling. Glasses high in  $Al_2O_3$  have a greater tendency to devitrify than do glasses high in  $SiO_2$ , as shown by the production of matte glazes, which are glasses so high in  $Al_2O_3$  content that devitrification takes place spontaneously on cooling. Crystalline materials in general have a higher density than glasses of the same composition. Crystalline quartz and fused quartz are good examples. An examination of Figure 3 will show that those bodies fired at  $1300^\circ C$  exhibit the usual trend of high

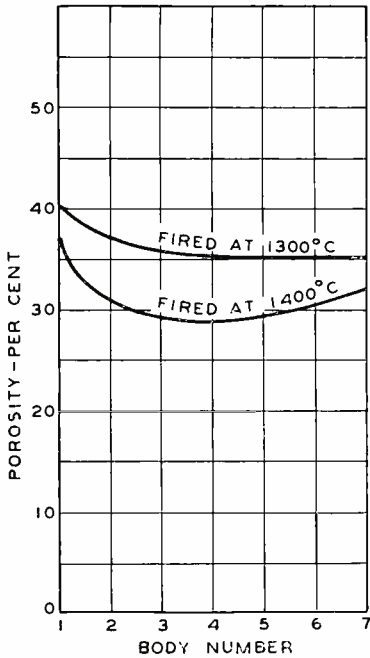


Fig. 3

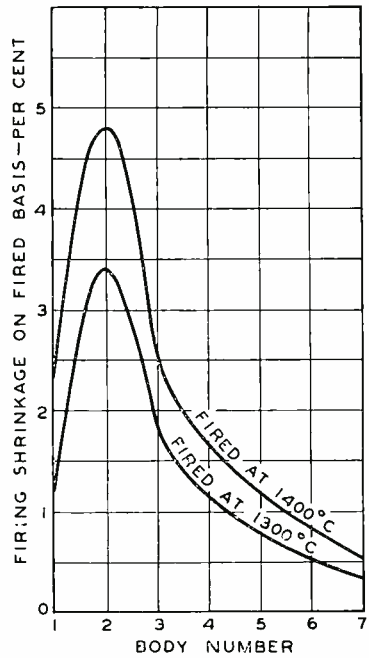


Fig. 4

flux and low porosity, while the same bodies fired at  $1400^\circ C$  show a tendency toward increased porosity with increasing flux. This increase in porosity is caused by the devitrification of glasses higher in  $Al_2O_3$  content (since more  $Al_2O_3$  is taken into solution at  $1400^\circ C$ ). The recrystallized material occupies less space than the original glass, and thus leaves a larger percentage of void space. When the porosity exceeds 20 per cent, the exhausting of vacuum tubes is accelerated due to the fact that the gas can be pumped from the spacer material without heat treatment. Insulators which have a vitreous vesicular structure are sources of future trouble in a tube, due to the possibility of the thin walls collapsing under stress or bombardment and releasing the enclosed gas into the tube envelop. For this reason, it has been

considered advisable to use extremely porous spacers rather than those which are highly vitreous.

Linear firing shrinkage is of direct interest in the manufacturing of insulating spacers, since it is the control of this shrinkage that determines the tolerance that must be allowed in manufacturing specifications. It is self-evident that the lower this value, the greater the control. Figure 4 shows the linear firing shrinkage of the bodies investigated. It seems unfortunate that the composition with the best electrical properties (Body No. 2) should have the greatest linear firing shrinkage, but this value is still well within the limits of control. This apparently abnormal shrinkage is caused by the fact that there is only enough flux present to cement together the particles of the inert material, but not enough to form sufficient glassy matrix of lower density than the original components to show an increase in volume, which would partially compensate for the original shrinkage. As the flux content increases, this latter condition becomes more pronounced: this is shown by the lower shrinkage of those bodies high in talc. Though this glass devitrifies, as explained above, this has little effect on the shrinkage value, since most of this recrystallization takes place after the glass has cooled to a temperature where the increased viscosity prevents the glass from flowing around the newly formed crystals.

The results of the measurements on this series of insulators demonstrate the value of accurate control over the porosity and crystalline content of ceramic insulating materials for use in vacuum tubes in order to obtain good electrical properties at elevated temperatures and high frequencies.

# FLUCTUATIONS IN SPACE-CHARGE-LIMITED CURRENTS AT MODERATELY HIGH FREQUENCIES

BY

B. J. THOMPSON, D. O. NORTH, AND W. A. HARRIS  
RCA Manufacturing Company, Inc., Harrison, N. J.

## PART V — FLUCTUATIONS IN VACUUM TUBE AMPLIFIERS AND INPUT SYSTEMS

BY

W. A. HARRIS

*Summary*—The determination of fluctuation-noise magnitudes in amplifiers can be accomplished by comparing the amplifier circuits with equivalent circuits including noise generators which simulate the fluctuation-noise sources. Noise-equivalent resistance or noise-equivalent conductance values based on thermal-agitation formulas may be used to represent the voltage-squared or current-squared outputs of these generators. In this PART V applications of the "noise generator" method of analysis to various systems using vacuum-tube amplifiers are illustrated. Formulas, based on the theoretical analyses of the preceding Parts, are given for noise-equivalent resistance values applicable to space-charged-limited vacuum tubes. These formulas are arranged for use with published tube data. A table of noise-equivalent resistance values for a number of tube types is included. Formulas for the noise-equivalent conductance values applicable to phototubes and television camera pick-up tubes are given.

It is shown that noise picked up by the antenna of a radio receiver can be represented by a noise-equivalent resistance proportional to (but in general, not equal to) the antenna-radiation resistance.

The effect of feedback on signal-to-noise ratio is discussed. Even when the feedback does not affect the signal-to-noise ratio to a serious degree, the possibility of the presence of feedback must be taken into account before inferences are drawn from experimental data as to the relative importance of noise sources.

### INTRODUCTION

IN THE preceding Parts of this series it is shown that there is a definite, predictable fluctuation in the plate current of a space-charge-limited vacuum tube; detailed theoretical studies are presented and formulas, verified by experimental work, are given to permit the calculation of fluctuation magnitudes and the prediction of the results of changes in tube parameters and operating conditions. The present section is written with the object of illustrating the application of the results and formulas of the preceding sections in the design of vacuum-tube amplifier systems and in the prediction and explanation of their performance.

The method of presentation followed will be based on the discussion of examples and problems of types encountered in design work. In

most cases the fluctuation phenomena are of interest because they produce noise, so the term "noise" will usually be used instead of the expression "fluctuation phenomena." Formulas for tube noise, based on those given in the preceding Parts, will be presented in simplified forms with, at times, some sacrifice in accuracy. This does not detract in any way from the importance of the more rigorous forms of the equations. It is our knowledge of the soundness of the underlying theory which gives us confidence in the approximate formulas, within their limitations, and when discrepancies and doubts do arise we can turn to the complete forms to find out whether the difficulties are due to the approximations made or to some other cause. Reference to the historical summary given in Part I should be sufficient to suggest the result of the absence of detailed analytical studies in the past.

Tube noise is one of three major components of the fluctuation noise in an amplifier system, the others being thermal-agitation noise in the input circuit and noise entering the system with the input signal. The grid of the first tube in an amplifier system is a convenient reference point for comparing the effects of noise from these sources and for comparing the resulting total noise level with the signal level at which the system is designed to operate.

#### EQUIVALENT CIRCUITS AND NOISE GENERATORS

In the consideration of an amplifier system, we want to be able to identify sources of fluctuation noise and to evaluate the contributions from these sources without concerning ourselves each time with such details as the mechanism by which the shot-effect fluctuations in the emission of electrons from the cathode of a tube are related to fluctuations in the plate current. One method of avoiding these details is to treat an amplifier as if all the fluctuation noise comes from "noise generators" connected at appropriate points in the circuit. These "noise generators" may have the noise-producing properties of resistors or of temperature-limited diodes. The equations describing these properties are the shot-effect and thermal-agitation formulas discussed in the preceding Parts.<sup>1</sup>

The mean-square fluctuation current  $\overline{i^2}$  from a temperature-limited diode, measured in a frequency band  $\Delta f$ , is given by the equation:

$$\overline{i^2} = 2eI\Delta f$$

where  $e$  is the electronic charge,  $1.59 \times 10^{-19}$  coulomb, and  $I$  is the diode current. Consequently,

$$\overline{i^2} = 3.18 \times 10^{-19} I\Delta f$$

<sup>1</sup> Part II, pp. 450, 460-471, April (1940) *RCA Review*; Part III, pp. 245-255, Oct. (1940) *RCA Review*. See also Part I, p. 272 and references, Jan. (1940) *RCA Review*.

when  $I$  and  $i$  are expressed in amperes and  $\Delta f$  is expressed in cycles per second. We can describe a constant-current noise generator producing an output of  $3.18 \times 10^{-10}$  current-squared units per kilocycle of bandwidth by stating that "the noise-equivalent diode current of the generator is one milliampere". We retain the current-squared unit because the noise power output of a system including a noise generator of this type is proportional to the mean-square current output of the generator and noise power outputs are quantities which can be added directly. Two noise generators connected in parallel, each having a noise-equivalent-diode-current rating of one milliampere, would produce the same results as a single generator with a noise-equivalent-diode-current rating of two milliamperes.

A short-circuited resistor produces a mean-square fluctuation current  $\bar{i}^2$  in a frequency band  $\Delta f$  in accordance with the equation:

$$\bar{i}^2 = 4kTg\Delta f$$

where  $g$  is the conductance of the resistor, or the reciprocal of its resistance;  $k$  is Boltzmann's constant,  $1.372 \times 10^{-23}$  joule per degree; and  $T$  is the temperature, degrees Kelvin. We can compare the mean-square current output of one of our noise generators with that of a short-circuited resistor at a given temperature; for a temperature of 290° K the mean-square current from a resistor with conductance  $g$  is

$$\bar{i}^2 = 1.59 \times 10^{-20}g\Delta f$$

The temperature 290° K is near enough to "room temperature" for practical purposes, so the relation between the "room-temperature" noise-equivalent-conductance rating and the noise-equivalent-diode-current rating of a constant-current noise generator can be written<sup>2</sup>

$$g_{cq} = 20 I_{cq}$$

The symbols  $g_{cq}$  and  $I_{cq}$  will be used for "noise-equivalent conductance" and "noise-equivalent diode-current", respectively. The constant-current noise generator referred to above ( $I_{cq} = 1$  milliampere) would have a noise-equivalent conductance of 20 milliamperes per volt, or 20,000 micromhos.

The mean-square thermal-agitation voltage  $\bar{e}^2$  across the terminals of a resistor in a frequency band  $\Delta f$  is

$$\bar{e}^2 = 4kTR\Delta f$$

or, for a temperature of 290° K

$$\bar{e}^2 = 1.59 \times 10^{-20}R\Delta f$$

<sup>2</sup> It is of little consequence whether we say that the coefficient 20 is obtained by using 290° K for room temperature, or that it is obtained by rounding the coefficient obtained for some other assumed temperature. The coefficient is actually  $5800/T$ , so "room temperatures" of 300°, 294°, and 290° give coefficients 19.3, 19.7, and 20.0, respectively. The corresponding Fahrenheit temperatures are 81°, 70°, and 63°.

The choice of a "noise-equivalent resistance" value to represent the output of a constant-voltage noise generator is made for the same reasons as those given above. The symbol  $R_{cq}$  will be used for "noise-equivalent resistance" in this Part<sup>3</sup>. A constant-voltage noise generator with a noise-equivalent resistance of 100,000 ohms produces a fluctuation-noise output of  $1.59 \times 10^{-12}$  voltage-squared units per kilocycle of bandwidth.

The application of the usual circuit theorems in connection with the noise-equivalent diode current, conductance, or resistance values assigned to our "noise generators" becomes evident when we remember that these values correspond to current-squared and voltage-squared outputs. Thus, a constant-voltage noise generator with a noise-equivalent-resistance value  $R_{cq}$  at the grid of a tube produces the same result as a constant-current noise generator at the plate with a noise-equivalent conductance value  $g_{cq}$  when

$$g_{cq}(\text{plate}) = g_m^2 R_{cq}(\text{grid})$$

The symbol  $g_m$  is the tube transconductance.

Since the numerical value of the noise-equivalent diode current is one-twentieth of the value of the noise-equivalent conductance, we have

$$I_{cq}(\text{plate}) = 20g_m^2 R_{cq}(\text{grid})$$

and by definition<sup>4</sup>

$$I_{cq}(\text{plate}) = I^2 I_b$$

where  $I^2$  is the shot-effect reduction factor for the tube.  $I^2$  is the factor determined from theoretical considerations in Parts II and III.

A constant-current noise generator  $g_{cq}$  in parallel with an admittance  $Y$  is equivalent to a constant-voltage noise generator

$$R_{cq} = \frac{g_{cq}}{|Y|^2}$$

in series with an impedance  $1/Y$  in any frequency band  $\Delta f$  small enough so that  $Y$  can be considered constant in that band; and conversely, a constant-voltage noise generator  $R_{cq}$  in series with an impedance  $Z$  is equivalent to a constant-current noise generator

$$g_{cq} = \frac{R_{cq}}{|Z|^2}$$

in parallel with an admittance  $1/Z$  in any frequency band  $\Delta f$  small enough so that  $Z$  can be considered constant in that band.

The diagrams of Figure 1 illustrate the use of "noise generators".

<sup>3</sup> The symbol  $R_{eff}$  and the name "effective resistance" used in Parts II and III in connection with tube noise are ambiguous when applied to circuit noise. The effective resistance of a circuit may be an entirely different quantity than the noise-equivalent resistance applicable to the circuit.

<sup>4</sup> Part II, Summary, p. 441; Apr. (1940) *RCA Review*.

The first diagram (Figure 1-a) represents an amplifier system consisting of an input circuit, the first vacuum tube, an amplifier including the output circuit of the first tube and additional stages, and an output system which might include a loudspeaker or a television screen, or alternatively a load circuit and a power-output meter. Noise in the output system is due to the combined effect of fluctuation voltages from tubes, input-circuit thermal agitation, and noise from external sources; the major part of the tube noise is due to reduced shot-effect fluctuations in the plate current of the first tube, as discussed in Parts II and III. When the gain of the first stage is low, it may be necessary to take into account the noise introduced by the interstage coupling circuit and by the second tube.

Figure 1-b indicates the substitution of a noise-free tube and a constant-current noise generator for the tube of Figure 1-a. The "generator" can have the characteristics of a temperature-limited diode; then we can determine the noise-equivalent diode current, which is the product of the plate current and the shot-effect reduction factor  $I^2$ , as determined by such equations as (43-a), Part II, and assign this current to the noise generator. The fluctuation-noise output from the "diode" noise generator is similar in both frequency-distribution and amplitude-distribution characteristics to the fluctuation-noise output of the actual tube. Thus, we can obtain the same noise-power output and at the same time produce noise which "sounds" the same as the noise from the original tube by this substitution. We describe the generator by stating that it has the characteristics of a temperature-limited diode which introduces the same current fluctuations into the circuit as did the original tube. The use of a noise generator of this type in our hypothetical equivalent circuit is directly comparable to the use of a "comparator diode" for the measurement of tube noise.<sup>5</sup>

It is also feasible to represent the plate-current fluctuations as if they were derived from thermal-agitation in a resistor. Since we want a "constant-current" (i.e. infinite-impedance) generator we cannot draw a noise-producing resistor as part of the circuit, but we can assign the appropriate noise-equivalent-conductance value to the noise generator of Figure 1-b. If we must draw a resistor we can draw a noise-free negative resistance of equal magnitude in parallel with it.

The third diagram (Figure 1-c) is a more useful representation for many purposes, since it shows tube noise introduced by a noise generator at the grid of the tube.<sup>6</sup> This noise generator can be represented as having the noise-equivalent-resistance value  $R_n$ , and other noise can be represented as coming from a second noise generator

<sup>5</sup> Part II, pp. 108-110, Aug. (1940) *RCA Review*.

<sup>6</sup> Part II, p. 471, July (1940) *RCA Review*.

having the noise-equivalent-resistance value  $R_b$ ; then it is correct to say that the total noise from these two sources corresponds to the noise-equivalent-resistance value  $(R_n + R_b)$ . The ideal tube substituted in this case should have infinite input impedance so the voltages supplied by the noise generators will not be short-circuited or reduced. The impedance of the real tube can be considered as part of the input circuit.

The circuit of Figure 1-d may represent conditions in an actual amplifier more accurately. The noise generators are assumed to produce noise distributed in accordance with the thermal-agitation law, in a uniform manner at all frequencies, but the frequency distribution of noise in various parts of the system is controlled by selectivity factors. The filter shown between the two noise generators  $R_b$  and  $R_a$  in Figure 1-d is assumed to have a selectivity characteristic corresponding to that of the input circuit of Figure 1-a. If we assume that  $R_a$  and  $R_b$  are approximately equal, that the amplifier passes a frequency band of width 8 kc and the filter passes a band of width only 4 kc, the output noise will contain contributions from both generators (i.e. tube and circuit) in the 4-kc band, but noise from  $R_a$  only (tube) in the range between the limits of the 4-kc band and those of the 8-kc band. The noise would sound differently than the same total noise power in either the 4-kc or the 8-kc band.

When the object of drawing or considering an equivalent circuit is to facilitate the computation of noise-power output or signal-to-noise ratio, the question of the exact frequency distribution of the noise may be of little consequence. Then the circuit of Figure 1-e would be preferred to 1-d, since direct addition of the noise-equivalent-resistance values for the noise generators is possible in Figure 1-e.  $R_a'$  (Figure 1-e) is made enough greater than  $R_a$  to compensate for the effect of the filter; consequently, it does not represent the tube noise directly. The noise generators in Figures 1-c, 1-d, and 1-e become identical when the effect of the filter is negligible ("broad" input circuit, "sharp" amplifier).

Noise from the second tube and the coupling circuit can be taken into account by the addition of another "generator",  $R_c$  (Figure 1-f). Since the noise-equivalent resistance represents the mean-square voltage produced by the noise generator, a factor equal to the square of the stage gain is used to refer the noise-equivalent-resistance value for a noise generator at the second grid, to the first grid. The method indicated can be extended to any number of stages, but it is not likely that tubes beyond the second will make an appreciable contribution to the total noise. In Figure 1-f,  $R_a$  and  $R_b$  represent noise-equivalent-resistance values for the first tube and the input circuit;  $R_c$  can be

described as representing the noise-equivalent-resistance value for the additional (second tube and circuit) amplifier noise, referred to the grid of the first tube. The total noise-equivalent resistance (excluding noise which might be introduced from external sources) is

$$R_{eq} = R_a + R_b + R_c$$

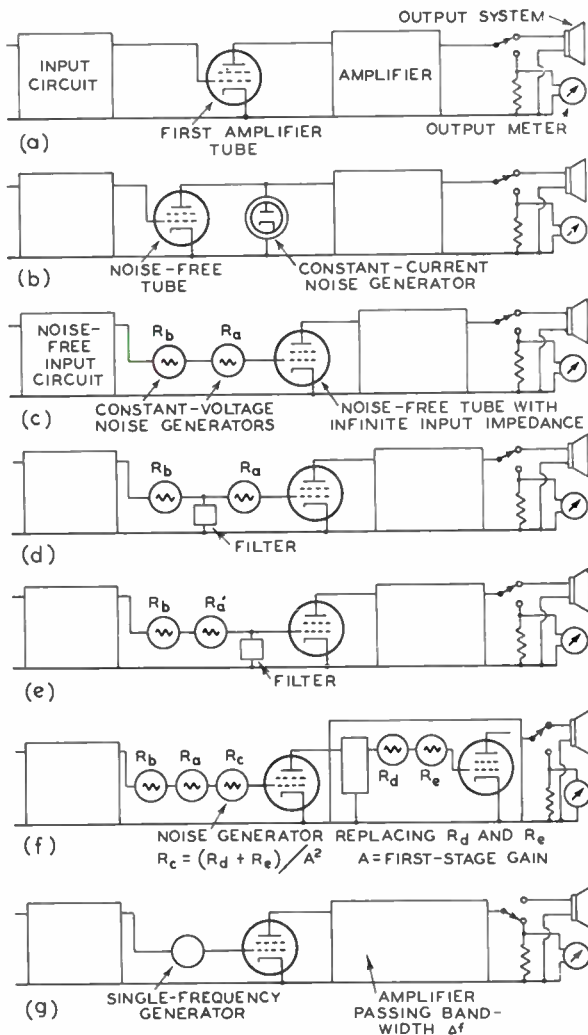


Fig. 1

The noise generators introduced in Figures 1-b to 1-f have an important property in common with the noise sources which they replace, in that they produce noise distributed in a uniform manner over a wide frequency band. However, there are some cases in which

we prefer to consider constant-frequency generators equivalent to the others in the sense that they cause the same output-meter deflection as the original noise sources of the amplifier. In such cases, we can use the equivalent circuit shown in Figure 1-g, and assume the substitution of an amplifier with a rectangular band-pass characteristic of bandwidth  $\Delta f$  and a noise-equivalent voltage generator operating at a frequency inside this passed band. The bandwidth  $\Delta f$  must be determined from the frequency characteristic of the amplifier in such a manner as to satisfy the relation

$$\sqrt{\overline{e^2}} = \sqrt{4kTR_{eq}\Delta f}$$

or,

$$\Delta f = \overline{e^2}/4kTR_{eq}$$

The quantity  $\Delta f$  will be referred to as the effective bandwidth of the amplifier.

In these equations  $\sqrt{\overline{e^2}}$  is the rms voltage of the new generator and  $R_{eq}$  is the total noise-equivalent resistance used in the previously discussed method of representation. When room-temperature noise-equivalent-resistance values are considered, the equations become

$$\sqrt{\overline{e^2}} = 1.3 \times 10^{-10} \sqrt{R_{eq}\Delta f} \quad (1)$$

or,

$$\Delta f = 0.6 \times 10^{20} \overline{e^2}/R_{eq}$$

If we want to assume separate generators corresponding to the separate noise sources, we must also assume that each operates at a different frequency inside the passed band so that their contributions to the power output will be added in the proper manner. Generally, it is easier to determine the noise-equivalent-resistance values first, add them, and obtain the noise-equivalent voltage from this result.

The effective bandwidth of an amplifier can be determined from a curve of power output against frequency by dividing the area under that curve by the ordinate corresponding to the chosen "noise-equivalent-voltage" frequency. When a curve of output voltage against frequency is available, the same result is obtained by using the squares of the ordinates of that curve. An approximate value obtained by measuring the frequency difference between the half-maximum ordinates of the curve of power output against frequency or between the corresponding (0.707 maximum) ordinates on the curve of power output against voltage can be used in many cases. An effective-bandwidth determination is referred to in the description of the amplifier used for measurements, Part II.<sup>7</sup>

The effective bandwidth determined for fluctuation-noise computa-

<sup>7</sup> Part II, p. 108, July (1940) *RCA Review*.

tions is generally considerably less than the bandwidth which represents the "frequency range" of an amplifier. This difference can be illustrated by a comparison of two amplifiers, one "cutting off" sharply at, say, 3000 cycles and the second giving some attenuation at 3000 cycles, but some response at 6000 cycles. The two amplifiers will not sound alike, although they may produce the same noise-power outputs when they are connected to similar input systems.

#### APPLICATION TO RADIO RECEIVERS

The generality of the method of analysis discussed is illustrated by considering its application to a radio receiver of the superheterodyne type. In a receiver the output system passes a band of frequencies from possibly 100 to 5000 cycles. To represent a superheterodyne receiver the amplifier shown as a block in Figures 1-a to 1-g must include a frequency-conversion stage for converting the signal to the intermediate frequency and a detector for producing the audio-frequency output. The detector makes noise analysis quite troublesome when we try to predict the noise-power output in the absence of any signal, but this is not an important condition. When a signal is being received the "carrier" component of the signal establishes the receiver gain because it determines the detector sensitivity, and the amount of a-c voltage developed. With a given carrier voltage, the audio-frequency voltage output is proportional to the sideband amplitudes, and the ratio between output and sideband amplitude is substantially constant so long as the modulation does not exceed 100 per cent and the audio system is not overloaded. The sidebands do not have to be those produced by modulation of the signal at its source. If we introduce a second signal differing by an audio frequency from the carrier we observe that the output is proportional to the amplitude of the second signal when this amplitude is not too great. Moreover, when the carrier is present we can introduce a second signal differing by an audio frequency from the intermediate frequency, into the i-f amplifier and obtain a similar result. The noise generators in Figures 1-a to 1-g produce signals corresponding to the "second signal" referred to, so the receiver functions as a linear amplifier with respect to the noise when a carrier is present.

The signal-to-noise ratio in a radio receiver depends on the relation between the sidebands of the received signal and the outputs of the noise generators. Consequently, when we decide to turn from consideration of noise-equivalent resistances to noise-equivalent voltages (as in Figure 1-g) it is proper to refer to the noise-equivalent rms voltage as the "equivalent-noise sideband input." This expression is

generally abbreviated to "ensi" when it is used in receiver-measurement discussions. In a double-side-band system the effective bandwidth to be used in making the conversion from noise-equivalent resistance to noise-equivalent voltage (ensi) is twice the effective audio-frequency bandwidth. The effective audio-frequency bandwidth can be obtained from a curve of power output against modulation frequency by dividing the area under the curve by the ordinate chosen to correspond to the noise-generator frequency. In this case the actual noise-generator frequency is the carrier frequency plus or minus the chosen audio-frequency value.

### NOISE FORMULAS

Use of the method of analysis described in the preceding sections depends on assignment of noise-equivalent-resistance and noise-equivalent-conductance values to the "noise generators" shown in the diagrams. The following equations are recommended for this purpose:

For triode amplifiers

$$R_{eq} = \frac{2.5}{g_m} \quad (2)$$

For pentode amplifiers

$$R_{eq} = \frac{I_b}{I_b + I_{c2}} \left( \frac{2.5}{g_m} + \frac{20I_{c2}}{g_m^2} \right) \quad (3)$$

For triode mixers

$$R_{eq} = \frac{4}{g_c} \quad (4)$$

$$\text{or, } R_{eq} = \frac{2.5\overline{g_m}}{g_c^2} \quad (4a)$$

For pentode mixers

$$R_{eq} = \frac{I_b}{I_b + I_{c2}} \left( \frac{4}{g_c} + \frac{20I_{c2}}{g_c^2} \right) \quad (5)$$

$$\text{or, } R_{eq} = \frac{I_b}{I_b + I_{c2}} \left( \frac{2.5\overline{g_m}}{g_c^2} + \frac{20I_{c2}}{g_c^2} \right) \quad (5a)$$

For multigrid converters and mixers

$$R_{eq} = 20 \frac{I_b(I_a - I_b)}{I_a g_c^2} \quad (6)$$

The following approximate relations for triode and pentode mixers are useful when the data required for Equations (4) and (5) are not available. The values "as amplifier" refer to conditions at the peak of the assumed oscillator cycle.

$$g_c \text{ (as converter)} = \frac{1}{4} g_m \text{ (as amplifier)} \tag{7}$$

$$I_b \text{ (as converter)} = \frac{1}{4} I_b \text{ (as amplifier)} \tag{8}$$

$$I_{c2} \text{ (as converter)} = \frac{1}{4} I_{c2} \text{ (as amplifier)} \tag{9}$$

$$R_{eq} \text{ (as converter)} = 4R_{eq} \text{ (as amplifier)} \tag{10}$$

Equation (10) applies to pentode mixers only. For triode mixers, use Equations (7) and (4) to obtain  $R_{eq}$ .

The noise from phototubes and television camera pick-up tubes operating without internal (gas or secondary-emission) current amplification can be represented by constant-current noise generators with outputs corresponding to noise-equivalent conductances as follows:

$$g_{eq} = 20I \tag{11}$$

The equation for a similar device with an internal current-amplification factor  $N$  (to a first approximation) is

$$g_{eq} = 20NI \tag{12}$$

Conversion from noise-equivalent resistance to noise-equivalent rms voltage is effected by use of Equation (1):

$$\sqrt{\overline{v^2}} = 1.3 \times 10^{-10} \sqrt{R_{eq} \Delta f} \tag{1}$$

Conversion from noise-equivalent conductance to noise-equivalent rms current is effected by use of the corresponding equation:

$$\sqrt{\overline{i^2}} = 1.3 \times 10^{-10} \sqrt{g_{eq} \Delta f} \tag{1-a}$$

The relation between noise-equivalent conductance and noise-equivalent diode current is

$$I_{cq} = 0.05 g_{eq} \tag{13}$$

Most of the symbols used in these equations have been defined or have conventional significance. The definitions are:

$R_{eq}$ , noise-equivalent resistance

$g_{eq}$ , noise-equivalent conductance

$I_{cq}$ , noise-equivalent diode current

$g_m$ , grid-plate transconductance

$\overline{g_m}$ , average transconductance (frequency converters and mixers)

$g_c$ , conversion transconductance (frequency converters and mixers)

- $I_b$ , average plate current  
 $I_{c2}$ , average screen-grid current  
 $I_c$ , average cathode current  
 $\sqrt{\overline{e^2}}$ , noise-equivalent rms voltage for bandwidth  $\Delta f$   
 $\sqrt{\overline{i^2}}$ , noise-equivalent rms current for bandwidth  $\Delta f$   
 $\Delta f$ , effective bandwidth  
 $I$ , Equations (11), (12), average output current  
 $N$ , Equations (11), (12), ratio of output current to photo-emission current.

Equations (2) to (6) are derived from the equations for fluctuation noise in triodes and pentodes given in Parts II and III and from equations for fluctuation noise in converters and mixers given by E. W. Herold.<sup>8</sup> Equations (7) to (10) are approximations derivable from certain idealized tube characteristics.

Equation (2) is derived from Equation (56) of Part II,

$$R_{eff} = \frac{\theta T}{\sigma T_o g_m}$$

In Part II it is demonstrated that the quantity  $\theta$  has a value of approximately  $\frac{2}{3}$  (the asymptotic value is 0.644). The quantity  $\sigma$  will be near unity for triodes likely to be of interest in input-circuit applications. Assignment of the value  $8/9$  to  $\sigma$ ,  $1000^\circ$  K to  $T$  (for an oxide-coated cathode), and  $300^\circ$  K to  $T_o$  gives Equation (2). The coefficient 2.5 is reasonably accurate over most of the expected range of variation for the significant quantities. Substitution of a tungsten filament for the oxide-coated cathode would make the use of a different coefficient necessary, but practically all tubes of current interest use oxide-coated cathodes operating at temperatures near  $1000^\circ$  K.

Equation (3) is derived from Equation (13), Part III. In this case the original equation was first written as the sum of two terms. The coefficient 20 is the quotient  $e/2kT_o$  which determines the relation between noise-equivalent conductance and noise-equivalent diode current.

Equations (4), (4-a), (5), and (5-a) are developed from equations given by Herold.<sup>8</sup> Equations (4) and (5) apply for approximately optimum oscillator voltage and (4-a) and (5-a) may be used for conditions deviating considerably from optimum conditions. Herold's equations are given in terms of conditions at the peak of the assumed oscillator cycle, but the ratios between average and peak values for

<sup>8</sup> E. W. Herold "Superheterodyne Converter System Considerations in Television Receivers," *RCA Review*, Vol. IV, pp. 324-337, Jan. (1940).

currents and transconductances given in the same paper enable us to rewrite the equations in terms of the average quantities. As a final step, the coefficients for Equations (4) to (5-a) were adjusted slightly to make them consistent with those of Equations (2) and (3).

Use of Equation (6) amounts to the substitution of the factor

$$\frac{I_a - I_b}{I_a} \text{ for the factors } \frac{I_a - \overline{I_b^2}/I_b}{I_a} \text{ and } F^2 \text{ used in Herold's equations}$$

for heptodes and hexodes, for outer-grid and inner-grid injection, respectively. The substitution gives values for  $R_{eq}$  which are higher than Herold's values by as much as 30 or 40 per cent under some conditions, but use of Equation (6) has an advantage over an arbitrary choice of  $F^2$  in that it predicts "full shot-effect" for  $I_b$  as the limiting condition for high signal-grid biases.

There is a difference in meaning for a noise-equivalent resistance value applicable to an amplifier and for a value applicable to a frequency converter or to a mixer. In either instance the noise-equivalent-resistance value can be considered as derived from a noise-equivalent-conductance value representing the plate-current fluctuations, but in the case of a converter or a mixer this derivation (division by conversion transconductance squared) yields a noise-equivalent-resistance value which is applicable only in a frequency band which centers at the chosen signal frequency and which does not extend half way to the intermediate frequency or half way to any adjacent image frequency. An equivalent circuit of the type of Figure 1-e is implied with a band-pass filter between the noise generator and the grid of the tube.

Use of Equations (11) and (12) amounts to the assumption that photoelectric emission is subject to shot-effect fluctuations, an assumption adequately justified by theory and experiment.<sup>9</sup> Equation (12) neglects additional noise from the amplification mechanism.

#### TUBE NOISE: TABULATED VALUES OF $R_{eq}$

The data in the following table were obtained by using Equations (1) to (9). The noise computations for each type were made by using published data conditions (as noted) with the appropriate equations; the values for triode and pentode converters were obtained by use of Equations (7) to (9) for currents and conversion-transconductance values and Equations (4) and (5) for noise-equivalent resistance. In some instances it is possible to obtain higher transconductance values by changing operating conditions, but this does not

<sup>9</sup> V. K. Zworykin, G. A. Morton, and L. Malter, "The Secondary Emission Multiplier—A New Electronic Device" *Proc. I. R. E.*, Vol. 23, No. 3, pp. 351-375, March (1936).

## TUBE NOISE VALUES

Type	Application	Voltages			Currents			Transcon- ductance Micromhos	Noise-Equivalent Resistance		Noise- Equivalent Input Voltage (d) Microvolts
		Plate Volts	Screen Volts	Bias Volts	Plate ma	Screen ma	Cathode ma		Calculated Ohms	Measured Ohms	
6SK7	Pentode Amplifier	250	100	-3	9.2	2.4	11.6	2,000	10,560	9,400-11,500	0.94
6SJ7	Pentode Amplifier	250	100	-3	3	0.8	3.8	1,650	5,800	5,800	0.70
6SG7	Pentode Amplifier	250	125	-1	11.8	4.4	16.2	4,700	3,300	600-760	0.53
6AC7/1852	Pentode Amplifier	300	150	-2	10	2.5	12.5	9,000	720	600-760	0.25
956	Pentode Amplifier	250	100	-3	5.5	1.8	7.3	1,800	9,400		0.90
1T4	Pentode Amplifier	90	45	0	2.0	0.65	2.65	750	20,600		1.3
6SA7	Frequency Converter	250	100	0	3.4	8.0	11.9	450 (c)	240,000	210,000	4.5
6K8	Frequency Converter	250	100	-3	2.5	6.0	8.5 (b)	350 (c)	290,000		4.9
1R5	Frequency Converter	90	45	0	0.8	1.8	2.75	250 (c)	170,000		3.8
6L7	Pentagrid Mixer	250	100	-3	2.4	7.1	9.5	375 (c)	255,000	210,000	4.6
6J5	Triode Amplifier	250	—	-8	9.0	—	—	2,600	960	1,250	0.28
955	Triode Amplifier	180	—	-5	4.5	—	—	2,000	1,250		0.32
6AC7/1852	Triode Amplifier	150	150	-2	—	—	12.5	11,200	220	200	0.14
6AC7/1852	Pentode Mixer	300	150	-1 (a)	5.2	1.3	6.5	3,400 (c)	2,750	3,000	0.48
6SG7	Pentode Mixer	250	125	-1 (a)	3.0	1.1	4.1	1,180 (c)	13,000		1.0
956	Pentode Mixer	250	100	-1 (a)	2.3	0.8	3.1	650 (c)	33,000		1.7
6J5	Triode Mixer	100	—	-1 (a)	2.1	—	—	620 (c)	6,500		0.74
6AC7/1852	Triode Mixer	150	150	-1 (a)	—	—	6.5	4,200 (c)	950		0.28
955	Triode Mixer	150	—	-1 (a)	2.8	—	—	660 (c)	6,100		0.72

(a) At peak of oscillator cycle.

(b) Hexode section only. Triode section takes its current from a separate part of the cathode.

(c) Conversion transconductance value.

(d) For effective bandwidth of 5000 cycles.

result in any radical change in the noise-equivalent resistance values. The noise-equivalent voltage input values were obtained by using Equation (1) and are included to facilitate comparisons with experimental data. It is generally preferable to use the noise-equivalent resistance values for circuit computations.

Most of the measured values in the table are from data supplied by E. W. Herold. The acorn types (955, 956) are seen to have about the same noise-equivalent values as Types 6J5 and 6SK7 respectively, as might be expected. Type 6AC7/1852 is in a class by itself with respect to noise because of its very high transconductance.

#### POSITIVE-ION NOISE

The fluctuation-noise component produced by collision ionization, discussed in Part IV, is quite properly omitted from the equations for noise-equivalent resistance. Residual gas in sufficient quantity to cause an appreciable increase in the fluctuation noise is not desirable from any point of view connected with normal tube operation. It is desirable, however, that we be able to determine the conditions under which residual gas will cause an appreciable increase in the noise power output of a system.

An estimate of the effect of residual gas can be obtained from the equation,

$$R_{eq}(\text{gas}) = \left( 20R^2 + A_1 \frac{I_a}{g_m^3} \right) I_{ip} \quad (14)$$

where

$R$  = grid-circuit resonant impedance

$I_a$  = cathode current

$I_{ip}$  = positive-ion current to grid

$g_m$  = transconductance

$A_1$  is a coefficient of the order of 40,000

The term  $20R^2 I_{ip}$  represents shot-effect voltage fluctuations produced by the gas current in the grid circuit. It may be increased several fold by induction effects connected with ion-transit time, even at frequencies of a few megacycles. The second term is derived from Equation (20), Part IV.<sup>10</sup>

When  $A_1$  is 40,000, the two terms are equal for

$$R^2 = 200 I_a / g_m^3$$

By substituting typical values for  $I_a$  and  $g_m$ , we find that the first term is probably the greater when  $R$  exceeds 20,000 ohms.

<sup>10</sup> Part IV, p. 384, Jan. (1941) *RCA Review*.

The noise-equivalent resistance value for thermal agitation in the grid-circuit resonant impedance is numerically equal to that impedance at frequencies near resonance. The total noise-equivalent resistance component depending on this impedance (neglecting transit-time effect) is

$$R_{eq} = R + 20R^2I_{ig} = R(1 + 20RI_{ig})$$

The fluctuation noise due to gas exceeds that due to thermal agitation when the product  $RI_{ig}$  exceeds one-twentieth of a volt. When the grid-circuit impedance is one-tenth megohm a positive-ion grid current of one-half microampere doubles the mean-square fluctuation noise.

When the grid-circuit impedance is low, the second term of Equation (14) predominates and at the same time the tube noise is likely to predominate over the circuit thermal-agitation noise. An equation for fluctuation noise in a system using a pentode amplifier connected to an input circuit with resonant impedance  $R$  can be written

$$R_{eq} = R + 20R^2I_{ig} + \frac{I_b}{I_b + I_{c2}} \left( \frac{2.5}{g_m} + 20 \frac{I_{c2}}{g_m^2} \right) + A_1 \frac{(I_b + I_{c2})I_{ig}}{g_m^3}$$

and the most important terms can be compared for any conditions which may be of interest.

#### INPUT-CIRCUIT NOISE

The input circuit used with an amplifier can introduce noise because of thermal agitation in the resistance of that circuit, and it can also transfer the noise generated in or picked up by the microphone, phototube, antenna, or any other input device to the grid of the first amplifier tube. It is evident that the noise from either cause may be the controlling factor in the choice of the first amplifier tube, since there is little object in using a tube with an inherent noise level much lower than that introduced by the input circuit. When the input-circuit noise is predominantly that due to thermal agitation, the determination of the noise level and the comparison with the amplifier noise are fairly simple matters. The general method to be used in such cases has already been indicated.

#### MICROPHONE AMPLIFIER

As a specific illustration we can consider the case of a microphone amplifier (Figure 2). The microphone is assumed to be of a type having a definite internal resistance; it may be one of the types using a ribbon or a moving coil as the voltage-generating element. Noise will be generated in this element in accordance with the thermal-

agitation law. The input transformer shown in Figure 2 can have a ratio high enough to make the noise from this source at the secondary of the transformer considerably greater than the noise-equivalent input voltage applicable to the first amplifier tube. This condition is realized when the reflected resistance at the secondary terminals (microphone resistance times voltage ratio squared) is considerably greater than the noise-equivalent resistance of the first tube.

As an example, let the first tube be a Type 6SJ7 pentode operated under resistance-coupled amplifier conditions. Reference to a table containing data for this method of operation<sup>11</sup> shows that for a supply voltage of 300 volts a plate-load resistor of 0.1 megohm followed by a second-tube grid resistor of 0.5 megohm, and a screen resistor of approximately 0.5 megohm give suitable operating conditions. The voltage gain is approximately 100. The value of the transconductance indicated by this gain and these specified load resistors is 1200 micromhos.

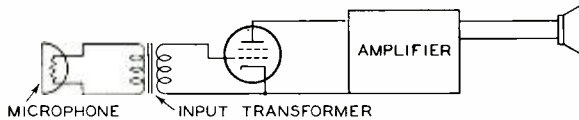


Fig. 2

The currents may be estimated by assuming that the plate-voltage drop is about one-half the supply voltage and that the screen current is about one-fourth of the plate current; resulting values are 1.5 milliamperes and 0.37 milliampere, respectively. The noise-equivalent resistance, determined by using Equation (3), is approximately 6000 ohms. The reflected impedance at the transformer secondary is likely to be of the order of 100,000 ohms, so the tube fluctuation noise is not important.

The noise-power level in the input circuit can be determined from the thermal-agitation formula when the effective bandwidth is known or assumed. The equation for the mean-square thermal-agitation voltage across the terminals of a resistor is

$$\overline{e^2} = 4kTR\Delta f$$

and the average power  $\overline{e^2}/R$ , is, therefore,

$$\overline{P} = 4kT\Delta f$$

For a temperature of 290° K, the equation becomes

$$\overline{P} = 1.6 \times 10^{-20} \Delta f$$

<sup>11</sup> RCA Receiving Tube Manual RC-14; resistance-coupled amplifier chart.

The noise-power level in decibels, referred to a standard 10-milliwatt level is

$$\text{Noise (db)} = 10 \log \Delta f - 178$$

When  $\Delta f = 10,000$  cycles, the noise power output is 138 db below 10 milliwatts.

The microphone signal output level is likely to be of the order of  $-40$  or  $-50$  db. The fluctuation-noise level is, therefore, 70 or 80 db below the signal. In some amplifiers a multigrid tube, Type 6L7 or 1612, is used because it offers the advantage of a second control grid for volume-control use. The noise-equivalent resistance of such a type as a resistance-coupled amplifier might be 100,000 ohms at maximum gain and a megohm or more when the gain is reduced by application of negative bias, but even these values permit satisfactory signal-to-noise ratios. The choice of a first tube for an audio-frequency amplifier quite evidently depends on factors other than fluctuation noise. Hum, microphonics and mechanical or leakage noises are generally far more important.

#### PHOTOTUBE INPUT CIRCUITS

A high-vacuum phototube produces noise in accordance with the shot-effect law,

$$\begin{aligned} \overline{i^2} &= 2eI\Delta f \\ \text{Consequently } I_{cq} &= I \\ \text{and } g_{cq} &= 20I \end{aligned} \quad (11)$$

Here  $\overline{i^2}$  is the mean-square fluctuation current and  $I$  is the average phototube current.

When the light input to the phototube is modulated in a sinusoidal manner the relation between the mean-square signal current and the average current is

$$\overline{I^2} = \overline{I}M^2/2 = \frac{1}{2} I^2 M^2$$

The factor  $M$  is the modulation factor for the light input or the current output.

The signal-to-noise power ratio (or current-squared ratio) is, therefore,

$$\overline{I^2}/\overline{i^2} = \frac{1}{2} I M^2 / e\Delta f$$

For values  $I = 1$  microampere,  $\Delta f = 10,000$ , and  $M = 1$ ,

$$\overline{I^2}/\overline{i^2} = 1.6 \times 10^8, \text{ or } 82 \text{ db.}$$

The phototube noise can be considered as coming from a constant-current generator with a noise-equivalent conductance value of twenty times the average phototube current. Equivalent circuits for this substitution are shown in Figures 3-a and 3-b.

When the phototube load resistance is one megohm, the fluctuation-noise contributions from phototube and resistor are equal for a phototube current of 0.05 microampere. At higher current levels the phototube noise predominates, but the current of 0.05 microampere gives noise 69 db below the signal level for a 10,000-cycle effective bandwidth and 100 per cent modulation.

Direct amplification of the current emitted by the photo cathode can be accomplished by "gas amplification" or by secondary-emission amplification. The effect of such amplification is to increase the signal and the noise outputs in the same ratio, except for the addition of a small amount of noise associated with the amplification mechanism." If we assume as a first approximation that the signal-to-noise ratio in

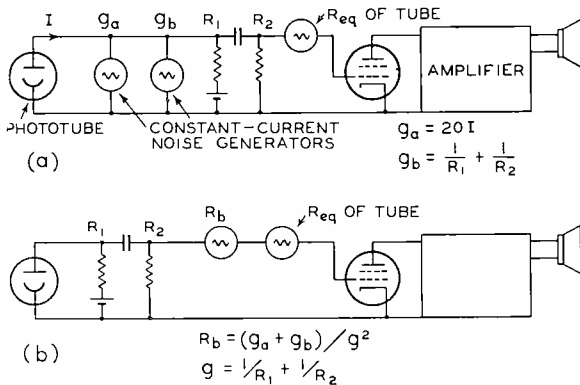


Fig. 3

the phototube output is unchanged by this amplification we find that the noise-equivalent conductance would be

$$g_{eq} = 20 IN \tag{12}$$

$N$  is the current-amplification ratio. When  $N = 5$ , the phototube noise becomes equal to the noise from a one-megohm load resistor for an output current of only 0.01 microampere. This value corresponds to a photo-emission current of only 0.002 microampere. If we were interested in a tube working at audio frequencies at such a low output level we would still obtain a signal-to-noise ratio of 55 db for 100 per cent modulation and a 10,000-cycle bandwidth from the tube itself. Subtraction of 3 db for the added resistor noise and 10 db as an allowance for lower modulation levels leaves a 42-db signal-to-noise ratio as an approximate theoretical value for the assumed conditions. Use of a high-vacuum phototube without current amplification, with the same load and the same light input, would result in a total noise reduction of 3 db and a signal reduction of 14 db, so the result would be a 31-db

ratio with the same allowances as in the other case. At these low operating levels the signal-to-noise improvement with current amplification would be quite marked, but the assumed outputs are considerably below those usually encountered in practice. The real value of gas amplification in phototubes used for sound work comes from the fact that the input signal to the amplifier becomes greater in comparison to the hum, microphonics, or other disturbances which might be present. The high assumed load resistor permits us to ignore normal tube fluctuation noise in this case also. The one-megohm value is not inconsistent with the assumed 10,000-cycle effective bandwidth if the input-circuit capacitance, including that of the phototube, does not exceed 15  $\mu\mu\text{f}$ .

*(To be continued)*

## ANNOUNCEMENT

RCA Laboratories, a new center for radio and electronic research, to be built this year at Princeton, N. J.

THE world's largest radio research laboratories will be built by the Radio Corporation of America, at Princeton, N. J., David Sarnoff, President of RCA, announced on March 6th, 1941. The Princeton laboratories will be the headquarters for all research and original development work of RCA, and for its patent and licensing activities.

"To equip our research staff with the best and most modern facilities and conveniences, we have purchased a large tract of land at Princeton," said Mr. Sarnoff, "upon which we will erect a laboratory building which will include a lecture auditorium and the combined technical and patent libraries of the RCA organization. We hope to have the building completed before the end of this year.

"We believe that this step marks a milestone in the progress of radio. Such important fields as television, facsimile, electron optics, wave propagation and ultra-high frequencies open to radio a future even greater than its past. The developments in these fields will contribute to the creation of new industries and to the improvement of existing services.

"More and more of our research work is being concentrated on problems of national defense. The new RCA Laboratories will make it possible to increase these efforts and to insure the maximum use of our research facilities for defense.

“By the establishment of the new Laboratories, radio quickens its pace alongside the older industries—electrical, steel, automobile, wire communications, chemical, metallurgical and others—which, through research, have contributed to the industrial leadership and progress of this country.”

More than 130 manufacturers in radio and other fields, Mr. Sarnoff pointed out, are now licensed under the patents of RCA. He said that the new Laboratories will continue to make inventions available to competitors and others, and to cooperate with them in the fullest development of the radio art.

Otto S. Schairer, heretofore Vice President in Charge of the RCA Patent Department, will be Vice President in Charge of RCA Laboratories, which will include the Patent Department.

At a meeting of RCA engineers held at Princeton a few days after the original announcement, Mr. Sarnoff further stated:

“I think we are fortunate that we are living in a generation that has given science the green light. And we are fortunate to live and work in a country that has come to look upon change and invention, new methods and new services as an inherent part of American culture and civilization, rather than upon something to deny or to obstruct or to prevent.

“We happen to be living at a time when the world is determined to move forward. We are not likely to go back to the methods of yesterday. We must not stand in the way of change. Our aim should be to help direct change along useful lines and to strike the happy balance between those who would destroy everything because they belong to yesterday, and those who would try anything because it has not been tried before. That is the balance where experience and integrity count most.

“Radio at the moment stands in need of redefinition. The great developments of the radio art, beginning with communications between

ship-and-shore, continent-and-continent, and followed by communication to the home through broadcasting, have already arrived at a stage which perhaps may not be called stabilization, but a stage of development where they, too, point the way to change.

"The services of radio are many—many more than we can comprehend even with our daily contact with the art. Anything that can make a sound, or a mark on a piece of paper, or control some device at a distance, and transmit sound and sight through space, lends itself to a multiplicity of uses depending upon the needs of the time and upon the opportunities of the moment.

"New inventions are geared to the times and to the generations in which people live. There was the Steam Age, then the Electrical Age, and later came the Radio Age. Now I think we are on the eve of a new age—the Electronic Age. Just as electricity *electrified* industries and life in general, so these developments that you gentlemen are producing with tubes and circuits will *electronize* industries and create the Electronic Age.

"The applications of electronics to the various uses of industries are more numerous than people outside of radio have any notion; they are more numerous than even those of us on the inside of radio can see today. Many problems in industrial mass production may be solved in large measure by the application of electronic devices.

"There is no security in standing still. Those who rest on the rock of stabilization, sooner or later find that that rock becomes their tombstone. There is no security for the future in the mere knowledge of today. There is hope and opportunity in what we can learn tomorrow. That is the greatest asset on the balance sheet of humanity and on the balance sheet of any organization engaged in scientific pursuits. And so I believe that this united front of scientific attack upon the problems of our particular art and its relationship to other industries is the greatest forward step in the direction of security and in individual opportunity.

“Whatever may be said about consolidations and mergers of physical assets and stocks and bonds, I have yet to hear the slightest word of criticism about the mobilization of brains. What we seek to consolidate in the new RCA Laboratories is the knowledge, the “know-how,” the experience and the intelligence of those who represent the vanguard of our development. Our hope lies in you. To you we look for the discovery of new needs, the creation of the new products, new services and new opportunities.”

## OUR CONTRIBUTORS



DUDLEY E. FOSTER received his E.E. degree at Cornell University in 1922. Prior to entering college he served during the war as a radio operator for the American Marconi Company. Following graduation from Cornell he became associated with the Electrical Alloy Company and Driver-Harris Company. In 1925 he joined the Malone-Lemmon Products Company as Production Engineer, and the next year became Chief Engineer of the Case Electric Company. Two years later that company was merged with the United States Radio and Television Company and soon thereafter Mr. Foster was promoted to Chief Engineer. In 1933 he became Chief Radio

Engineer of the General Household Utilities Company, and in 1934 took up his present duties as engineer in the RCA License Laboratory. He also is lecturer in television engineering at Stevens Institute of Technology and is a member of the Institute of Radio Engineers.

RAYMOND F. GUY entered the marine service of the Marconi Wireless Telegraph Company in 1916, resigning in 1918 to enlist in a regular army Signal Corps Replacement Company. After a year overseas he entered Pratt Institute, graduating in Electrical Engineering in 1921. After short periods as Inspector for the Shipowners Radio Service and The Independent Wireless Telegraph Company, he became, in 1921, one of the small pioneering group that built and operated WJZ, at that time licensed by the Westinghouse Company and located in the Newark plant. After three years of supervisory activities, Mr. Guy



transferred to the RCA Research Department, heading the Broadcast Engineering Section, where he engineered the RCA stations, did consulting work for RCA clients, and directed the development of all broadcast transmitting apparatus used or sold by RCA. In 1929 he became the Radio Facilities Engineer of NBC. Since that time he has been responsible to the Vice President and Chief Engineer for the design, construction, and engineering of all of NBC's Standard Broadcasting, Television, UHF and International Radio Facilities, coverage studies and surveys, cost studies, frequency allocation, power tube engineering, development and design of antenna systems, propagation, etc. He is licensed to practise as a Professional Engineer in New York and New Jersey, is a Fellow of the Institute of Radio Engineers, a Fellow of the Radio Club of America, and a Member of the New York Electrical Society. During the last 10 years he has been active on technical committees of the IRE and other bodies.

H. E. HALLBORG received his degree of B.Sc. in Electrical Engineering from Brown University in 1907, and continued with a general course in the Testing Department of the General Electric Company at Schenectady, N. Y., through 1909. He engaged in high-power communications development by the National Electric Signalling Company at Brant Rock, Mass., under Professor Fessenden through 1912, and then served the American Marconi Company in the study of high-power station technique in England. Upon return to America he became Engineer in Charge and supervised the construction of the New Brunswick and Belmar stations. He was elected to Sigma Xi by Brown University in 1914. In 1915-23 he was Expert Radio Aid in the U. S. Navy and served as Civilian in charge of Radio Activities in the 5th Naval District, during the World War. After the armistice, he served the Navy at Washington, D. C. In 1923-25 he was engaged by the C. Brandies Co., New York, as Consulting Engineer and joined R.C.A. Communications, Inc., New York, as Research Engineer in 1925.



WILLIAM A. HARRIS is a native of Indiana. He received his B.S. degree in Electrical Engineering from the Rose Polytechnic Institute in 1927. He was in the radio department of the General Electric Company, 1927-1928, and in receiver development work for the same company, 1928-1929. Since 1930 he has been engaged in research and engineering work for the RCA Victor Company and the RCA Manufacturing Company at Harrison, N. J. Mr. Harris is an associate member of the Institute of Radio Engineers.

VERNON D. LANDON, following his graduation from Detroit, Jr. College, became a Westinghouse engineer and for six years was in charge of their radio frequency laboratories. In 1929 he went with the Radio Frequency Laboratory in Boonton, N. J., as Assistant Chief Engineer, and in 1931 became Assistant Chief Engineer for Grigsby-Grunow. Since 1933 he has been with the Engineering Department of RCA Manufacturing Company.



LOUIS MALTER received his B.S. degree from C. C. N. Y. in 1926 and his M.A. and Ph.D. degrees from Cornell in 1931 and 1936 respectively. He taught physics at C. C. N. Y. from 1926 to 1928. He was with the Acoustic Research Division of the RCA Manufacturing Co., Inc., from 1928 to 1930 and during the Summer of 1931. From 1933 to 1936 he was in the Electronics Research Division, RCA Manufacturing Company, Camden, N. J.; from 1936 to 1938 in the High Vacuum Section and from 1938 to date in the Research Laboratories of the RCA Manufacturing Company at Harrison. He is a member of the Americal Physical Society and the Institute of

Radio Engineers.

JOHN A. RANKIN received his degree of B.S. in Electrical Engineering from Michigan State College in 1934. From 1934 to date he has been an engineer in the RCA License Laboratory. He is a member of Tau Beta Pi. In 1935 he became an associate member of the Institute of Radio Engineers.



STUART W. SEELEY received his B.Sc. Degree in Electrical Engineering from Michigan State College in 1925. He was an amateur experimenter and commercial radio operator from 1915 to 1924. Following this he joined the experimental research department of the General Electric Company, and a year later became Chief Radio Engineer for the Sparks Withington Company. Since 1935 he has been Section Engineer in the RCA License Laboratory.

L. R. SHARDLOW received his B.S. degree in Ceramic Engineering at Alfred University in 1929, and the M.S. in Ceramic Engineering at the University of Illinois in 1931, while working as a Special Research Assistant on high-voltage insulation problems. Since 1932 he has been with the RCA Manufacturing Company in the Research and Engineering Department at Harrison, engaged in research and development on various phases of electrical insulation for vacuum tubes. He is a member of Sigma Xi.



## TECHNICAL ARTICLES BY RCA ENGINEERS

Published First Quarter, 1941

- ANDERSON, L. J.—A Line Type of Microphone for Speech Pick-Up—*Journal of the Society of Motion Picture Engineers*, March.
- BATSEL, C. W. and C. W. FAULKNER—Operation of the Variable-Intensity Recording System—*Journal of the Society of Motion Picture Engineers*, February.
- BOHLKE, W. H.—Communication and Electronic Maintenance, Part 3—*Radio News*, January.  
—— Communication and Electronic Maintenance, Part 4—*Radio News*, February.
- BROWN, GEORGE H.—A Vestigial Side-Band Filter for Use With a Television Transmitter—*RCA Review*, January.
- CROSBY, MURRAY G.—Band Width and Readability in Frequency Modulation—*RCA Review*, January.  
—— Band Width and Readability in Frequency Modulation—*QST*, March, 1941.
- FERRIS, W. ROBERT—see NORTH and FERRIS.
- FREDENDALL, B. F.—Lateral Disc Recording—*Broadcast News*, February.
- HANSON, O. B.—RCA-NBC Television Presents a Political Convention as First Long-Distance Pick-Up—*RCA Review*, January.
- HATHAWAY, J. L.—Automatic Audio-Gain-Control Design Considerations—*ATE Journal*, February.
- HEACOCK, R. H.—A New High-Quality Soundhead—*RCA Review*, January.
- KELLOGG, E. W.—Ground-Noise Reduction Systems—*Journal of the Society of Motion Picture Engineers*, February.
- KOWALSKI, R. J.—Modern Microphone Types, Structure and Operating Technique—*International Projectionist*, January.
- LANDON, V. D.—Cascade Amplifiers With Maximal Flatness—*RCA Review*, January.  
—— Impulse Noise in F-M Reception—*Electronics*, February.  
—— The Distribution of Amplitude With Time in Fluctuation Noise—*Proceedings Institute of Radio Engineers*, February.
- LYNN, R. A.—Noise Reduction in Disc Recording—*ATE Journal*, January.
- MEIKELL, O. S.—An Analysis of Constant-K Low and High-Pass Filters—*RCA Review*, January.
- NIXON, GEORGE M.—The Operation of Automatic Audio-Gain-Control Amplifiers—*ATE Journal*, February.
- NORTH, D. O.—see THOMPSON and NORTH.  
—— and W. ROBERT FERRIS—Fluctuations Induced in Vacuum-Tube Grids at High Frequencies—*Proceedings Institute of Radio Engineers*, February.
- OLSON, HARRY F.—Line Microphones—*Journal of the Society of Motion Picture Engineers*, March.  
—— Tone Guard—*The Journal of the Acoustical Society of America*, January.
- PREISMAN, ALBERT—Bridged Tee Pads—*Communications*, February.
- SEE, HAROLD P.—Televising the National Political Conventions of 1940—*Journal of the Society of Motion Picture Engineers*, January.
- STOLZENBERGER, E.—The RCA High-Fidelity MI-4887 Recording Head and General Notes on Recording—*ATE Journal*, January.
- THOMPSON, B. J. and D. O. NORTH—Fluctuations in Space-Charge-Limited Currents at Moderately High Frequencies, Part IV—Fluctuations Caused by Collision Ionization—*RCA Review*, January.
- VANCE, A. W.—Stable Power Supplies for Electron Microscopes—*RCA Review*, January.
- WILLIAMS, D.—Motor-Driven Faders—*ATE Journal*, February.
- WING, A. K. and J. E. YOUNG—A Transmitter for Frequency-Modulated Broadcast Service Using a New Ultra-High-Frequency Tetrode—*RCA Review*, January.  
—— A New Ultra-High-Frequency Tetrode and Its Use in a 1-Kilowatt Television Transmitter—*Proceedings Institute of Radio Engineers*, January.
- YOUNG, J. E.—see WING and YOUNG.